

Role Of Transmembrane Protein Strabismus In Motor Neuron Migration In The Zebrafish Hindbrain

A Dissertation
Presented to
The Faculty of the Graduate School
University of Missouri-Columbia

In Partial Fulfillment
of the Requirements for the Degree
Doctor of Philosophy

by
VINOTH SITTARAMANE

Dr. Anand Chandrasekhar, Dissertation Advisor

December, 2008

The undersigned, appointed by the Dean of the Graduate school, have examined the dissertation entitled

**ROLE OF TRANSMEMBRANE PROTEIN STRABISMUS IN MOTOR
NEURON MIGRATION IN THE ZEBRAFISH HINDBRAIN**

Presented by Vinoth Sittaramane

A candidate for the degree of Doctor of Philosophy

And hereby certify that in their opinion it is worthy of acceptance.

Professor Anand Chandrasekhar

Professor Andrew McClellan

Professor Troy Zars

Professor Steven Nothwehr

Professor Richard Tsika

ACKNOWLEDGEMENTS

I would like to acknowledge many people for helping me during my doctoral work. I am deeply indebted to my advisor, Anand Chandrasekhar, for giving me guidance and counsel, and for having faith and confidence in me. He continually stimulated my analytical thinking and greatly assisted me with scientific writing. I am especially thankful to him, for his patience towards me during tough times like missing several deadlines and reading my rusty drafts. He has always amazed me with his dedication and discipline and made me realize that I still have a lot to learn from him. Anand, I would be grateful to you forever.

I am also very grateful for having an exceptional doctoral committee and wish to thank Drs. Andrew McClellan, Richard Tsika, Troy Zars and Steven Nothwehr for their continual support and encouragement. My special note of thanks goes to Stephanie Bingham and Gary Vanderlaan for teaching valuable techniques and more importantly for being there whenever I needed any help. It has been a pleasure working and learning with my colleagues, Derrick, Anagha, Xiufang and Seng Kai. I deeply thank them for investing time and energy discussing ideas with me and tolerating my arrogant opinions and attitude many a times. My warm thanks are due to Denise, for all those long grumbling conversations. Denise, I learnt a lot from you and you will always be special. Thanks!

I would like to thank Moe Baccam for taking care of us as well as fish facility. You are wonderful and thanks for all the pep talks. I also would like to

thank all the undergrads that I worked with especially Drew, Andy, Larry, Neal and Chimwemwe. I thoroughly enjoyed working with you all.

Finally, I'd like to thank my family. My father has always extended his passion for research and encouraged me to pursue science, while my mother was a constant source of support. I'm grateful to my sisters Sudha and Kappu for their everlasting love and enthusiasm. I deeply owe to my best friends, Subbu, Karthik, Bala and Chandra for helping me keep my life in proper perspective and balance.

I am very grateful to the biological sciences and neurosciences graduate program in the University of Missouri-Columbia. I have gained a lot from the program and thank all the people responsible for it.

TABLE OF CONTENTS

| | |
|--|------|
| ACKNOWLEDGEMENTS | ii |
| LIST OF TABLES | x |
| LIST OF FIGURES | x |
| ABSTRACT | xiii |
| CHAPTER I: INTRODUCTION | 1 |
| 1.1 <u>Neural Development</u> | 1 |
| 1.2 <u>Neuronal Migration</u> | 2 |
| 1.2.1 Leading Edge Extension..... | 3 |
| 1.2.2 Nucleokinesis..... | 5 |
| 1.3 <u>Neuronal Migration In The Forebrain</u> | 8 |
| 1.3.1 Radial Migration..... | 8 |
| 1.3.2 Tangential Migration..... | 10 |
| 1.4 <u>Molecular Mechanisms Regulating Neuronal Migration</u> | 11 |
| 1.4.1 Extracellular Signals In Neuronal Migration..... | 11 |
| 1.4.1.1 Long-Distance Guidance Molecules..... | 14 |
| 1.4.1.2 Short Distance Instructive Molecules And Cell Adhesion Complexes..... | 15 |
| 1.4.2 Non-receptor Kinases..... | 18 |
| 1.4.3 Cytoskeletal Proteins In Neuronal Migration..... | 19 |
| 1.4.3.1 Microtubules and Its Associated Proteins..... | 19 |
| 1.4.3.2 Actin and Its Associated Proteins..... | 20 |
| 1.5 <u>Facial Branchiomotor Neuron Migration in the Hindbrain</u> | 23 |

| | | |
|--|---|----|
| 1.6 | <u>Molecular Mechanisms Regulating FBMN Migration</u> | 27 |
| 1.6.1 | Chemoattractive Mechanisms..... | 27 |
| 1.6.2 | Transcription Factors In FBMN Migration..... | 29 |
| 1.7 | <u>PCP Molecules In FBMN Migration</u> | 32 |
| 1.7.1 | Role Of <i>stbm</i> In FBMN Migration..... | 33 |
| 1.7.2 | Genetic Interactions Between <i>stbm</i> and Other PCP Genes In Regulating FBMN Migration..... | 34 |
| 1.7.3 | Genetic Interactions Between <i>stbm</i> and Non-PCP Genes In Regulating FBMN Migration..... | 39 |
| CHAPTER II: MATERIALS AND METHODS | | 41 |
| 2.1 | <u>Fish Care And Maintenance</u> | 41 |
| 2.2 | <u>Fish Strains</u> | 41 |
| 2.2.1 | <i>trilobite (tri)</i> | 41 |
| 2.2.2 | <i>Islet1</i> -GFP Transgenic Line..... | 42 |
| 2.3 | <u>Probe and RNA Synthesis</u> | 42 |
| 2.3.1 | Template DNA Preparation..... | 42 |
| 2.3.2 | Probe Synthesis..... | 43 |
| 2.3.3 | mRNA Synthesis..... | 44 |
| 2.3.4 | RNA Gel Electrophoresis..... | 44 |
| 2.4 | <u>mRNA or Morpholino Injection</u> | 45 |
| 2.5 | <u>In Situ Hybridization</u> | 46 |
| 2.6 | <u>Immunohistochemistry</u> | 48 |
| 2.7.1 | Antibody Labeling..... | 49 |

| | | |
|--|--|----|
| 2.7.2 | Fluorescent Antibody Labeling..... | 50 |
| 2.7 | <u>Genetic Mosaic Analysis</u> | 51 |
| 2.8 | <u>The FBMN Migration Index - A Sensitive Measure of Neuronal Migration in a Population of Embryos</u> | 51 |
| 2.9 | <u>Imaging of Embryos</u> | 52 |
| 2.10 | <u>Western Blotting</u> | 52 |
| 2.10.1 | Protein Isolation..... | 52 |
| 2.10.2 | Protein Preparation and SDS-PAGE | 53 |
| 2.10.3 | Transfer of Proteins to Nitrocellulose Membrane and Western Blotting..... | 53 |
| 2.11 | <u>Cell Death Detection Using Acridine Orange</u> | 54 |
| 2.12 | <u>Common Reagents and Solutions</u> | 55 |
| | | |
| CHAPTER III: STRABISMUS FUNCTION IS REQUIRED IN THE FLOORPLATE AND NEUROEPITHELIAL CELLS TO MEDIATE THE MIGRATION OF FACIAL MOTOR NEURONS IN ZEBRAFISH HINDBRAIN..... | | |
| 3.1 | <u>Introduction</u> | 57 |
| 3.2 | <u>Results</u> | 62 |
| 3.2.1 | <i>Stbm</i> and <i>pk1a</i> Expression Overlap in Mesoderm and Endoderm..... | 62 |
| 3.2.2 | <i>Stbm</i> and <i>pk1a</i> genetically Interact to Regulate FBMN Migration..... | 65 |
| 3.2.3 | Endoderm is Not Required for Normal Migration of FBMNs. | 69 |

| | | |
|-------|---|----|
| 3.2.4 | Mesodermal <i>stbm</i> is Not Required for FBMN Migration..... | 74 |
| 3.2.5 | <i>Stbm</i> Functions in the Floorplate and Neuroepithelial Cells to Regulate FBMN Migration..... | 81 |
| 3.3 | <u>Discussion</u> | 84 |

CHAPTER IV: ROLE OF STRABISMUS DOMAINS IN MEDIATING FBMN MIGRATION IN ZEBRAFISH HINDBRAIN.....89

| | | |
|-------|--|-----|
| 4.1 | <u>Introduction</u> | 89 |
| 4.2 | <u>Results</u> | 92 |
| 4.2.1 | <i>Stbm</i> /Trilobite/ <i>Vangl2</i> is a Four-pass Transmembrane Protein..... | 92 |
| 4.2.2 | Developing an FBMN Migration Rescue Assay Using Wild-type Embryos..... | 96 |
| 4.2.3 | The FBMN Migration Index – A Sensitive Measure of Neuronal Migration in a Population of Embryos..... | 99 |
| 4.2.4 | FBMN Rescue Assay in <i>stbm</i> Morphant Embryos..... | 99 |
| 4.2.5 | <i>Stbm</i> C- and N-Terminal Domains can Independently Rescue FBMN Migration..... | 102 |
| 4.2.6 | Development of Heat Shock Inducible <i>stbm</i> Transgenic Lines... | 103 |
| 4.3 | <u>Discussion</u> | 109 |

CHAPTER V: THE CELL ADHESION MOLECULE Tag1, TRANSMEMBRANE PROTEIN *Stbm*/*Vangl2*, AND Laminin α 1 EXHIBIT GENETIC INTERACTIONS DURING MIGRATION OF FACIAL BRANCHIOMOTOR NEURONS IN ZEBRAFISH.....115

| | | |
|-----|---------------------------|-----|
| 5.1 | <u>Abstract</u> | 115 |
| 5.2 | <u>Introduction</u> | 116 |

| | | |
|-------|--|-----|
| 5.3 | <u>Materials and Methods</u> | 119 |
| 5.3.1 | Animals..... | 119 |
| 5.3.2 | Immunohistochemistry and In situ Hybridization..... | 119 |
| 5.3.3 | Morpholino and mRNA Injections..... | 120 |
| 5.3.4 | In vivo Time-lapse Analysis of GFP-expressing Migrating Motor Neurons..... | 122 |
| 5.4 | <u>Results</u> | 124 |
| 5.4.1 | Transient Axonal glycoprotein-1 (Tag1) is expressed in the Facial Branchiomotor Neuron (FBMNs) | 124 |
| 5.4.2 | <i>Tag1</i> is necessary for the Tangential Migration of FBMNs in Zebrafish..... | 127 |
| 5.4.3 | Neuronal Development in <i>tag1</i> Morphants..... | 127 |
| 5.4.4 | <i>Tag1</i> , <i>stbm</i> (<i>vangl1</i>) and <i>laminina1</i> Genetically Interact with each Other to Mediate FBMN Migration..... | 136 |
| 5.4.5 | <i>Tag1</i> , <i>stbm</i> and <i>lama1</i> Regulate Persistent Movement of FBMNS..... | 145 |
| 5.5 | <u>Discussion</u> | 146 |

CHAPTER 6: EXPRESSION OF UNCONVENTIONAL MYOSIN GENES

| | | |
|---------|---|-----|
| | DURING NEURONAL DEVELOPMENT IN ZEBRAFISH | 158 |
| 6.1 | <u>Abstract</u> | 158 |
| 6.2 | <u>Introduction</u> | 162 |
| 6.3 | <u>Results and Discussion</u> | 162 |
| 6.3.1 | Phylogenetic Analysis of Zebrafish Unconventional Myosins.... | 167 |
| 6.3.2 | Expression Analysis of Zebrafish Myosins..... | 167 |
| 6.3.2.1 | Expression in Hindbrain Segments..... | 170 |

| | | |
|---------|---|-----|
| 6.3.2.2 | Expression in Hindbrain Neurons..... | 170 |
| 6.3.2.3 | Expression in the Forebrain and Midbrain..... | 171 |
| 6.3.2.4 | Expression in the Otic Vesicle..... | 176 |
| 6.3.2.5 | Expression in the Eye..... | 179 |
| 6.3.2.6 | Expression in the Spinal Cord and Trunk..... | 179 |
| 6.3.2.7 | Expression of <i>myo2hc2</i> in Cranial Muscles..... | 182 |
| 6.4 | <u>Materials and Methods</u> | 182 |
| 6.4.1 | Animals..... | 183 |
| 6.4.2 | Cloning and Phylogenetic Analysis of Zebrafish Myosins..... | 183 |
| 6.4.3 | Histological Procedures..... | 186 |
| | REFERENCES | 189 |
| | Vita | 216 |

LIST OF TABLES

| | | |
|------------------|---|-----|
| Table 5.1 | Genetic Interactions During FBMN Migration Between <i>trilobite</i> (<i>stbm</i> ⁻), <i>bashful</i> (<i>lama1</i> ⁻) and <i>tag1</i> Morphants..... | 151 |
| Table 5.2 | Differences in Dynamic Behaviors Between FBMNs Located in r4 of Morphant embryos..... | 152 |
| Table 6.1 | Myosin Genes Characterized in this Report..... | 188 |

LIST OF FIGURES

| | | |
|-------------------|--|----|
| Figure 1.1 | Basic Steps in Neuronal Migration..... | 6 |
| Figure 1.2 | Radial and Tangential Migration of Neurons..... | 12 |
| Figure 1.3 | Schematic of the Organization of the Cranial Motor Neurons in Zebrafish, Chick and Mouse Embryos..... | 25 |
| Figure 1.4 | Wnt/PCP Independent Signaling by <i>Stbm</i> to Regulate FBMN Migration in Zebrafish Hindbrain..... | 36 |
| Figure 3.1 | <i>Strabismus</i> and <i>prickle1a</i> Expression Overlap in Mesoderm and Endoderm..... | 60 |
| Figure 3.2 | <i>Strabismus</i> and <i>prickle1a</i> Genetically Interact to Mediate FBMN Migration..... | 63 |
| Figure 3.3 | Endoderm is Not Required for FBMN Migration..... | 66 |
| Figure 3.4 | Schematic Representation of Transplantation Experiments..... | 70 |
| Figure 3.5 | Targeted Transplantation of Donor Cells into Mesoderm and Endoderm of Host Embryos Using <i>tar</i> RNA..... | 72 |
| Figure 3.6 | <i>Strabismus</i> Deficient Cells in Mesoderm and Endoderm Do Not Affect FBMN Migration in Wild-type Embryos..... | 76 |
| Figure 3.7 | Donor Derived <i>stbm</i> Deficient Neuroepithelial and Floorplate Cells Block the Migration of FBMNs in Wild-type Embryos..... | 79 |
| Figure 3.8 | Donor Derived Wild-type Neuroepithelial and Floorplate Cells Rescue the Migration of FBMNs in <i>tri</i> ⁻ / <i>stbm</i> Morphants..... | 82 |
| Figure 4.1 | <i>Strabismus</i> Domains..... | 94 |

| | | |
|-------------------|---|-----|
| Figure 4.2 | Convergent-Extension and FBMN Migration Indices..... | 97 |
| Figure 4.3 | Convergent-Extension and FBMN Migration Indices in Normal and <i>stbm</i> Morphant Embryos..... | 100 |
| Figure 4.4 | Full length and Δ 5' UTR <i>stbm</i> RNA Can Rescue Defective FBMN Migration in <i>stbm</i> Morphants..... | 104 |
| Figure 4.5 | <i>stbm</i> N- and C- terminal Domains Can Rescue Defective FBMN Migration in <i>stbm</i> Morphant Embryos..... | 107 |
| Figure 4.6 | Development of Heat Shock Inducible Transgenic Lines..... | 111 |
| Figure 5.1 | Expression of <i>tag-1</i> in the Migrating Facial Branchiomotor Neurons..... | 125 |
| Figure 5.2 | FBMN Migration is Affected in <i>tag1</i> Morphants..... | 128 |
| Figure 5.3 | Rescue of the <i>tag1</i> Morphant Phenotype..... | 130 |
| Figure 5.4 | Neuronal Defects in <i>tag1</i> Morphants..... | 133 |
| Figure 5.5 | Genetic Interactions Between <i>tag1</i> and <i>stbm</i> | 137 |
| Figure 5.6 | Genetic Interactions Between <i>stbm</i> and <i>lama1</i> | 139 |
| Figure 5.7 | Genetic Interactions Between <i>tag1</i> and <i>lama1</i> | 142 |
| Figure 5.8 | Quantification of Genetic Interaction Data..... | 147 |
| Figure 5.9 | FBMNs Deficient in <i>tag1</i> , <i>stbm</i> or <i>lama1</i> Function Exhibits Non-polarized Protrusive Activity..... | 149 |
| Figure 6.1 | Domain Organization of Myosins Examined in this Report..... | 163 |
| Figure 6.2 | Phylogenetic Relationship of Unconventional Myosin Family Members Between Zebrafish (<i>Danio rerio</i>), Mouse (<i>Mus musculus</i>), and Man (<i>Homo sapiens</i>)..... | 165 |
| Figure 6.3 | Myosins Exhibiting Restricted Patterns in the Hindbrain..... | 168 |
| Figure 6.4 | Myosin Expression in the Forebrain and Midbrain..... | 172 |
| Figure 6.5 | Myosin Expression in the Developing Ear..... | 174 |

| | | |
|-------------------|---|-----|
| Figure 6.6 | Myosin Expression in the Eye..... | 177 |
| Figure 6.7 | Myosin Expression in the Trunk and Spinal cord..... | 180 |
| Figure 6.8 | Myosin 2 Expression in Head Muscles..... | 184 |

ABSTRACT

Nervous system development involves extensive cell migration, causing immature neurons to move from proliferative zones to specific locations to generate functional circuits. Defective in neuronal migration can cause severe anomalies including mental retardation and learning disabilities. Therefore, it is important to understand the molecular mechanisms underlying neuronal migration. We use zebrafish as a model to study one such migration. In the zebrafish and mouse hindbrain, Facial Branchiomotor Neurons (FBMNs), which mediate jaw and facial movements in mammals, migrate caudally (tangentially) from rhombomere 4 (r4) into r6 and r7. The transmembrane protein Strabismus (Stbm) is a component of the non-canonical Wnt/PCP pathway and is necessary for the normal migration of FBMNs. To understand the mechanisms by which *stbm* regulates neuronal migration, I sought (1) to identify the cell types where *stbm* function is required for FBMN migration (2) to analyze the various domains of Stbm and their requirement for FBMN migration and (3) to analyze other genes interacting with *stbm* to regulate FBMN migration.

Previous analyses showed that *stbm* is expressed ubiquitously, and function non-cell autonomously during FBMN migration. Expression analysis of *stbm* and its interacting partner *prickle1a* (*pk1a*) raised the possibility that *stbm* and *pk1a* may function in non-neural tissues such

as the paraxial mesoderm or endoderm to regulate FBMN migration. FBMN migration occurs normally in embryos lacking endoderm suggesting that endoderm-expressed *stbm* is not necessary for FBMN migration. Targeted transplantation of *stbm*-deficient cells into the mesoderm of wild-type host embryos does not affect FBMN migration indicating that mesoderm-expressed *stbm* is also not essential for FBMN migration. However, transplanted wild-type cells generating ventral neural tube cells including floorplate were able to rescue FBMN migration in *stbm*^{-/-} mutants. Conversely, transplanted *stbm*-deficient cells generating ventral neural tube cells such as floorplate were able to block FBMN migration in wild-type zebrafish embryos, suggesting strongly that *stbm* expression in the floorplate is necessary and sufficient for FBMN migration. Strabismus (Stbm) is predicted to be a four pass transmembrane protein with N- and C- terminal cytoplasmic domains, and a PDZ domain binding motif at the C-terminus. To identify regions of Stbm that are essential for mediating FBMN migration, we tested the abilities of the cytosolic N- & C- terminal fragment to rescue migration in the *stbm*^{-/-} mutants. Surprisingly, both constructs rescued defective FBMN migration, suggesting that both N- and C- terminal domains of Stbm can independently facilitate downstream events mediating FBMN migration in zebrafish hindbrain.

Genetic mosaic analyses have indicated that *stbm* functions in the environment especially in the ventral neural tube cells such as

floorplate to regulate FBMN migration. This result suggests that *stbm* expressed outside motor neurons genetically interact with other genes expressed in FBMNs and the ventral neural tube to mediate FBMN migration. To test this hypothesis, we examined the roles of *Transient axonal glycoprotein-1 (Tag-1)* and *Laminin α 1*, which respectively encode cell adhesion and extracellular matrix protein, during FBMN migration. *Tag-1* is expressed in FBMNs and its knockdown using antisense morpholinos leads to loss of FBMN migration. It genetically interacts with *stbm* to regulate FBMN migration. *Laminin α 1 (lama1)* also interact genetically with *stbm* to regulate FBMN migration. These results indicate that FBMN expressed *tag-1* may be interacting with *stbm* in adjacent cells and *lama1* to regulate FBMN migration.

CHAPTER ONE

INTRODUCTION

1.1 Neural Development

The nervous system is the most complex organ in humans consisting of billions of neurons that are organized in a highly specific pattern of connections creating functional circuits. Early development of the vertebrate nervous system broadly involves four major processes: neural plate induction, neurulation, and neurogenesis, and neuronal migration (Nicholls et al., 2001).

The neural plate is induced when a sheet of ectodermal cells in the dorsal side of gastrula stage embryo acquires neural properties and forms a tissue consisting of elongated neuroectodermal cells (Nicholls et al., 2001). The edge of the neural plate along its length thickens and moves upward to form neural folds, which fuse dorsally to form a hollow neural tube. This morphogenetic process is called neurulation. Following neurulation, medial regions of the neural plate are located ventrally, and generate floor plate cells and motor neuron and interneuron populations. Lateral regions of the neural plate are located dorsally, and generate roof plate cells and sensory neuron and some interneuron populations (Lewis and Eisen, 2003).

Neurogenesis is the process by which neural progenitors are specified from a common pool of neuroectodermal cells. Notch signaling controls acquisition of neural fate via lateral inhibition, whereby activated Notch signaling in neighboring cells blocks proneural development thereby promoting neuroectodermal status (Baker, 2000; Gridley, 1997).

1.2 Neuronal Migration

Nervous system development is characterized by organized patterns of cell movements. Numerous neurons migrate within the vertebrate forebrain and they travel distances up to centimeters in primates (Hatten, 1999). The complex architecture of mammalian brain is directly generated by intricate neuronal migrations that occur during development. Disturbances in neuronal migration can result in mental retardation, epilepsy and severe learning disabilities (Marin and Rubenstein, 2003). Understanding how neurons migrate within the developing brain is therefore essential to diagnose and treat neuronal migration disorders. In this introduction, first I will briefly describe the basic steps that a migrating neuron follows in its journey and later will elucidate the various modes and molecular mechanisms involved in the neuronal migration.

As in any other migrating cell, neurons migrate in phases (Figure 1.1). First, filopodia and lamellipodia explore the micro-environment and

extend leading edge. Second, the nucleus within the neuron moves into the leading process, termed as nucleokinesis and third, the trailing process is retracted (Lambert de Rouvroit and Goffinet, 2001). Collectively, these events enable the neuron to migrate in response to the extracellular and intracellular signals.

1.2.1 Leading Edge Extension

Migrating neurons respond to attractive and repulsive signals in their micro-environment. Responses to these signals are integrated by small GTPase switches of the Rho family (Luo, 2000) and influence the peripheral microfilament network by regulating actin polymerization. Leading edge extension may be either through axonal growth cone or dendritic extension. Neuronal migration following axonal growth cone elongation is referred to as neurophilic, and it mostly occurs tangentially and superficially, close to the pial surface (Rakic, 1990). Best known neurophilic migrations are the subpial migration of external cerebellar granule cells from the rhombic lip over the cerebellar cortex (Hatten, 1999) and the circumferential migration of inferior olivary neurons from the rhombic lip around the brainstem (Bourrat and Sotelo, 1988). Leading edge extensions, in the dendritic domain are morphologically described as dendritic growth cones or tips. Dendritic processes usually elongate along the radial aspect of the neuroepithelium and radial glial cells and migrations through dendritic extensions are termed as

gliophilic migration (Rakic, 1990; 2000a,b). Radial glial cells are thought to provide the substrate and guidance cues for the extension for the dendritic processes. Gliophilic migration accounts for the majority of the neuronal migration in cerebral cortex and cerebellum (Nadarajah and Parnavelas, 2002; Lambert de Rouvroit and Goffinet, 2001). Apart from the axonal and dendritic tip leading edge extensions, there are other types of neuronal migrations. Some examples are: radial non-gliophilic migrations of cortical neurons by nuclear translocation (Nadarajah et al., 1999); Chain migrations by which neurons migrate with a tangential orientation from subventricular zones in the lateral ganglionic eminences to the olfactory bulb by following a glial tunnel that extends through the tissue (Luskin, 1993; Wichterle et al., 1997; Law et al., 1999); and the migration of GABAergic neurons with one or two prominent, horizontally elongated leading processes (Denaxa et al., 2000), from the medial ganglionic eminence to the cerebral cortex (Anderson et al., 1997; Parnavelas, 2000).

Existence of a variety of leading processes indicates the diversity of micro-environmental cues and diverse signaling pathways involved in their growth. Morphological studies suggest that the shape of a leading process reflects its rate of extension, which is maximal for growth cones, less rapid for tangential extension and even slower for radial migration (Lambert de Rouvroit and Goffinet, 2001).

1.2.2 Nucleokinesis

The translocation of the nucleus into the leading process during neuronal migration is termed as nucleokinesis (Figure 1.1). Nucleokinesis is distinct and differentially regulated from leading edge extension, and critically dependent on the microtubule cytoskeleton, as shown in many organisms, from slimes molds to vertebrates. Aberrant nucleokinesis is implicated in human brain malformations known as type 1 lissencephalies, which are characterized by defective migration of immature cortical neurons to the cerebral cortex and are occasionally associated with defective migration in the cerebellum (Lambert de Rouvroit and Goffinet, 2001). Atleast two genetic mutations have been identified as a cause for type 1 lissencephaly, namely lissencephaly 1 (PAFAH1B1/Lis1) (Reiner et al., 1993; Hattori et al., 1994) and doublecortin (DCX) (des Portes et al., 1998; Gleeson et al., 1998). Both Lis1 and doublecortin proteins interact with microtubules, and are components of the dyenin motor complex and of the microtubule organizing centers (Lambert de Rouvroit and Goffinet, 2001). The third step in cell migration, which is the retraction of the trailing process, is poorly understood.

Although neuronal migration occurs throughout the developing nervous system, it has been best studied in the mammalian forebrain and cerebellum. In the following topics, I will discuss specific examples and mechanisms of neuronal migration.

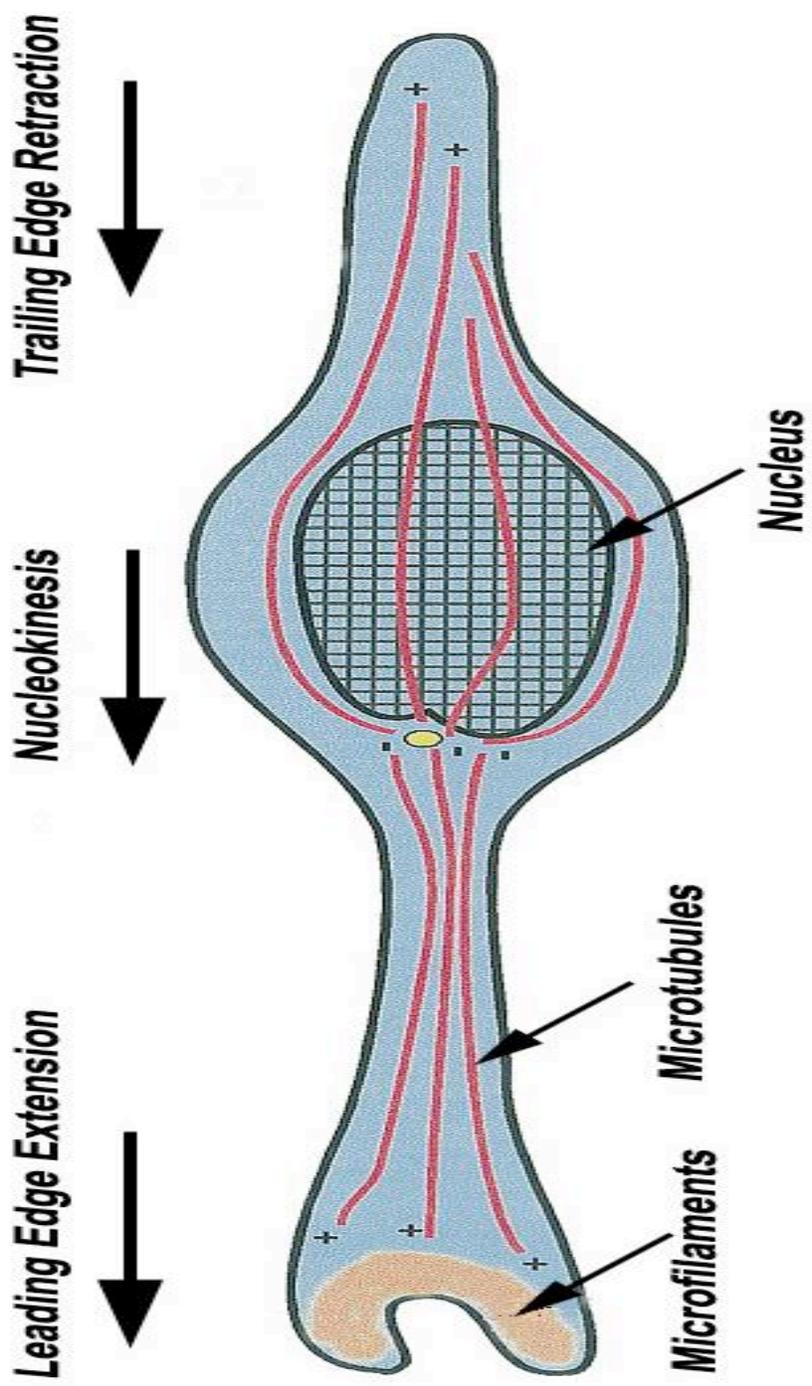


Figure 1.1 Basic Steps in Neuronal Migration

Schema of the steps involved during the migration of a neuron. Neurons generally form many extensions, but only one becomes the leading edge followed by the nuclear migration. Actin filaments at the leading tips polymerize to form the leading edge and the nucleokinesis is dependent on microtubules organization and the trailing edge retraction is poorly understood. (Modified from Lambert de Rouvroit and Goffinet, 2001)

1.3 Neuronal Migration in the Forebrain

The forebrain arises from the most anterior part of the neural tube and becomes an enlarged vesicle called the prosencephalon (Marin and Rubenstein, 2003). All the structures of the forebrain including the cerebrum, hippocampus, and thalamus originate from a continuous sheet of neuroepithelial cells lining the prosencephalon. Cortical neurons arise from the proliferative pseudostratified epithelium at the margin of the embryonic cerebral ventricles (Rakic, 1982). Neural progenitors in the ventricular zone of the cortex proliferate and become specified as neurons. Once specified, the neuronal precursors migrate out of the ventricular zone towards their resting place in the developing neocortex. Two general types of migration (Figure 1.2) have been identified in the forebrain on the basis of the orientation of migrating neurons: radial migration, in which cells migrate from the progenitor zone towards the surface of the brain following the radial glial cells of the neural tube; and tangential migration, in which cells migrate orthogonally to the direction of the radial migration (Marin and Rubenstein, 2003).

1.3.1 Radial Migration

Radial migration is the major route employed to construct the highly laminated structures in the CNS such as cerebral and cerebellar cortices as well as other structures like the spinal cord, striatum, and

thalamus (reviewed by Ayala et al., 2007). About 80-90% of neurons formed in the cortical proliferative zones migrate radially to their final positions in the cortex. As neuroepithelial cells proliferate, each radial glial cell has its cell body (soma) anchored to the ventricular zone and extends a process that reaches the pial surface and attaches to the basal membrane (Gadisseux et al., 1989) (Figure 1.2). Radial glial cells not only support cortical neuron migration by providing a pathway for directed migration, but also undergo mitosis to produce new neurons (Heins et al., 2002; Malatesta et al., 2000; Miyata et al., 2001; Noctor et al., 2001, 2002). In mouse embryos, the first group of neurons that migrates out of the ventricular zone constitutes the preplate (Allendoerfer and Shatz, 1994). An intermediate zone of axons is laid down by the emigration of the first wave of neurons and separates the germinal layer from the mantle of postmitotic cells. The subsequent waves of neuronal migration split the preplate into two layers: the more superficial marginal zone, which consists of the Cajal-Retzius cells born in the first wave of migration; and the deeper subplate, which is constituted by the rest of the immature neurons (Figure 1.2). The development of the cerebral cortex progresses with successive waves of migration that position neurons within different layers in the cortical plate (Hatten, 1999). As a result, the marginal zone and subplate contain the earliest-generated neurons of the cortex (Chun et al., 1987; Kostovic and Rakic, 1980; Luskin and Shatz, 1985), whereas the

cortical plate contains progressively older neurons. Detailed analysis of the migratory behavior of the neurons has revealed the existence of two distinct modes of radial migration (Figure 1.2). i) Neurons adopting glial-guided migration have a short leading process that is not attached to the pial surface and display a saltatory pattern of locomotion, composed of short and rapid forward movements followed by relatively long stationary phases (Figure 1.2B) (Nadarajah et al., 2001). ii) In somal translocation, neurons extend a long leading process with branched ends to attach to the pial surface and by shortening this process, the cell body is progressively pulled towards the pial surface (Figure 1.2A) (Nadarajah et al., 2001). However, these two modes are not cell-type specific, since many migrating neurons switch to somal translocation when the leading process reaches the pial surface at the final stage of their migration (Nadarajah et al., 2001).

1.3.2 Tangential Migration

Neuronal migrations perpendicular to the plane of radial glial fibers is called tangential migration (Figure 1.2C). Although most cortical neurons undergo radial migration, some subpopulations of neurons also undergo tangential migration. Tangential migrations differ primarily in the type of substrate used by the migrating cells, for example, some neurons migrate using each other to promote their migration, as in the case of olfactory bulb interneuron precursors (Marin

and Rubenstein, 2003). Migrating neurons may follow growing axons to reach their destination or some may not follow any specific substrates and instead disperse individually to reach their position such as the cells migrating from subpallium to pallium (Marin and Rubenstein, 2003). Two major tangential routes identified in the forebrain are: (1) the neuronal migrations from medial ganglionic eminence (MGE) to the neocortex and hippocampus and (2) neuronal migrations from the lateral ganglionic eminence (LGE) to the olfactory bulb (Kriegstein and Noctor, 2004; Marin and Rubenstein, 2001).

1.4 Molecular Mechanisms Regulating Neuronal Migration

Extracellular and intracellular molecular events directly control the migratory behavior of the neurons in a given microenvironment. Extracellular guidance cues are interpreted through receptors that relay signals to a network of signaling pathways, ultimately converging on cytoskeletal machinery. As a result, neuronal migration is a concerted mechanical decision made by a large interactive signaling network. In the following section, I will discuss various molecules that regulate neuronal migration starting with extracellular signaling molecules followed by kinases and cytoskeletal proteins.

1.4.1 Extracellular Signals In Neuronal Migration

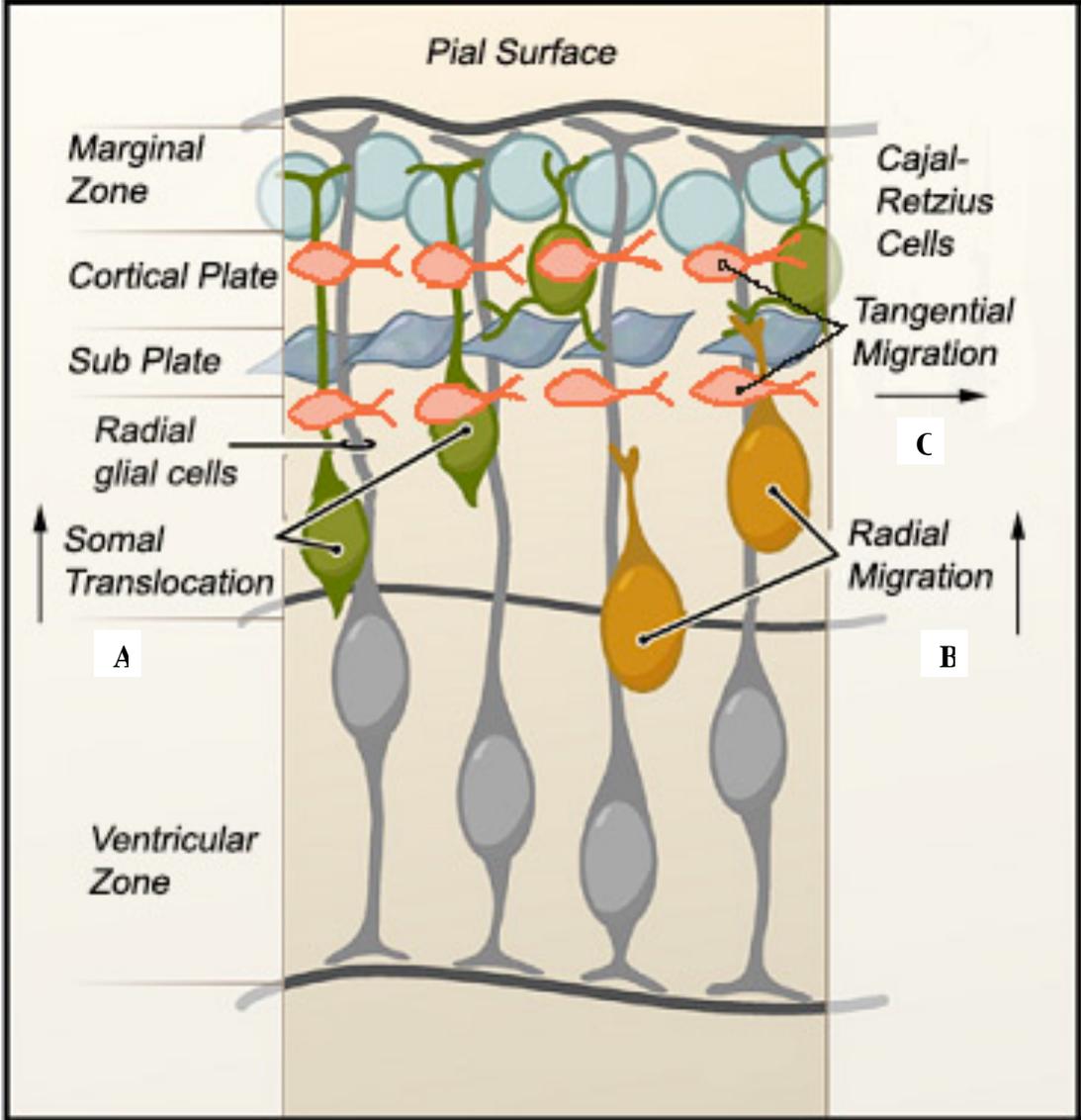


Figure 1.2 Radial and Tangential Migration of Neurons

Cortical neurons can migrate to their final position in two pathways (i) Radial migration and (ii) Tangential migration. Radial migration can be of two types (A) Projection neurons send their process to the pial surface where it attaches and serves as an anchor for the soma to translocate itself to the pial surface. (B) New neurons born in the ventricular surface use radial glial fibers to migrate to the pial surface called locomoting cells. Tangentially migrating cells move across perpendicular to the plane of the radial glial fiber system (C) to reach their final position. (Modified from Ayala et al., 2007).

Wide range of molecules functions as extracellular signals for migrating neurons. Chemotropic molecules such as Semaphorins, Netrin and Slits can act as guidance cues that attract or repel the migrating neurons towards or away from the location and are called long distance guidance molecules. Another group of molecules such as extracellular matrix and cell adhesion complexes surrounding the neurons provide an environment rich in signaling molecules for the neurons to migrate and are called short-distance instructive molecules.

1.4.1.1 Long-Distance Guidance Molecules

Many families of chemotropic molecules such as Netrins, Semaphorins, and Slits that were originally identified as axonal guidance cues have also been implicated in neuronal migration (Tessier-Lavigne and Goodman, 1996). Netrin1 is expressed in the midline of the hindbrain and attracts the tangential migration of pontine neurons from the rhombic lip via its receptor deleted in colorectal cancer (DCC) (Yee et al., 1999). Conversely, Netrin1 and DCC mediate the repulsion of the cerebellar neurons from the external granule layer and the striatal neurons from the subventricular zone of the MGE (Alcantara et al., 2000; Marin and Rubenstein, 2003). Recent studies indicate that netrin1 act by stimulating the GSK3 β and CDK5-dependent phosphorylation of MAP1B, thus potentially regulating microtubule and actin dynamics (Del Rio et al., 2004).

Slit2 and its receptor Roundabout (Robo) may regulate neuronal migration. In vitro migration assays and in vivo expression patterns suggests that Slit2/Robo may guide both tangential and radial migration of neurons. Slit2 has also been implicated in a novel pathway through Robo to inactivate Cdc42 (Wong et al., 2001). However, studies in Slit1/2 null mice indicate that the migration of interneurons from basal telencephalon to the neocortex is intact (Marin et al., 2003; Ward et al., 2003). Therefore, the possible function of Slit2 in neuronal migration is unclear.

Semaphorins are another family of guidance molecules implicated in neuronal migration. Semaphorin 3A and 3F bind to their neuropilin and plexin coreceptors and regulate the sorting of cortical and striatal interneurons from MGE (Marin and Rubenstein, 2003). The plexin receptors serve as scaffolds for several members of the Rho family of GTPases, thus regulating actin dynamics. Plexins also regulate microtubule dynamics by regulating the tyrosine kinases Fes and Fyn, in a semaphorin 3A dependent manner (Bagri and Tessier-Lavigne, 2002; Kruger et al., 2005; Uchida et al., 2005).

1.4.1.2 Short-Distance Instructive Molecules and Cell Adhesion Complexes

The extracellular matrix (ECM) and surrounding cellular architecture provide an environment rich in signaling molecules. For

instance, neuron-glia interaction is very essential for radial migration and several proteins such as astrotactin, integrins, and neuregulins have been implicated in regulating this association. By contrast, TAG-1, an N-CAM member, and the cadherin/catenin complex are thought to mediate neuron-neuron interactions. Also, ECM glycoprotein γ 1 laminin and its receptors integrin α 6 and β 1 have an indirect effect on neuronal migration by regulating the formation of the basal membrane and the anchorage of radial glia endfeet (Georges-Labouesse et al., 1998; Graus-Porta et al., 2001; Halfter et al., 2002).

Secreted factors such as brain-derived neurotrophic factor (BDNF) and NT4, members of the neurotrophin family, were shown to promote the migration of cortical and cerebellar granular neurons (Behar et al., 1997; Borghesani et al., 2002). TrkB, the high affinity receptor of BDNF and NT4, is expressed in migrating neurons in the cortical plate. Both BDNF and NT4 stimulate the motility of embryonic cortical cells in vitro through a Ca^{2+} ion-dependent mechanism that involves the auto-phosphorylation of TrkB (Behar et al., 1997).

Several neurotransmitters are also implicated in modulating the migration of cortical projection neurons. For example, γ -amino butyric acid (GABA) induces dissociated embryonic cortical neurons to migrate in vitro, and it is mediated through GABA receptors (Ayala et al., 2007). GABA is also expressed in the developing neocortex in a pattern suitable to influence migrating cortical neurons (Behar et al., 2001).

Another receptor that modulates the movement of projection neurons is the N-methyl-D-aspartic acid (NMDA) subtype of glutamate receptor. Blockade of NMDA signaling decreases cell migration, whereas enhancement of NMDA receptor activity increases the rate of cell movement (Komuro and Rakic, 1993).

Matrix and membrane bound molecules also directly instruct neuronal migration. The classical members of this family include Reelin (Rice and Curran, 2001), EphB2 and its ligand EphrinB2, and heparin sulfate glycosaminoglycans (Conover et al., 2000; Hu, 2001).

Reelin is a large extracellular glycoprotein that binds to VLDLR and ApoER2, both members of the lipoprotein family of receptors, and induces tyrosine phosphorylation of the adaptor protein, Dab1. Mutations in *Reelin* and *Dab1* display neuronal migration defects that are highly similar, indicating that they all function in a linear signaling pathway. The tyrosine phosphorylation of Dab1 holds a central position in the understanding of the Reelin function because mice expressing Dab1 with all five phosphorylation sites mutated phenocopy *Reelin* mutant (*Reeler*) mice (Howell et al., 2000). Family members of nonreceptor protein kinase Src and Fyn have been shown to phosphorylates Dab1 (Arnaud et al., 2003; Bock and Herz, 2003). In addition, mouse mutants with a combined deletion of *Src* and *Fyn* have a significant reduction of Dab1 tyrosine phosphorylation and developmental defects in the fetal cortex and cerebellum very similar to

those of the *Dab1* mutant mice (Kuo et al., 2005). It is speculated that Fyn and Src are presented to Dab1 through the Cadherin related neuronal receptor (CNR) and integrin $\alpha3\beta1$, the other two receptors for Reelin (Dulabon et al., 2000; Senzaki et al., 1999). The Reelin pathway is involved in the regulation of microtubule dynamics by regulating phosphorylation of Tau (Hiesberger et al., 1999; Beffert et al., 2004) and interacting with Lis1 (Assadi et al., 2003).

1.4.2 Non-receptor Kinases

Kinases mediate neural positioning by phosphorylating the key components of multiple pathways. Key components include Src, Fyn, PI3K, Cdk5, GSK3 β , MAPK-upstream protein kinase (MUK), members of c-Jun N-terminal kinase family (JNK), and extracellular signal-regulated kinase (ERK) (Hirai et al., 2002; Kawauchi et al., 2006; Konno et al., 2005; Simo et al., 2006). We will use Cdk5 as an example to illustrate how such a kinase interacts with its numerous substrates to regulate neuronal migration.

Mice depleted of Cdk5 or its regulators P35 and P39 exhibit severe neuronal positioning defects in the brain regions, including the neocortex, hippocampus, and cerebellum (Dhavan and Tsai, 2001). Interestingly, *P35* mice mutants display an abnormal “branched migration” of neurons, suggesting that a failure to consolidate one leading neurite may contribute to the neuronal positioning defect (Gupta

et al., 2003). Cdk5 phosphorylates a wide range of substrates that include cytoskeletal structural proteins such as intermediate and heavy chains of neurofilaments, MAPs, MAP1b, Tau, Nde1, doublecortin (DCX), and the actin regulatory proteins, PAK1 and p27kip1. Cdk5 also phosphorylates other kinases and adaptor proteins including focal adhesion kinase (FAK), Src, and Dab1, as well as the cell adhesion protein, β -catenin (Kato and Maeda, 1999; Kawauchi et al., 2005; Keshvara et al., 2002; Paglini et al., 1998; Takahashi et al., 2003; Tanaka et al., 2004; Xie et al., 2003).

1.4.3 Cytoskeletal Proteins in Neuronal Migration

Signaling pathways regulating neuronal migration eventually engage cytoskeletal proteins such as microtubules and actin to mediate cell movement. Though it is not entirely clear how the extracellular signals coordinate the cytoskeletal response, it is believed that the actin and microtubule networks have complementary roles in mediating neuronal migration.

1.4.3.1 Microtubules and Its Associated Proteins

Microtubule dynamics regulate neuronal migration by providing stability to the growing neurites and by associating the centrosome to the nucleus during nucleokinesis. Microtubule regulators include classical microtubule-associated proteins (MAPs) such as MAP1A,

MAP1B, MAP2 and Tau (Dehmelt and Halpain, 2004) and non-classical MAPs such as Lis1 and DCX family members. Classical MAPs are involved in stabilization of microtubules. While mutation of *MAP1b* in mice show subtle neuronal migration defects, double mutations with *MAP1b/Tau* and *MAP1b/MAP2* show more severe neuronal migration defects (Dehmelt and Halpain, 2004) suggesting that MAP1B, MAP2 and Tau act synergistically to facilitate neuronal migration.

Non-classical MAP Lis1 is a centrosome and microtubule associated protein that promotes microtubule stability by reducing the frequency of microtubule catastrophe in vitro (Sapir et al., 1997). Humans with hemizygous deletion of *Lis1*, suffer from type 1 lissencephaly, a severe brain developmental disorder that manifests a smooth brain surface, abnormal cortical layering, enlarged ventricles, and neuronal heterotopias (Ozmen et al., 2000). DCX is a member of another family of non-classical MAPs that are involved in microtubule stability. DCX was first identified in humans as the gene responsible for X-linked lissencephaly in males and subcortical heterotopia (or doublecortex) in females (Ayala et al., 2007).

1.4.3.2 Actin and Its Associated Proteins

Disruption of actin dynamics using cytochalasin B, impairs the migration of granule neurons along radial glial processes in vitro (Rivas and Hatten, 1995). In addition, mutations that destabilize the actin

network have profound effects on the development of the CNS. Periventricular heterotopia is a migration disorder, where neurons fail to migrate out of the germinal layers and form clusters that line the lateral ventricles (Fox et al., 1998). It is caused by mutations in filamin 1, an actin binding protein that cooperates with Arp2/3 complex to form actin networks. Filamin 1 also interacts with variety of transmembrane proteins and acts as scaffold for signaling proteins of the Rho family of GTPases, which are also implicated in neuronal migration (Dhavan and Tsai, 2001; Luo, 2000; Stossel et al., 2001). Another family of actin regulators includes mammalian Ena (Mena), vasodilator-stimulated phosphoprotein (VASP), and Ena-VASP-like protein (EVL). Ena/VASP proteins in lamellipodia facilitate actin polymerization. In neurons, Mena binds to profilin, another actin binding protein, and is concentrated in filopodia tips of the growth cone. When Ena/VASP proteins were inhibited through in utero retroviral injection, it results in the ectopic localization of the early-born neurons to the more superficial layers (Krause et al., 2003) indicating the requirement of these proteins during neural development.

Non muscle myosin II is another important actin-associated protein that regulates neuronal migration. In vitro inhibition of non muscle myosin II using a specific inhibitor, blebbistatin, results in an impairment of nucleokinesis. Mouse myosin II mutants show severely abnormal brain development such as enlargement of the ventricles and

disordered neuronal architecture (Tullio et al., 2001), and abnormal migration of cerebellar granular neurons and impaired tangential migration of neurons originating in the MGE (Ma et al., 2004).

Unconventional non muscle myosins are actin-based motors known to play fundamental roles in eukaryotic motility such as cell crawling, phagocytosis and organelle trafficking (Libby and Steel, 2000; Tuxworth and Titus, 2000; Wu et al., 2000; Soldati, 2003). Furthermore, unconventional myosins have been localized to neuronal growth cones and regulate growth cone motility in vitro (Wang et al., 1996; Evans et al., 1997; Suter et al., 2000; Difenbach et al., 2002; Sousa et al., 2006). Nevertheless, the in vivo functional role of unconventional myosins during neuronal migration and growth cone guidance is not clear. **In order to begin addressing the functions of various unconventional myosins in the developing vertebrate embryo, we have carried out an extensive characterization of the expression of unconventional myosin genes in the developing zebrafish in Chapter 6.**

We use zebrafish as a model to study neuronal migration, particularly the migration of facial branchiomotor neurons in the developing hindbrain. In the next few sections, I will discuss the migration of facial branchiomotor neurons and various molecular mechanisms regulating it.

1.5 Facial Branchiomotor Neuron (FBMN) Migration in the Hindbrain

The anterior aspect of the neural tube undergoes morphological changes and forms forebrain, midbrain and hindbrain. The hindbrain region is further partitioned into seven or eight compartments called rhombomeres (Figure 1.3). Rhombomeres are polyclonal compartments (Lumsden, 1990) that are distinguished from each other by limited cell movements (Fraser et al., 1990; Birgbauer and Fraser, 1994), differential cell adhesion (Guthrie and Lumsden, 1991; Wizenmann and Lumsden, 1997), differential cell repulsion (Xu et al., 1995, 1999; Cooke et al., 2001; Cooke and Moens, 2002), and compartment specific expression of homeobox genes (Wilkinson and Krumlauf, 1990; Lumsden and Krumlauf 1996). Each rhombomere contains a characteristic, segmentally reiterated set of neurons, including motor neurons and reticulospinal interneurons (Kimmel et al., 1985; Metcalfe et al., 1986; Lumsden and Keynes, 1989; Clarke and Lumsden, 1993; Glover, 2001; Chandrasekhar, 2004).

Within the rhombomeres, a variety of neurons are generated at a defined dorsoventral (D-V) position in response to morphogen gradient created by sonic hedgehog (Shh) and others (Jessell, 2000). Likewise, segmental specific expression of various Hox genes assigns the positional information along anterior-posterior (A-P) axis of the

hindbrain (Jessell, 2000). The facial branchiomotor neurons (FBMNs) are generated in r4 and their axons innervate muscles derived from the second branchial arch. In zebrafish and mouse, these neurons migrate caudally from r4, adjacent and parallel to the floorplate, into r6 and r7 (zebrafish) and r6 (mouse) (Chandrasekhar, 2004; Song, 2007). In chick, the FBMNs are induced in r4, with a few cells also induced in r5 and they do undergo limited migration (Jacob and Guthrie, 2000). The cell bodies appear to move into a leading edge protrusion, in a process called perikaryal translocation (Book and Morest, 1990). While the cell bodies migrate caudally, their axonal process is left behind in manner that reflects their migratory path and their motor axons exit in r4.

Here on, I will discuss various molecular mechanisms involved in the migration of facial branchiomotor neurons from r4 to r6 and r7. The facial branchiomotor neurons (FBMNs) of several vertebrates, including mouse and zebrafish, but not chick, migrate tangentially along the rostrocaudal axis from their birth place in r4 into more caudal rhombomeres as far as r7 (Gilland and Baker, 1993; Goddard et al., 1996; Studer et al., 1996; Chandrasekhar et al., 1997; Higashijima et al., 2000). Several molecules have been identified to play a role in regulating the tangential migration of FBMNs in mouse and zebrafish. I will attempt to broadly classify them based on their mode of action and pathways.

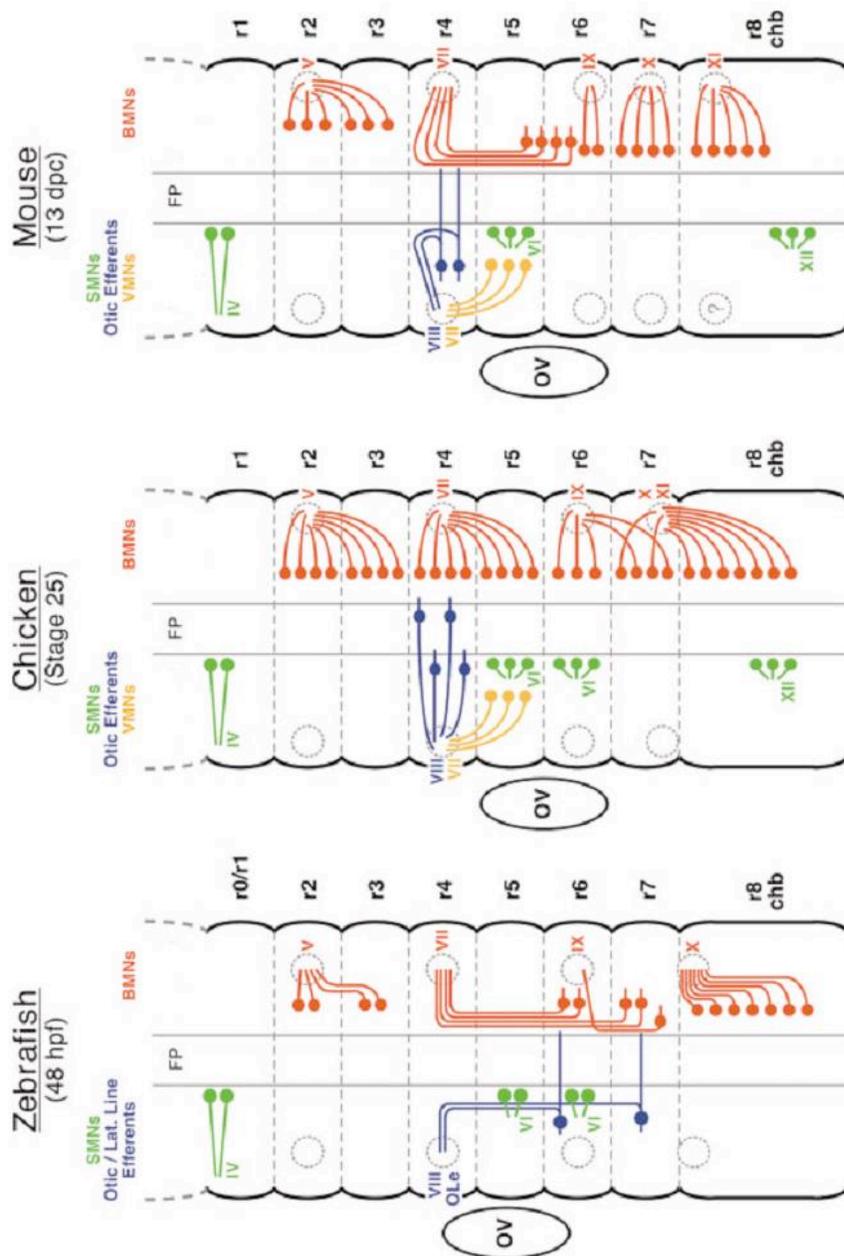


Figure 1.3 Schematic of the Organization of Cranial Motor Neurons in Zebrafish, Chick and Mouse embryos.

Embryo Ages: Zebrafish, 48 hours post fertilization (hpf); Chick, stage 25; mouse, 13 days post coitum (dpc). Hindbrain is shown in an open book configuration with anterior end at the top. The rhombomeres are shown as bulges separated by broken grey lines and labeled as r0/r1 to r8 or caudal hindbrain (chb). The branchiomotor neurons (BMNs) and axons are shown in red. The somatomotor neurons (blue), visceromotor (orange) and otic and lateral line efferents (green) are also shown here, but not discussed. The nerve exit points are shown as dotted circles. OV, Otic vesicle. (Chandrasekhar, 2004).

1.6 Molecular Mechanisms Regulating FBMN Migration

1.6.1 Chemoattractive Mechanisms

Evidence from various mice and zebrafish mutants with defects in axon guidance and cell body migration of FBMNs suggests that these functions may utilize similar genetic program (Chandrasekhar, 2004; Song, 2007). Several axon guidance cues are implicated in FBMN migration, either attracting or repelling them away from their original position (Chandrasekhar, 2004).

FBMNs migrate from r4 to r6 and r7, thus it is possible that chemoattractive cues are present around their final destination or along their migratory pathway and guide their migration. The existence of environmental cues has been demonstrated in transplantation experiment. When a chick r4 is homotypically transplanted in the place of a mouse r4, the chick FBMNs migrate caudally into the host (mouse) r5 and r6 (Studer, 2001), demonstrating that chick FBMNs have the ability to respond to mouse signals. Conversely, when mouse r4 is transplanted into the chick hindbrain, mouse FBMNs fail to migrate caudally, suggesting that cues necessary for initiation and maintenance of caudal migration is absent in chick hindbrain (Studer, 2001). In *Krox20* null mice and *Kreisler* null mice, which lack r5, the FBMNs were able to initiate their caudal migration but prematurely undergo radial movements before reaching r6 (Manzanares et al., 1999; Schneider-Maunoury et al., 1993; Seitanidou et al., 1997). Likewise, zebrafish

valentino mutants, in which r5 and r6 is transformed into a single rhombomere with mixed identity, also exhibit a similar migration defect (unpublished). Together these findings suggest that r5 derived signals may guide the migration of FBMNs. Though the exact nature of signaling is not known, two possible mechanisms are implicated namely VEGF and Reelin signaling.

VEGF Signaling - VEGF is Vascular endothelial growth factor and it has been implicated in various neuronal and blood cell migrations. VEGF is expressed in the ventral neural tube (Schwarz et al., 2004), while its receptor Neuropilin1 (Npn1) is expressed in the floorplate and FBMNs during migration (Kitsukawa et al., 1995; Schwarz et al., 2004; Takagi et al., 1995). *VEGF120* and *Npr1* null mice exhibit FBMN migration defect, where FBMNs migrate upto r5 to form smaller facial nucleus (Schwarz et al., 2004). Also, placing VEGF164 coated beads in the explanted hindbrain tissue, causes FBMNs to migrate toward it, showing that VEGF acts as a chemoattractant for FBMNs (Schwarz et al., 2004). Thus, VEGF could be signaling through its receptor Neuropilin1 to regulate FBMN migration in mouse.

Reelin Signaling - The Reelin (Reln) gene encodes a secreted extracellular matrix protein and in mouse it is expressed in the areas surrounding the facial nucleus in r6 and also in lower levels within the

FBMNs (Ohshima et al., 2002). In *reeler* mutant, there are defects specifically in radial FBMN migration. Dab1 is the adaptor protein for reelin receptor and Cdk5 is the kinase involved in the reelin pathway. *Dab1* and *Cdk5* mutants show similar defects as the *reeler* mutants (Ohshima et al., 2002). Thus, reelin expressed in r6 could have a chemoattractive effect on the radial FBMN migration.

1.6.2 Transcription Factors in FBMN Migration

In developing hindbrain, multiple transcription factors are implicated in cell specification and subsequent differentiation of neurons (Chandrasekhar, 2004). Several of these molecules are also involved in neuronal migration.

Ebf1 - Early b-cell factor (*Ebf1*) is a transcription factor with both a novel HLH domain and an atypical zinc finger structure (Hagman et al., 1993, 1995). In mouse, *Ebf1* is expressed within the FBMN cell bodies as well as rhombomeric boundaries in mouse embryos during their migration (Garel et al., 1997). In *Ebf1* mutants, many FBMNs undergo a premature dorsolateral migration in r5. In *Ebf1* mutant embryos, expression of cell adhesion molecule TAG-1 is downregulated within r5, while receptor molecule Ret and adhesion molecule Cdh8 are ectopically activated in r4 (Garel et al., 1997). These results suggest that *Ebf1* helps FBMNs to properly interpret environmental cues.

Gata2* and *Gata3 - *Gata2* and *Gata3* are zinc finger transcription factors and are expressed in nearly identical patterns in the ventral neural tube and are strictly excluded from FBMNs (Nardelli et al., 1999; Pata et al., 1999). Interestingly, both *Gata2* and *Gata3* deficient embryos have defective FBMN migration. In *Gata2* mutants, expression of other transcription factors such as *Isl1* and *Nkx6.1* are reduced and more restricted to the ventral neural tube near the floorplate (Nardelli et al., 1999), suggesting that *Gata2* may be required for proper FBMN development. In addition, genetic interaction studies using *Hoxb1*, *Gata2* and *Gata3* null mice suggest that these genes exist in a linear pathway in the order of *hoxb1*, *Gata2* and *Gata3* (Pata et al., 1999).

***Hox* genes** - Several *Hox* genes are expressed in overlapping fashion to control the A-P patterning of the hindbrain and are involved in regulating the rhombomeric identity. Importantly, *Hoxa1* and *Hoxb1* are highly expressed around r4 and closely associated with FBMNs. *Hoxa1* is expressed from r4 to r8. In *Hoxa1* mutant mice, r3/r4 boundary is not defined and r5 is missing and more importantly FBMNs born in r4 are mis-specified and assume a partial r2 identity. Therefore, some FBMNs migrate dorsally in r3-r4, while others migrate caudally to form small FBMN nucleus (Carpenter et al., 1993; Gavalas et al., 2003; Gavalas et al., 1998). *Hoxb1* is specifically expressed in r4. In *Hoxb1* mutant mice, r4 is mis-specified to acquire r2 identity and therefore all

FBMNs migrate laterally like trigeminal motor neurons in r2 (Goddard et al., 1996; Studer et al., 1996). In zebrafish, *Hoxb1a* is expressed in r4 and is necessary for the migration of FBMNs (McClintock et al., 2002).

Phox2a* and *Phox2b - Paired-like homeobox 2a and 2b (*Phox2a* and *Phox2b*) are homeodomain transcription factors expressed in all branchiomotor neurons. While *Phox2b* is present in both progenitors and postmitotic neurons, *Phox2a* is expressed only in postmitotic neurons. *Phox2b* mutant mice lack all BM neurons including FBMNs (Pattyn et al., 2000) whereas *Phox2a* mice have no developmental defects. This is probably due to the redundant role of *Phox2b*. When *Phox2a* is knocked in for *Phox2b* FBMNs are born but failed to migrate caudally indicating a role for *Phox2b* in FBMN migration (Coppola et al., 2005).

Mash1* and *Math3 - These are bHLH transcription factors that define neuronal identity among progenitors and are expressed mainly in the progenitor domain (Ohsawa et al., 2005). While *Mash1* null mice have no migration defect, *Math3* null mice show severe migration defects where small subset of FBMNs migrate normally and rest of them migrate laterally in the border of r4 to form a nucleus in r5. *Mash1;Math3* compound mutant also have a similar defect in FBMN migration (Ohsawa et al., 2005).

Nkx6.1* and *Nkx6.2 - *Nkx6* genes are homeodomain transcription factors that are expressed in the progenitor domain as well as FBMNs in the hindbrain. While *Nkx6.1* is expressed throughout their migration, *Nkx6.2* is expressed mainly in pre-migratory FBMNs (Pattyn et al., 2003). In *Nkx6.1* null mice, cell bodies are generated normally, but FBMNs migrate only laterally with r4 with no caudal migration. In contrast, *Nkx6.2* null mice exhibit no migration defect, suggesting a redundant role for *Nkx6.1* (Muller et al., 2003; Pattyn et al., 2003).

Tbx20 - *Tbx20* is a T-box transcription factor and is highly expressed in all BM neurons. *Tbx20* is selectively expressed in postmitotic FBMNs during their migration. In *Tbx20* null mice, FBMNs are formed normally but they fail to migrate caudally as well as laterally (Song et al., 2006). Furthermore, *Tbx20* null mice showed down regulation several planar cell polarity (PCP) genes within FBMNs including *prickle1* and *vangl* which in zebrafish have been shown as necessary for FBMN migration (Carriera-Barbosa et al., 2003; Jessen et al., 2002). Therefore *Tbx20* may control the expression of PCP genes to regulate the migration of FBMNs.

1.7 PCP Molecules in FBMN Migration

The non-canonical (Wnt) signaling pathway mediates planar cell polarity (PCP) (Figure 4) processes from flies to mammals (Tada et al.,

2002; Tree et al., 2002). In vertebrates, the secreted glycoproteins Wnt11 and Wnt5a act as ligands (Heisenberg et al., 2000; Rauch et al., 1997; Tada and Smith, 2000), although a Wnt ligand mediating PCP is yet to be found in *Drosophila*. Core components of these pathways include: Frizzled (Fz) receptors; intracellular signal transducer, disheveled (Dsh); a 4-pass transmembrane protein, Van gogh /Strabismus/Trilobite (Vang/Stbm/Tri); an intracellular protein, Prickle1a (Pk1a); seven pass transmembrane proteins, Celsr1a, Celsr1b, Celsr2 (Cadherin, EGF like, LAG like, seven pass receptor); small GTPases RhoA and Cdc42; and a RhoA effector, Rho kinase 2 (Darken et al., 2002; Djiane et al., 2000; Goto and Keller, 2002; Habas et al., 2001; Heisenberg et al., 2000; Jessen et al., 2002; Marlow et al., 2002; Park and Moon, 2002; Tada and Smith, 2000; Wallingford et al., 2000). Several of these molecules have been implicated in FBMN migration.

1.7.1 Role of *stbm* in FBMN Migration

Stbm/Vangl2, is required for both convergent extension (CE) movements (Marlow et al., 1998) and FBMN migration in zebrafish (Jessen et al., 2002; Bingham et al., 2001). Genetic mosaic analyses have shown that *stbm* functions mostly cell autonomously to mediate convergent extension cell movements and non-cell autonomously for FBMN migration (Jessen et al., 2002). However, the identity of the cell type where *stbm* function is required for FBMN migration is not known.

Therefore, we examined the identity of the cell types where *stbm* function is required to mediate FBMN migration in Chapter three.

1.7.2 Genetic Interactions between *stbm* and other PCP Genes in Regulating FBMN Migration

Stbm functions with *knypek* (*glypican4/6*), *pipetail* (*wnt5a*), *silberblick* (*wnt11*) and *dishevelled*(*Dsh*) to mediate CE movements in Wnt/PCP pathway (Park and Moon, 2002; Jessen et al., 2002). However, we believe that *stbm* functions independently of Wnt/PCP pathway to regulate FBMN migration in zebrafish due to the following reasons (1) Several *stbm/trilobite* alleles (*tri^{tc240a}*, *tri^{vu46}*, *tri^{vu48}*) have been identified that cause mild CE defect but a severe FBMN migration defect, suggesting that these two process are regulated differently by *stbm*, (2) *stbm* functions cell autonomously for CE movements and non-cell autonomously for FBMN migration (Jessen et al., 2002), (3) Mutations in other PCP molecules such as *knypek*, *pipetail* and *silberblick* produce CE defects, but do not affect FBMN migration. Also, specific inhibition of Wnt/PCP pathway by overexpression of a truncated, dominant negative Dishevelled protein reduces gastrulation movements (Xdd1; Sokol, 1996) but, has no effect on FBMN migration. These results strongly suggest that *stbm* mediates FBMN migration through Wnt/PCP independent mechanisms.

However, *stbm* may interact with other PCP core genes such as *prickle1a*, *frizzled*, *celsr1a*, *celsr1b* and *celsr2* to mediate FBMN migration (Figure 1.4). In *Drosophila*, *stbm* interacts with *prickle1* (Jenny et al., 2003) and *flamingo* (*fmi/Celsr*) (Rawls et al., 2003) to regulate planar cell polarity in a Frizzled (Fz)/Dishevelled dependent manner (reviewed by Strutt, 2003). Knockdown of *prickle1a* (*pk1a*) using morpholinos (MO) in zebrafish produces severe CE defects and a mild FBMN migration defect (Carriera Barbosa et al., 2003). Sub-optimal dose of *pk1a* MO injected into *tri^{m209}* heterozygotes produces strong FBMN migration defect, suggesting that *pk1a* genetically interacts with *stbm* to mediate FBMN migration (Carriera Barbosa et al., 2003). *Pk1a* expression is not detected in the FBMNs, thus, it probably functions non-cell autonomously.

Recently, another prickle1, *pk1b* was identified in zebrafish and is expressed in the FBMNs and functions cell autonomously (Rohrschneider et al., 2007) to regulate FBMN migration and also it genetically interacts with *stbm* in mediating FBMN migration (Oni Mapp and Victoria Prince, Unpublished). Together, both *pk1a* and *pk1b* genetically interact with *stbm* to mediate FBMN migration. *Scribble1* is another cell polarity gene encoding an intracellular protein that genetically interacts with *stbm* to mediate both CE movements and FBMN migration (Wada et al., 2005). *Scribble1* also functions non-cell autonomously to regulate FBMN migration (Wada et al., 2005). *Celsr1a*,

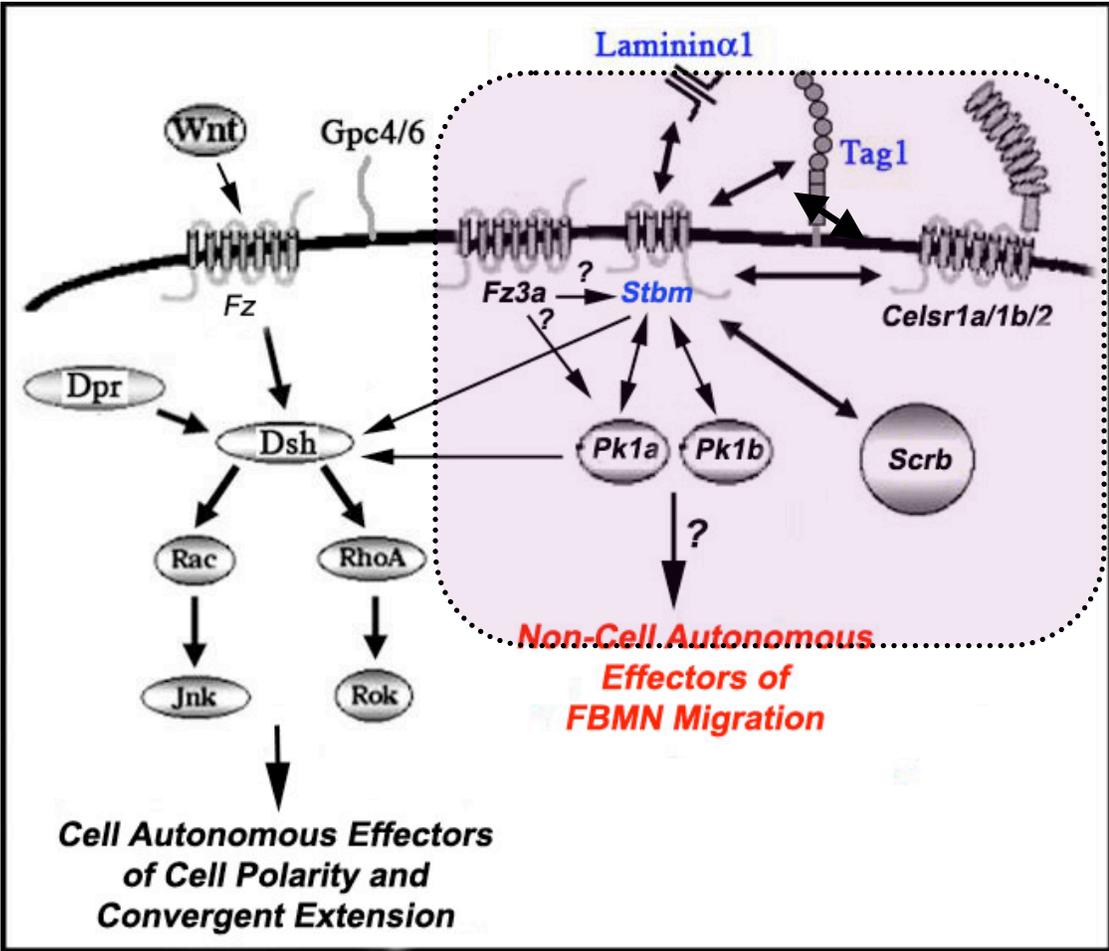


Figure 1.4 Wnt/PCP Independent Signaling by Stbm to Regulate Facial Motor Neuron Migration in Zebrafish

A model for the non-canonical Wnt/PCP pathway in zebrafish and specific molecules of this pathway (dotted box) interact to mediate FBMN migration in zebrafish. *Laminina1* and *tag1* genetically interact with *stbm* to mediate FBMN migration. *pk1a* and *pk1b* are two prickle genes that interact with *stbm* to regulate FBMN migration. Interactions between *fz3a*, *stbm* and *celsr* have not been studied yet. *Fz3a*, *stbm*, *celsr1a*, *celsr1b*, *celsr2*, *pk1a* and *lama1* are expressed more broadly in the neural tube and function non-cell autonomously while *pk1b* and *tag1* are expressed in the FBMNs and thought to be functioning cell autonomously. Double headed arrows indicate genetic interactions involved in regulating FBMN migration. Single headed arrows indicate the sequence of activation of molecules in the pathway. (Modified from Doudney and Stanier,2005),

Celsr1b and *Celsr2* are PCP genes that encode seven pass transmembrane receptor molecules which functions redundantly in a non-cell autonomous fashion to mediate FBMN migration (Wada et al., 2006). *Fz3a*, a frizzled receptor gene is also necessary for the FBMN migration in a non-cell autonomous manner (Wada et al., 2006). Both *Celsr2* and *Fz3a* genes function in the neuroepithelial cells adjacent to the migrating FBMNs to mediate FBMN migration. However, it is not known whether *Celsr2* and *Fz3a* genes interact with *stbm* to regulate FBMN migration.

Mouse *vangl2* and *Celsr1* mutants also show severe defect in FBMN migration (Glasco DM, Fritsch B, Vilhais-Neto GC, Pourquié O and Chandrasekhar A., Unpublished; Qu Y, Glasco DM, Fritsch B, Zhou L, Ravni A, Murdoch JN, Goffinet AM, Chandrasekhar A and Tissir F., Unpublished) However, mouse homologues for *Pk1a* and *Fz3* have not been studied yet. Taken together, several core genes of Wnt/PCP pathway such as *stbm*, *pk1a*, *pk1b*, *celsr2*, *celsr1a*, *celsr1b* and *Fz3a* are necessary for FBMN migration, but some of the key components such as *Wnt5a*, *Wnt11*, *Dsh* and *Glypican* do not play any role in FBMN migration (Bingham et al., 2001; Jessen et al., 2002) suggesting that *stbm* and these other genes function in a Wnt and Dsh independent novel mechanism to mediate FBMN migration.

One way to understand the mechanisms deployed by *Stbm*, would be to define the function of various domains of *Stbm*. **Therefore,**

in Chapter 4, we performed a structure-function analysis of *stbm* domains to examine their roles in FBMN migration.

1.7.3 Genetic Interactions between *stbm* and Non-PCP Genes in Regulating FBMN Migration

Since *Stbm* is a transmembrane protein with two extracellular loops that functions non-cell autonomously, it is possible that *stbm* may interact with other molecules in the environment or the ones expressed in the FBMNs to regulate migration. One such candidate that is expressed in the FBMNs is the transient axonal glycoprotein-1 (TAG-1) (Warren et al., 1999). TAG-1 is a cell adhesion molecule that belongs to the Immunoglobulin superfamily it has been implicated in axon guidance (Liu and Halloran, 2005, Wolman et al., 2008) and neuron migrations (Denaxa et al., 2001; 2005). But, the role of TAG-1 in FBMN migration has not been tested. **Therefore, we examined the role of TAG-1 in FBMN migration by using TAG-1 morpholinos and studied its interaction with *stbm* during FBMN migration in Chapter 5.**

Another candidate laminin α 1 (*Lama1*), is an extracellular matrix protein that is expressed in the environment of the FBMN migration in the hindbrain. *Lama1* is known to provide permissive and instructive cues for axon outgrowth and neuronal migration (Paulus and Halloran, 2005; Wolman et al., 2008). In *bashful* (*lama1*) mutants, some FBMNs

fail to migrate from r4 to r6 and r7 (Paulus and Halloran, 2005). But, the molecular mechanism by which Lama1 regulates FBMN migration is not clear. **Therefore, we examined the interaction between *lama1* with *stbm* and *tag1* to regulate FBMN migration in Chapter 5.**

CHAPTER 2

MATERIALS AND METHODS

2.1 Fish Care and Maintenance

Zebrafish, *Danio rerio*, stocks were maintained on a 14 hour light/ 10 hour dark cycle as described earlier (Westerfield, 1995). Embryos were obtained from pair-wise crosses and grown at 28.5°C in embryo medium (E3) to reach specific developmental ages. Embryos were treated with 0.2 mM phenylthiourea (PTU, Sigma) to prevent pigmentation when desired. Embryos were fixed in 4% paraformaldehyde in phosphobuffered saline (PFA-PBS) at required time-points in preparation for analysis.

2.2 Fish Strains

2.2.1 *trilobite* (*tri*)

Trilobite mutant alleles were identified during a large scale mutagenesis screen using ENU in Tübingen, Germany and Boston, USA (Solnica-Krezel et al., 1996; Hammerschmidt et al., 1996). The gene encoded by *trilobite* loci was positionally cloned and identified as *strabismus* (Jessen et al., 2002). Though different mutant alleles (*tri*^{tk50f}, *tri*^{tc240a}, *tri*^{m209}) have varied severity in convergence extension

phenotype (CE) phenotype, all of them exhibit identical branchiomotor neuron migration defect. The *tri*^{tk50f} allele carries a partial deletion in the coding sequence (Jessen et al., 2002) resulting in no transcription of *stbm*. The *tri*^{tc240a} allele carries a 39 base pair in-frame insertion resulting in 13 amino acid addition at Arg 21 of *Stbm*. The *tri*^{m209} allele contains a 13 base pair frameshift insertion in the C-terminus leading to the premature termination of translation at Ala 441.

2.2.2 Islet1-GFP transgenic line

The *islet1*-GFP transgenic line (Higashijima et. al., 2000) expresses green fluorescent protein (GFP) in all branchiomotor neurons (nV, nVII, nX), except the nIX motor neurons. We used this GFP transgenic line for assaying FBMN migration under fluorescent microscope and also for labeling branchiomotor neurons using GFP antibodies.

2.3 Probe and RNA Synthesis

2.3.1 Template DNA Preparation

Appropriate amount (~15 µg) of double stranded DNA is digested overnight at 37°C with a restriction enzyme that has a single site closely located downstream of the cDNA/Expressed Sequence Tags (ESTs) to create a linear DNA. To test if all the DNA is digested, a small amount of digested DNA could be run in the agarose gel (1%).

The digestion reaction is inactivated by incubating at 65° C for 10 minutes. Finally the digested DNA is purified by phenol chloroform extraction and ethanol precipitation. The precipitated DNA is washed with 70% ethanol and the pellet is resuspended in 20 µl of nuclease free water. The linearized DNA concentration is estimated using nanodrop spectrophotometer (ND-1000) and the quality of DNA can be visualized by running it in agarose gel. The template DNA is then suitable for preparing antisense probe for RNA insitu hybridization and full-length mRNA synthesis for injection.

2.3.2 Probe Synthesis

DIG (Digoxigenin) conjugated sense and antisense probes are prepared from appropriately linearized DNA templates using DIG RNA labeling kit (SP6/T7/T3, Roche Catalog # 11175025910). Briefly, 1 µg of linearized DNA is mixed with appropriate amounts of 10X transcription buffer, 10X hapten NTP mix, 25X RNasin, and 10X RNA Polymerase Mix (T3, T7, or Sp6), and brought to a final volume of 50 µl. Reactions are incubated in 37°C water bath for 2 hours. Probe RNA is then precipitated by adding 1 µl of 20 µg/µl glycogen, 5 µl of 0.2 M EDTA, 6.3 µl of 4M LiCl, and 190 µl of 100% ethanol, followed by overnight storage at -20°C. The next day, samples are microcentrifuged at 4°C for 20-30 minutes, washed with 70% ethanol, resuspended in 30 µl of nuclease-free ddH₂O. Probes are stored at -

20°C. Probes are run on an RNA agarose gel to assess quality of in vitro transcription.

2.3.3 mRNA Synthesis

Sense mRNA is synthesized using an appropriate Ambion Message Machine Kit (T7 or Sp6) as per manufacturer's recommendations. Briefly, 1 ug of linearized DNA template is incubated at 37°C with RNase-free water, 2X ribonucleotide mix, 10X transcription buffer and 10X RNA polymerase mix (T7 or Sp6), generating a final reaction volume of 20 µl. After 2 hours (3 hours for Sp6 RNAP) at 37°C, each tube receives 30 µl of nuclease-free ddH₂O and 30 µl of Lithium Chloride. To precipitate mRNA, samples are stored overnight at -20°C. The next day, samples are microcentrifuged for 20 minutes at 4°C, washed through 70% ethanol, and resuspended in 25 µl of nuclease-free ddH₂O. Messages are stored at -20°C. Yields and quality are determined by nano spectrophotometer and RNA gel electrophoresis.

2.3.4 RNA Gel Electrophoresis

Formaldehyde agarose gels are prepared for visualizing quality of synthesized RNA. Briefly, melt 1 gram of agarose in 84.8 ml of ddH₂O. Under the fume hood, add 5.2 ml of room-temperature 37% formaldehyde and swirl gently. Next, add 10 ml of 10X MOPS (0.2 M MOPS, 0.05 sodium acetate, 0.01 M EDTA, pH 7.0, stored at 4°C) and

swirl gently before casting gel. 1X MOPS buffer is used as running buffer. RNA samples are prepared by mixing 2ul of RNA, 1 ul of 1:10 diluted Ethidium bromide and 16 ul of 1.25X RNA loading buffer. RNA sample is then heated at 65⁰C for 10 min before loading in the gel. Smearred bands indicate a low quality synthesis while single clean band typically indicate a successful transcription reaction.

2.4 mRNA or Morpholino Injection

Zebrafish embryos are injected at 1 to 2 cell stage when the cells are syncytial, thereby the injected MO or mRNA can spread throughout the body. Embryos are lined up on glass slide trays, composed of two glass slides glued together, with the top slide cut in half. Embryos are orientated with animal layers pointing towards the injection needle. Pre-pulled microcapillary needles are loaded with either mRNA or morpholino depending on the experiment and then installed into a micro-manipulator. The micro-manipulator is connected to a gas-pressure pulse regulator that permits controlled pressure injections (~3-4 nl per embryos). Microcapillary needles must first be gently broken by smashing into the edge of the glass slide tray or using a micro-tweezer. Activated needles penetrate through the yolk for delivery of mRNA or morpholino either to the blastomere or the boundary between blastomere and yolk.

For overexpression studies, micro-inject embryos at the one to

eight cell stages. Micro-injection trays are made by cutting a glass slide in half and gluing it to the center of another slide. This provides a straight edge against which to line embryos prior to injection. Embryos (in their chorions) should be placed on the makeshift tray, animal pole facing the right edge of the cut slide with enough E3 to cover the embryos. Micro-injection is performed using borosilicate capillary tubes with or without filament (Stoelting Inc) pulled on a pipette puller to form micro-injection needles. The micro-injection needles can be loaded with the appropriate reagent (DNA, RNA, lineage-tracer, etc.) by capillary action (with filament) or with a pipette equipped with a tip for loading micropipettes (no filament). The micro-injection needle is fitted to a micro-manipulator and used to pressure inject the reagent into embryos (~4 nl/embryo). The tip of the micro-injection needle can be broken by gently touching it against the side of the broken slide against which the embryos are lined up. Embryos should be micro-injected directly into the blastomere (one cell stage) or the margin of the yolk and dividing blastomeres (two to eight cell stages).

2.5 In Situ Hybridization

Whole mount in situ hybridization is carried out on embryos fixed in 4% paraformaldehyde for at least 12 h (typically overnight) at 4°C and dehydrated in 100% methanol (Fisher) for at least 5 h (typically overnight) at -20°C. All steps are carried out at room temperature unless otherwise noted. Embryos are rehydrated in a

series of PBST/MeOH washes as follows: 1X5 min. in 50% MeOH/50% PBST, 1X5 min. in 30% MeOH/70% PBST, then 2X5 min. in PBST. Following a 30 min. room temperature fixation in 4% paraformaldehyde, wash embryos 3X5 min. in PBST, then treat with proteinase K (Sigma; 23mg/ml diluted to 10 $\mu\text{g}/\mu\text{l}$) for 5 to 20 min., depending on the age of the embryo. Wash 2X5 min. in PBST and fix for one hour. Wash embryos 3X5 min in PBST and 1X10 min in 50%PBST/50% hybridization buffer and incubate in hybridization buffer for at least two hours at 70°C. Incubate embryos overnight in ~100ng probe (1:100 dilution of stock probe in hybridization buffer) at 70°C.

Following the overnight incubation, remove used probe and save at -20°C if valuable (probes can be re-used 2-3 times without affecting the efficiency of the signal produced). Wash embryos at 70°C for 1 h in fresh hybridization buffer, then wash 2X30 min. in wash A, 1X30 min. in wash B and 2X30 min. in wash C, all at 70°C. Wash 1X10 min. at room temperature in 50% wash C/50% Maleic Acid Buffer + 0.1% (v/v) Tween20, 2X10 min. in Maleic Acid Buffer + 0.1% (v/v) Tween20, 1X10 min. in blocking solution. Incubate embryos for three hours in blocking solution and then overnight in anti-digoxigenin or anti-fluorescein, alkaline phosphatase-conjugated antibody (Fab; Boehringer Mannheim/Roche), diluted 1:5000 in blocking solution. Wash 8X15 min. in Maleic Acid Buffer + 0.1% (v/v) Tween20, then 3X10 min. in TMNT. Incubate embryos in the dark in TMNT + 0.45%

(v/v) NBT, 0.35% (v/v) BCIP(Vector) for blue chromagenic reaction and in 0.4mg/ml Naphthol in 1 M Tris HCl, pH7.4 (Fast Red,Sigma) until the color develops satisfactorily. The color reaction should be stopped by washing embryos 3X5 min. in 1XPBS. Fix embryos overnight in 4% paraformaldehyde at 4°C, then transfer to 70% glycerol, deyolk with pins, and mount on slides for analysis.

2.6 Immunohistochemistry

Primary antibodies used are as follows: for the visualization of hindbrain motor neurons, Islet1/2 (39.4D5), 1:500 (Korzh et al., 1993) (Developmental Studies Hybridoma Bank, DSHB); axonal morphology was analyzed using anti-acetylated tubulin, 1:500 (Chitnis and Kuwada, 1990) (Sigma); Mauthner reticulospinal neurons, 3A10, 1:500 (Hatta, 1992) (DSHB); commissural neurons, zn5, 1:10 (Trevarrow et al., 1990); noradrenergic locus coeruleus neurons, anti-tyrosine hydroxylase (anti-TH), 1:500 (Guo et al., 1999) (Chemicon). Secondary antibodies (1:250) were conjugated to biotin (Vector Labs) or rhodamine (Molecular Probes) and were all anti-mouse, except anti-TH which was raised in rabbit. All biotin-conjugated antibody experiments were performed using Vectastain Elite Kit (Vector Labs). For rabbit antibody, the rabbit kit was used initially. More recently, a universal mouse/rabbit kit that has the same secondary antibody

(1:250) to recognize primary antibodies generated in mouse or rabbit has worked very efficiently.

2.6.1 Antibody Labeling

Whole mount immunohistochemistry was carried out on embryos fixed in 4% paraformaldehyde for at least 12 h (typically overnight) at 4°C, to visualize numerous neuronal populations in the zebrafish hindbrain. All steps in this procedure are carried out at room temperature. Wash embryos 4X30 min. in incubation buffer (IB), incubate 1X30 min. in IB + 1% (v/v) horse serum (HS) (Sigma) and incubate overnight in primary antibody raised in either rabbit or mouse diluted in IB+HS. Next, wash embryos 2X30 min. in IB and then 1X30 min. in IB+HS. Incubate embryos 8h in secondary antibody (Vectastain) diluted 1:250 in IB+HS. Next, wash embryos 3X30 min. in IB. During the third wash, mix the avidin-biotin color development (A/B) solution as follows: 1% (v/v) reagent A, 1% (v/v) reagent B (Vectastain) in IB, and allow to sit for 30 min. Incubate embryos in the A/B solution overnight. On day three, wash the embryos at least 8X15 min. in IB. Incubate the embryos in 0.5 mg/ml diaminobenzidine (DAB) (Sigma) in 1XPBS + 1% (v/v) DMSO for 15 min. before starting the peroxidase color reaction with the addition of 0.1 volume, 0.03% hydrogen peroxide (Fisher). Upon satisfactory staining, the color reaction should be stopped by replacing the DAB solution with ice-cold

1XPBS + 0.1% (v/v) Sodium Azide (Sigma) and washing the embryos 3X5 min. with 1XPBS. Fix immunostained whole-mount embryos overnight in 4% paraformaldehyde and store at 4°C. Embryos should then be transferred to 70% glycerol, deyolked using pins and mounted on slides dorsally or laterally for analysis.

2.6.2 Fluorescent Antibody Labeling

Whole mount immunohistochemistry is carried out on embryos fixed in 4% paraformaldehyde for at least 12h at 4°C, to visualize numerous neuronal populations in the zebrafish hindbrain. All steps in this procedure are performed at room temperature. Wash embryos 4X30 min. in incubation buffer (IB), then 1X30 min. in IB + 1% horse serum (HS) (Sigma) and incubate overnight in primary antibody raised in either rabbit or mouse diluted in IB+HS. Next, wash embryos 2X30 min. in IB and then 1X30 min in IB+HS. Incubate embryos in the dark (the tubes can be covered with aluminum foil to block the embryos from becoming exposed to light) for 8-12 h in fluorescent secondary antibody (Molecular Probes) diluted in 1:500 in IB+HS. Rinse 3X5 min. in PBS and fix overnight in 4% paraformaldehyde. Transfer embryos to PBS and put through a glycerol series (25%, 50%, then 70% glycerol) right before mounting on slides and taking images. It is important to store the embryos in dark in order to avoid fading of the

fluorescent signals.

2.7 Genetic Mosaic Analysis

Transplantation studies were done using standard published protocols. Details of the protocol can be found in the previous dissertation from the lab (Bingham,S., 2004). Targeted transplantation to mesoderm and endoderm were done using *tar* RNA and the details are explained in chapter three with a schematic (Figure 3.4).

2.8 The FBMN migration index - A sensitive measure of neuronal migration in a population of embryos

To assay the ability of *Stbm* (or other) constructs to regulate CE cell movements and FBMN migration, we separate a collection of embryos into two groups for CE phenotypes at the 8-15 somite stage (wild-type and morphants; Figure 3.2 E, 4.3, 4.4, 4.5), and three groups for FBMN migration phenotypes at 36 hpf (wild-type, mutant and mixed; Figure 3.2 E, 4.3, 4.4, 4.5). The CE and FBMN migration indices are weighted averages of the distribution of embryos between the different phenotypic classes. For example, FBMN migration index = $[(N_0 \cdot 0) + (N_{0.5} \cdot 0.5) + (N_1 \cdot 1)]$ divided by $(N_0 + N_{0.5} + N_1 = \text{total number of embryos})$. For a completely wild-type collection, the index equals 1.0, and for a completely mutant population (where each embryo exhibits total loss of FBMN migration), the index equals 0. The CE movement

index is similarly calculated. Together, these indices provide sensitive measures for the status of CE and FBMN movements in a collection of embryos, as demonstrated below.

2.9 Imaging of Embryos

Mount embryos dorsally on slides in 70% glycerol (fixed) or embed in 1% agarose (live). Antibody and in situ-labeled embryos can be imaged on an Olympus BX60 microscope equipped with shutters for fluorescence and bright-field imaging. In addition, confocal images can be acquired of islet1GFP-transgenic embryos and/or rhodamine-conjugated antibody-labeled embryos using an Olympus IX70 microscope equipped with a BioRad Radiance 2000 confocal imaging laser system (Molecular Cytology Core, University of Missouri-Columbia).

2.10 Western Blotting

2.10.1 Protein Isolation

Dechorionate 10 embryos at appropriate stages and transfer them to a 1.5 ml tube. Homogenize the embryos in 100 μ l of $\frac{1}{2}$ Ginzburg Fish Ringer solution (55 mM NaCl, 1.8 mM KCl, 1.25 mM NaHCO₃) with 7x protease inhibitor cocktail mix. Spin the homogenized sample in refrigerated centrifuge for 30 sec at 300 g. Discard the supernatant and store the pellet which contains the zebrafish embryo

protein with minimal yolk. The entire procedure is done in ice in order to avoid protein denaturation. If large amounts of protein are required, several tubes of 10 embryos each can be made and stored at -80°C . Protein extracted from 10 embryos is usually loaded in one lane for the western blotting experiments.

2.10.2 Protein Preparation and SDS-PAGE

Stored protein samples are diluted with equal volume of Laemmli buffer (Biorad) and boiled for 10 minutes in a water bath. Then they are loaded into 12% SDS-PAGE gels and run at 200V for 45 minutes. The gels were prepared using standard protocols (Sambrook et al., 1989).

2.10.3 Transfer of Proteins to Nitrocellulose Membrane and Western Blotting

Transfer of proteins – Equilibrate SDS-PAGE in 1x transfer buffer for 5 minutes with shaking. Assemble transfer sandwich in Mini Protean III system with Bio-Ice cooling unit, magnet, and cold 1x transfer buffer (Bio-Rad Mini-trans blot manual). Run at 100V for 1 hour. Disassemble the sandwich and proceed to western blotting.

Hybridization – Block with 5% milk-PBST for 12 hours at room temperature with shaking. Rinse with 0.5% milk-PBST twice for 5

minutes each. Incubate with primary antibody in 0.5% milk-PBST for 12 hours at room temperature with shaking. Rinse with 0.5% milk-PBST twice for 5 minutes each. Incubate with secondary antibody in 0.5% milk-PBST for 12 hours at room temperature with shaking. Wash in 0.5% milk-PBST twice at room temperature for 15 minutes each.

Detection – Gather film, film cassette, plastic wrap, scissors, ECL western blotting detection reagents (Pierce biotechnology), pipette aid, pipettes (2 per membrane), 15 ml falcon tubes., paper towels, tweezers, timer and membrane (in final wash). Turn on developer and check for fixer and developer levels. Blot dry membrane by placing face up on a paper towel. Place membrane face up on plastic wrap. Mix equal amounts of ECL solution 1 and 2 to give a final volume of 0.125 ml/cm³ of membrane. Add ECL solution and let stand for 1 minute without agitation. Blot dry membrane by placing face up on a paper towel. Place membrane in cassette and cover with plastic wrap. Turn off lights. Fold upper-right hand corner of a piece of film and place over membrane, close cassette. Initially expose for desired time, usually 2-5 minutes, and develop. Repeat as necessary to achieve desired signal strength.

2.11 Cell Death Detection Using Acridine Orange

Cellular Degeneration in live embryos can be detected using Acridine orange (3,6-dimethylaminoacridine) which fluoresces green (FITC channel) when bound to double stranded DNA. Live dechorionated embryos were treated with acridine orange (2 mg/ml in PBS pH 7.1) in a petri dish for 1 hour. These embryos were then washed couple of times with PBS and embedded in methyl cellulose in a depression slide and viewed using an Olympus BX-60 microscope equipped with FITC filter.

2.12 Common Reagents and Solutions

Common solutions used in immunohistochemistry and in situ hybridization are prepared based on the recipes available elsewhere (Vanderlaan, G. 2006). Solutions used in western blotting and protein isolation are listed below.

½ Ginzburg Fish Ringer Solution – For Protein Isolation

55 mM NaCl

1.8 mM KCl

1.25 mM NaHCO₃

Tris-glycine electrophoresis buffer

25 mM Tris

250 mM Glycine (pH 8.3)

0.1% SDS

5X Stock

15.1 g Tris

94 g Glycine

900 ml deionized water

50 ml of 10% (w/v) SDS

Adjust volume to 1000 ml

30% Acrylamide/Bis Solution

Bio-Rad Laboratories. (Catalog # 161-0156)

Ammonium Persulfate

Bio-rad Laboratories. (Catalog # 161-0700)

10% (w/v) Solution is prepared in deionized water.

TEMED

Bio-rad Laboratories. (Catalog # 161-0800)

1.5 M Tris (pH 8.8) in deionized water – For making resolving gel

1.0 M Tris (pH 6.8) in deionized water– For making stacking gel

Transfer Buffer

To Make 1 liter (pH 8.3)

39 mM Glycine

2.9 g Glycine

48 mM Tris

5.8 g Tris

0.037% SDS

0.37 g SDS

20% Methanol

200 ml Methanol

Detection System

PIERCE ECL Western Blotting Substrate (Catalog # 32209)

CHAPTER THREE

***Stbm* function is required in the floorplate and neuroepithelial cells to mediate the migration of facial motor neurons in zebrafish hindbrain**

Unpublished: Sittaramane, V., Glasco, DM., Li, S., Matisse, M., and Chandrasekhar, A., (2008). (Manuscript in preparation).

3.1 Introduction

Development of the nervous system is a complex process which involves various cellular processes including migration of immature neurons from the proliferative zones to their final position which enable them to be a part of functional circuits. Disturbances in the neuronal migration may lead to severe anatomic anomalies interfering with normal functions of these neurons. While the cortical neurons in the neocortex are a major group of neurons that migrate, there are other neurons in the hindbrain that undergo migrations.

Facial Branchiomotor Neurons (FBMNs) are a subset of branchiomotor neurons which are born in rhombomere 4 (r4) of the hindbrain and undergo a characteristic caudal migration within the ventral neural tube to r6 and r7 in several vertebrates (Studer et al., 1996; Chandrasekhar, 2004). Recent studies have identified several

molecules that are necessary for the migration of FBMNs and lot of these modulates the Wingless/Planar cell polarity (Wnt/PCP) signaling either directly or indirectly. Wnt/PCP signaling regulates the convergent extension (CE) movements of gastrulation and more importantly establishes the anterior-posterior polarity of neural progenitors and facilitate neural tube formation (Ciruna et al., 2006). Loss of function of some of the key components of Wnt/PCP pathway like Strabismus (*stbm*) (Bingham et al., 2002; Jessen et al., 2002), Prickle1 (*pk1a*) (Carreira-Barbosa et al., 2003), Scribble1 (*scrb1*) (Wada et al., 2005) and Frizzled3a (*fz3a*), *Celsr1a*, *1b* and *Celsr2* (Wada et al., 2006) leads to elimination of FBMN migration in zebrafish. Importantly, *stbm* has been shown to genetically interact with *pk1a* (Carriera-Barbosa et al., 2003) and *scrb1* (Wada et al., 2005) in regulating neuronal migration indicating that these molecules are functioning together. However, disruption of the function of other major components of Wnt/PCP like Wnt11, Wnt5a, Glypican/knypek and Dishevelled do not affect the migration of FBMNs (Bingham et al., 2002; Jessen et al., 2002). Further, zebrafish *Stbm*, *Pk1a*, *Fz3a*, *Celsr1* and *2* and *Scrb1* functions non-cell autonomously (in different cell types like neuroepithelium and mesoderm) during FBMN migration (Jessen et al., 2002; Carriera-Barbosa et al., 2003; Wada et al., 2005, 2006), whereas existing models suggest cell autonomous roles for these molecules during convergent extension and gastrulation events. These results strongly

hint a possible Wnt/PCP independent mechanism involved in mediating FBMN migration. Nevertheless, the cellular and genetic machinery involved in this Wnt/PCP independent regulation of FBMN migration is largely unknown.

Recent studies have shown that zebrafish *fz3a* and *celsr2* functions in the surrounding neuroepithelial cells and mediate the FBMN migration by preventing the integration of FBMNs into the neuroepithelial layer (Wada et al., 2006). However, the cell-types where *stbm* function is required during neuronal migration is not clear. Though *tri/stbm* has been shown to be necessary for re-integration of daughter cells into neuroepithelial layer (Ciruna et al., 2006), the function of *stbm* during FBMN migration remains to be studied. While *stbm* is expressed ubiquitously in the hindbrain, *pk1a* has a more specific expression along the path of neuronal migration (Carriera-Barbosa et al., 2003). In this study, we show an overlapping expression pattern for *stbm* and *pk1a* in mesoderm and endoderm, raising an interesting possibility of them functioning together in either mesoderm or endoderm to mediate neuronal migration. We show that endoderm is not necessary for FBMN migration by depleting the endodermal tissue using *sox32/Casanova* morpholino (MO), which interrupts the nodal signaling responsible for endoderm formation. Genetic mosaic analyses revealed that *stbm* is required within the neural tube especially in the floorplate neuroepithelial cells to mediate FBMN migration.

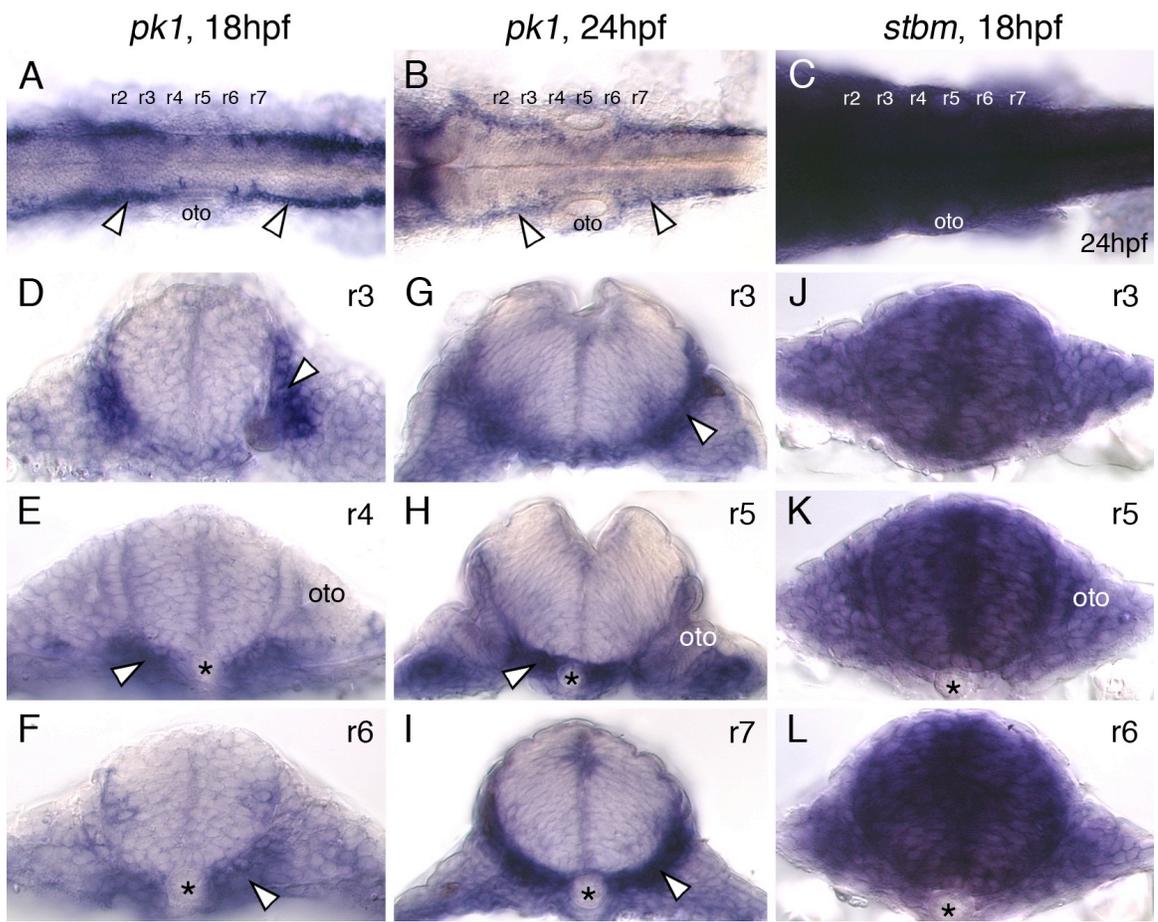


Figure 3.1 *stbm* and *pk1a* expression overlaps in mesoderm and endoderm. A-C show dorsal view of the hindbrain of zebrafish with anterior to the left. Oto, denotes otic vesicle. D-L shows the cross section of the hindbrain of zebrafish at different rhombomere levels. RNA in situ hybridization of *pk1a* probe show the expression of *pk1a* in lateral edges of rhombomere (arrowheads) at 18hpf and 24 hpf embryos respectively. Cross section of in situ stained embryos reveals the expression of *pk1a* specifically in mesoderm (white arrowheads) and endoderm (black arrowheads) at the level of r3 (D and G), r4 (E), r5 (H), r6 (F) and r7 (I) in 18 and 24 hpf embryos. *Stbm* is expressed ubiquitously within the hindbrain (C) at 24 hpf. Cross sections of in situ stained embryos reveal that *stbm* is expressed uniformly within the neural tube, mesoderm and endoderm (J, K and L). *star* denotes notochord.

3.2 Results

3.2.1 *stbm* and *pk1a* expression overlaps in endoderm and mesoderm

Previous studies have shown the *stbm* function is primarily required non-cell autonomously for FBMN migration (Jessen et al., 2002) and *pk1a* expression is not detected in the migrating FBMNs (Carreira-Barbosa et al., 2003; Veeman et al., 2002) suggesting a non-cell autonomous role for *pk1a* also. Given that *stbm* and *pk1a* are genetically interacting, it is possible that they are functioning within the same cell to regulate FBMN migration. To examine this hypothesis, we first verified the known expression pattern of *stbm* and *pk1a*. While *stbm* is expressed ubiquitously throughout development (Park and Moon, 2002), *pk1a* is expressed more in the lateral regions of the developing rhombomeres and also appears to be expressed at very low levels in the FBMN migratory pathway (Carreira-Barbosa et al., 2003). Detailed analyses of the expression pattern by cross-sectioning the embryos at different rhombomere and tissue levels (Figure 3.1). In-situ hybridization with *stbm* and cross-sectioning at different rhombomere levels especially r3 (Figure 3.1J), r4 (not shown), r5 (Figure 3.1K) and r6 (Figure 3.1L) reveal that *stbm* is expressed strongly and broadly (Figure 1C) both within the developing neural tube and outside in the mesoderm and endoderm excluding the notochord. However, *pk1a* expression during the period of FBMN migration at 18 hours post-

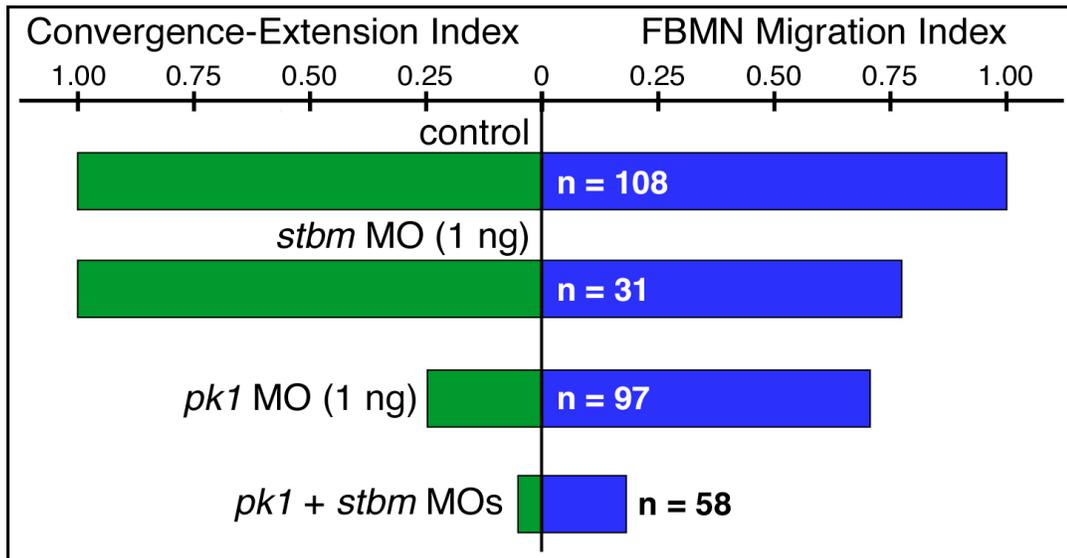
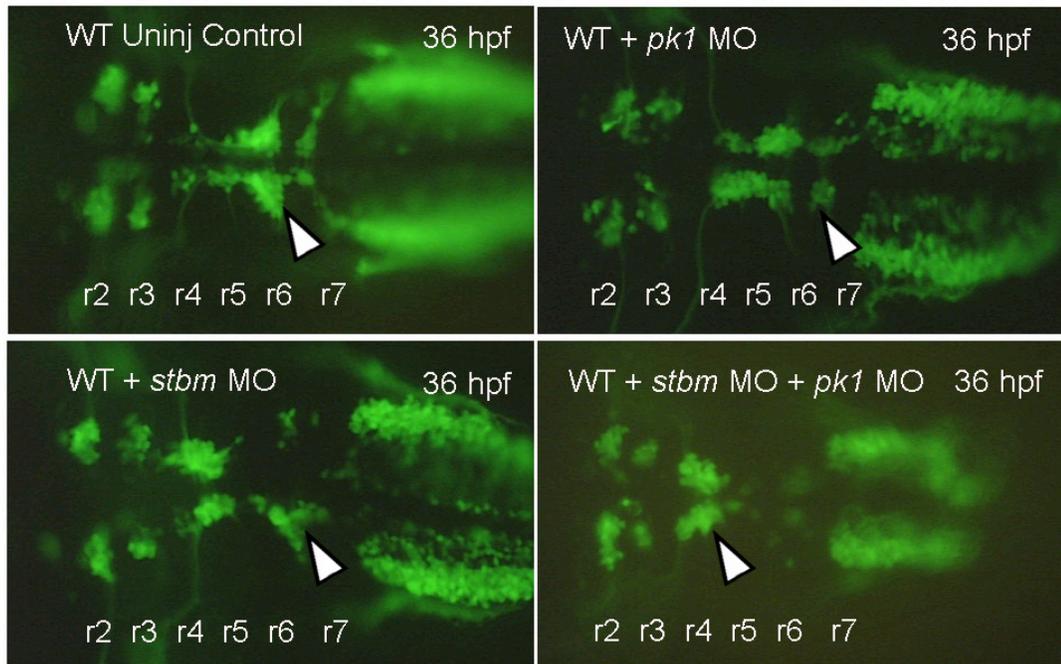


Figure 3.2 *stbm* and *pk1a* genetically interact to mediate FBMN migration. A-D are dorsal views of hindbrain showing branchiomotor neurons in a *isl1:gfp* embryos 36 hpf with anterior to the left. Sub-optimal doses of *pk1a* MO (1ng) (B) and *stbm* MO (1ng) (C) produce an intermediate phenotype in the FBMN migration, when compared to wild-type un-injected embryos (A). Co-injection of sub-optimal doses of *stbm* and *pk1a* MO leads to complete defect in FBMN migration (D). E, shows the quantitative data of the genetic interactions between *stbm* and *pk1a* with Convergent extension and FBMN migration index.

fertilization (hpf) and 24 hpf is predominantly found in the mesodermal and endodermal tissue outside the neural tube. Dorsal views and cross-sectioning at the different rhombomere levels show that *pk1a* is expressed laterally in the mesoderm upto r3 (Figure 3.1A, B, D and G), and while in r4 and r5 (Figure 3.1E and H) it is expressed strongly in ventral mesoderm and expands more laterally from r6 (Figure 3.1F and I). This study strongly indicates that *pk1a* is expressed mainly in the mesoderm and endoderm tissue outside the neural tube across different rhombomere levels, although a very low level of expression within the neural tube cannot be excluded. Nevertheless, *pk1a* and *stbm* expression still overlaps in the mesoderm and endoderm tissues during the period of FBMN migration, suggesting that they could be functioning outside the neural tube to regulate FBMN migration in the ventral neural tube within 1-2 cell diameters.

3.2.2 *stbm* and *pk1a* genetically interact to regulate FBMN migration

stbm and *pk1a* are crucial members of Wnt/PCP pathway and they genetically interact during CE movements (Carreira-Barbosa et al., 2003; Veeman et al., 2003). In addition, both *stbm* and *pk1a* are necessary for FBMN migration (Jessen et al., 2002; Carreira-Barbosa et al., 2003). Since, CE movements are governed by genetic interaction between *stbm* and *pk1a*, it is only rational to test whether these two

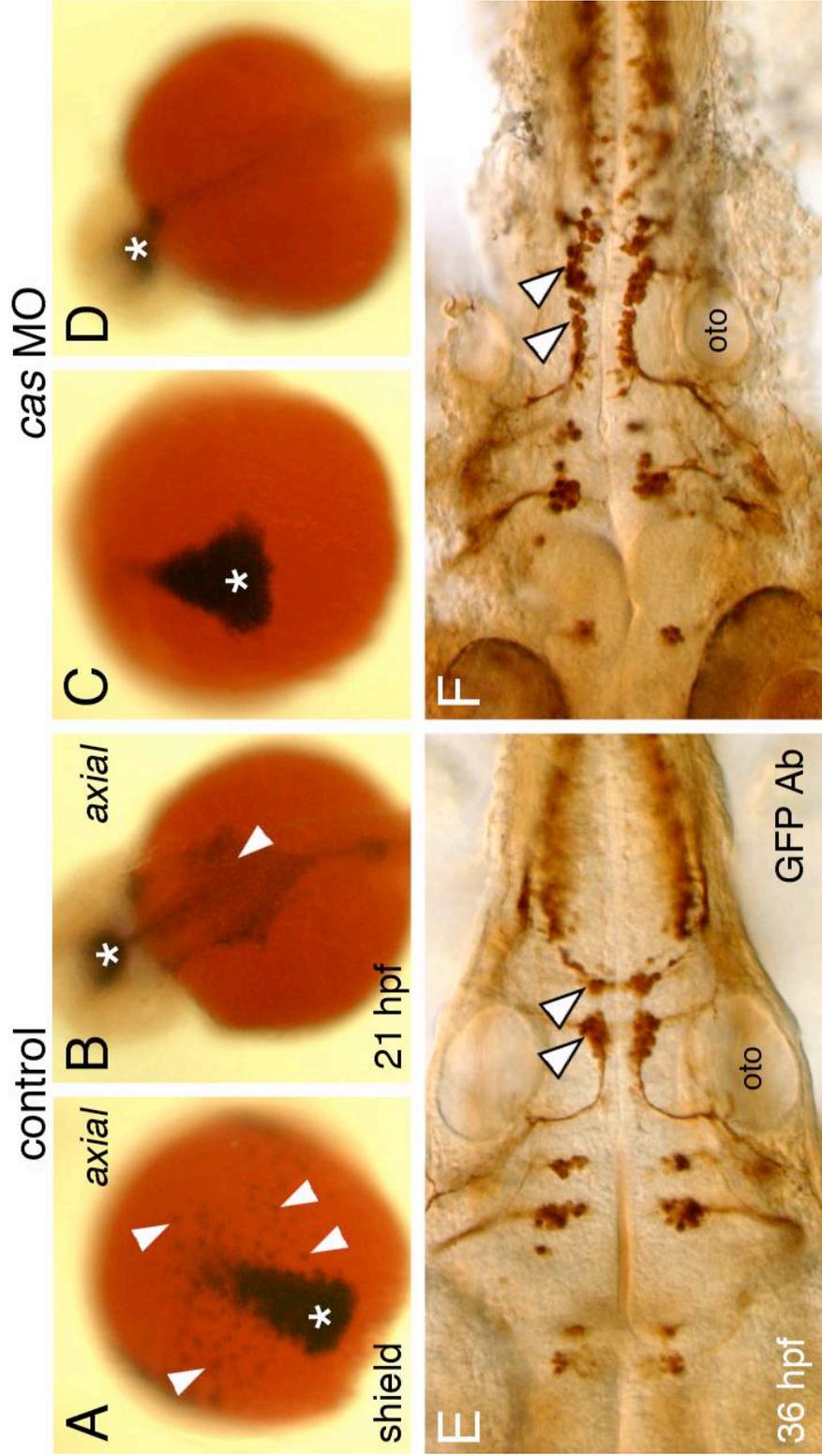


Figure 3.3 Endoderm is not required for FBMN

migration. A-D are embryos stained with axial, endoderm and mesoderm precursor marker. E and F are dorsal views of *Isl1::gfp* embryos stained with GFP antibody. Injection of *cas (sox32)* MO leads to depletion of endodermal precursors at shield stage (C) and 21 hpf (D) when compared to un-injected embryos (A and B). FBMN migration is not affected in endoderm depleted embryos (F) when compared to un-injected wild-type embryos (E).

genes genetically interact to regulate FBMN migration. Injection of sub-optimal dose of *pk1a* MO produced FBMN migration defect in *tri*^{m209} heterozygous embryos demonstrating a genetic interaction between *pk1a* and *stbm* (Carreira-Barbosa et al., 2003). However, *tri*^{m209} allele is known to generate a haplo-insufficient phenotype (L.Sonica-Krezel, Personal Communication). Indeed, *tri*^{m209} heterozygotes themselves exhibit defects in FBMN migration (unpublished data), potentially confounding the conclusions of Carreira-Barbosa et al. (2003). To clarify this issue, we examined their genetic interaction in the wild-type embryos by co-injecting sub-optimal doses of both *stbm* and *pk1a* MOs into 1-cell stage embryos obtained from wild-type, *Tg(isl1:gfp)* fish. If we decide to do this, we would be looking at migration defect in a population rather than at individual embryos, so we devised a measure to calculate the phenotype index. According to this method, we assign an index value for each classified phenotype namely normal wild-type like convergent extension would have a value of 1 (Figure 3.2A), defective convergent extension like *tri*^{-/-} would have 0 (Figure 3.2B) and likewise normal FBMN migration is 1 (Figure 3.2C), intermediate FBMN migration (where some FBMNs migrate to r6 and r7) is 0.5 (Figure 3.2B) and defective FBMN migration like *tri*^{-/-} is 0 (Figure 3.2C). Then, we calculate the weighted average for every population to assign an index value for FBMN migration. For example, in embryos injected with *stbm* MO (1 ng), the phenotypic index for CE is 1 and FBMN is 0.75

(Figure 3.3C and E), meaning that this dose of *stbm* MO does not affect the CE movements, but it mildly affects the FBMN migration. In *pk1a* MO (1 ng) injected embryos, the phenotypic index for CE is 0.25 and FBMN is 0.7 (Figure 3.3B and E), meaning that this dose of *pk1a* MO produces a strong CE defect but, a mild FBMN migration defect. However, when both *stbm* MO (1 ng) and *pk1a* MO (1 ng) are injected, the CE movements and FBMN migration are more severely affected bringing their phenotypic index values to less than 0.1 and 0.2 respectively (Figure 3.3D and E). These result, indicate a strong genetic interaction between *stbm* and *pk1a* during FBMN migration. Since, *stbm* and *pk1a* also have an overlapping expression in mesoderm and endoderm, we examined whether *stbm* is required in the endoderm or mesoderm to regulate neuronal migration.

3.2.3 Endoderm is not required for normal migration of FBMNs

To test whether endoderm is necessary for FBMN migration, we generated embryos lacking endoderm by injecting *casanova* (*cas/sox32*) MO (Holzschuh et al., 2005) into wild-type, *Tg(isl1:gfp)* embryos. Cas (Sox32) is a transcription factor that is essential for endoderm specification (Sakaguchi et al., 2001; Kikuchi et al., 2001). In *cas* MO-injected embryos (n=30), endoderm tissues fail to specify,

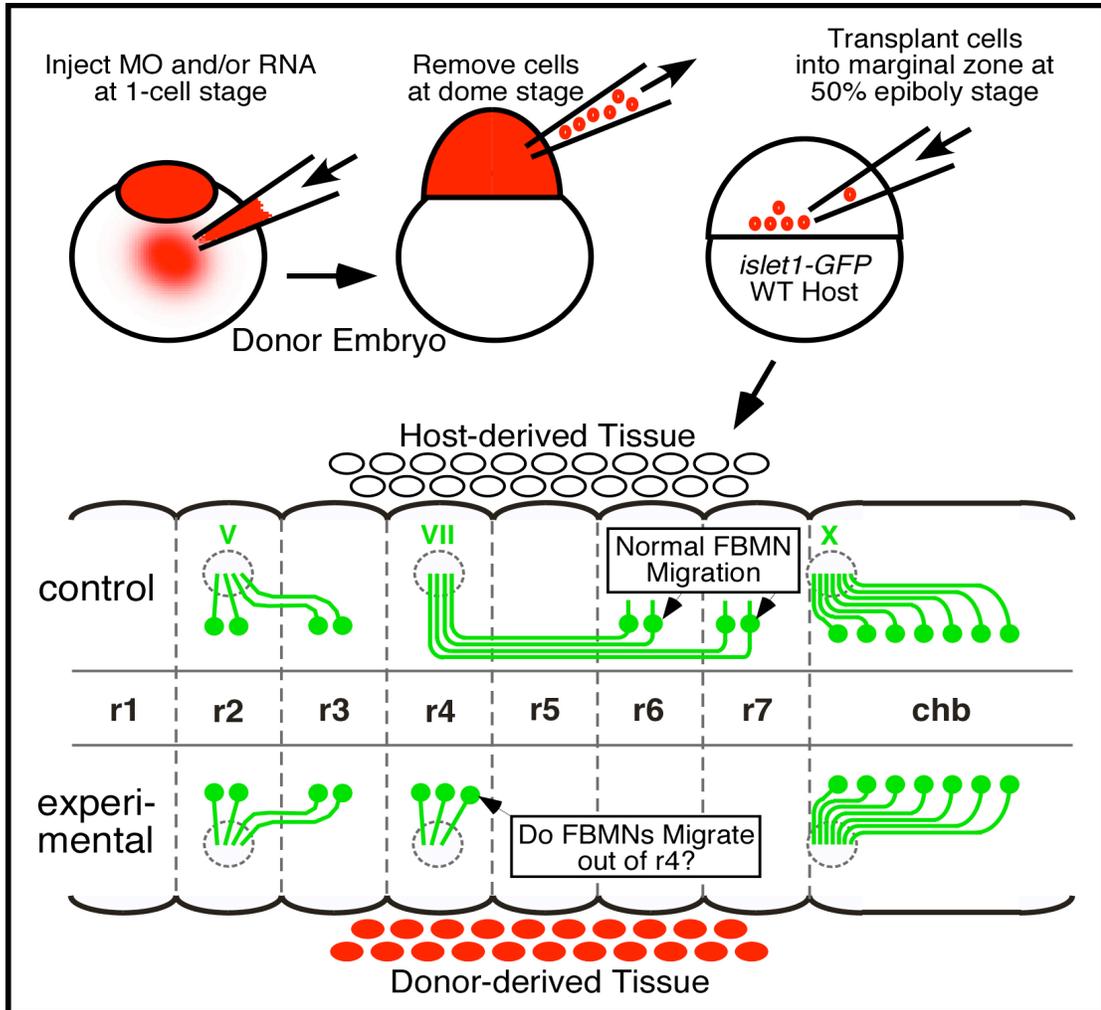
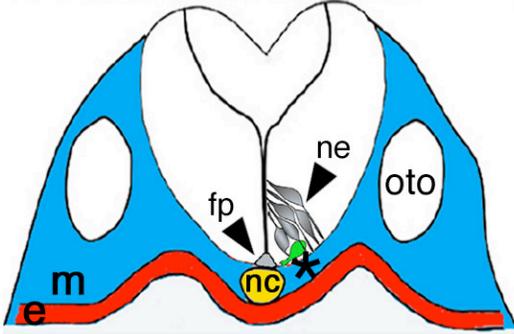
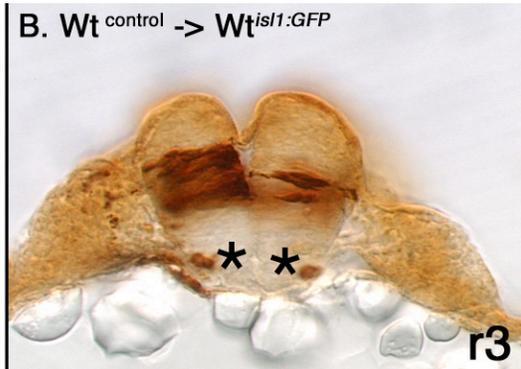


Figure 3.4 Schematic representation of the transplantation experiments Cells from donor embryos injected with *tar* RNA and are transplanted into the marginal zone of host embryos at 50% epiboly stage. Mesoderm on the transplanted side is predominantly formed from the donor derived cells.

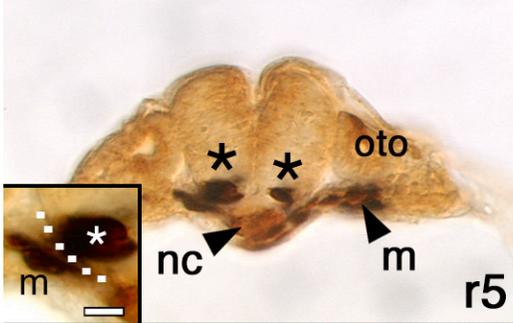
A. Schematic CS-Hindbrain



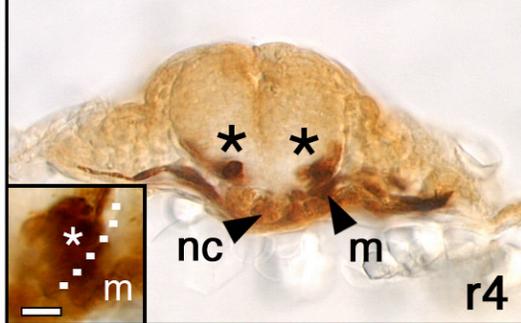
B. $Wt^{control} \rightarrow Wt^{isl1:GFP}$



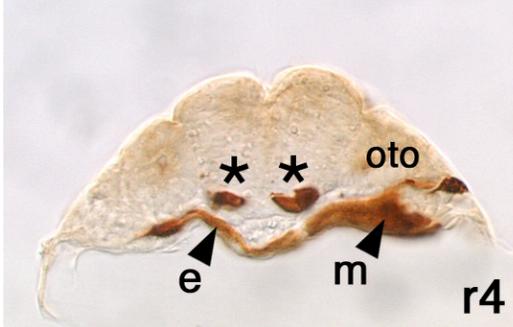
C. $Wt^{TAR RNA (low)} \rightarrow Wt^{isl1:GFP}$



D. $Wt^{TAR RNA (low)} \rightarrow Wt^{isl1:GFP}$



E. $Wt^{TAR RNA (high)} \rightarrow Wt^{isl1:GFP}$



F. $Wt^{TAR RNA (high)} \rightarrow Wt^{isl1:GFP}$

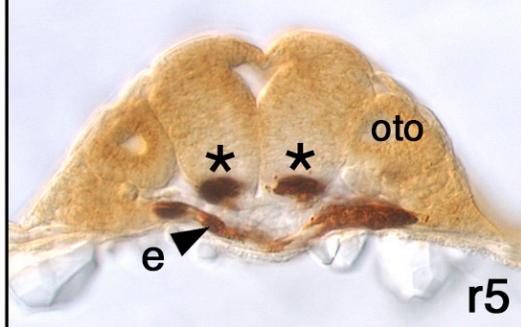


Figure 3.5 Targeted transplantation of donor cells into mesoderm and endoderm of host embryos using *tar* RNA.

All images are cross sections of transplanted zebrafish hindbrain stained with GFP antibody. Donor cells in the host embryos have biotinylated dextran and are stained during a normal antibody staining using ABC kit. Schematic of a cross section of hindbrain shows tissues of different germ layers (A), neural tube (white), mesoderm (m, blue), endoderm (e, red), notochord (nc, yellow), neuroepithelial cells (ne) and floorplate (fp) in the neural tube (black) and migrating FBMNs (green). Wild-type donor cells with no *tar* RNA are not targeted to any particular tissue and can be found inside in the neural tube (B). However, donor cells having low concentrations of *tar* RNA can be targeted efficiently to mesoderm (C and D), while donor cells with high concentrations of *tar* RNA are targeted to endoderm (E and F). Subsets in C and D show the close apposition of donor derived mesoderm and host FBMNs within the hindbrain. Stars point to motor neurons inside the neural tube.

which is shown by using an endoderm specific marker axial (Figure 3.4A, B, C and D). In *cas* MO-injected embryos, FBMN migration was largely unaffected even though axial-expressing endodermal cells were missing (Figure 3.4E and F). These results indicate that endodermal expression of *pk1a* and *stbm* is not required for FBMN migration, implicating that mesodermal expression of these genes may play a role in neuronal migration.

3.2.4 Mesodermal *stbm* is not required for FBMN migration

First, we hypothesized that *stbm* could be functioning in the mesoderm as shown in the schematic (Figure 3.6A). To test this hypothesis, we examined whether knocking down *stbm* function in the mesoderm can eliminate FBMN migration and also whether *stbm* expression in the mesoderm is sufficient to rescue FBMN migration in the *stbm* morphant embryos. We knocked down *stbm* function in the mesoderm in two steps as shown in schematic (Figure 3.5). First, wild-type, non-transgenic embryos were injected at the 1-cell stage with full-length TARAM-A^d (*TAR*) mRNA and *stbm* MO along with a lineage tracer (Biotinylated rhodamine dextran, Molecular Probes). After 3 hours, at the early blastula stage, cells were removed from these embryos and transplanted into wild-type host, *Tg(isl1:gfp)* blastulae at 50% epiboly stage near the margin. TARAM-A^d

(*TAR*) mRNA encodes a constitutively active activin type I receptor that cell autonomously drives cells into the mesodermal fate in host embryos (Thisse and Thisse, 1999; Figure 3.6). At high doses (200 pg RNA per embryo), TARAM-A^d drives mesoderm and endoderm formation (Figure 3.6E and F), but primarily induces mesoderm at lower doses (Figure 3.6C and D) (50 pg RNA per embryo), and the donor derived cells contribute to a significant fraction of the cranial mesoderm in the host embryos (Figure 3.6). Since the transplanted embryos also contain *stbm* MO, the function of *stbm* in donor-derived mesodermal cells were knocked down, as shown previously to knock down BMP function in the endoderm (Holzschuh et al., 2005). Since cells are transplanted on only side of the presumptive dorsal organizer (shield), donor-derived cells typically contribute to mesoderm on only one side of the embryo (Figure 3.6), providing an internal control for the manipulation and its effects on FBMN migration. The embryos were examined at 24-30 hpf under fluorescent microscope to determine whether GFP-expressing host-derived FBMNs migrate normally out of r4 when the rhodamine dextran-labeled, donor-derived cells were present in the mesoderm. Embryos were fixed, and processed for immunostaining with anti-GFP antibody and biotin-streptavidin alkaline phosphatase chemistry to simultaneously visualize donor-derived cells outside the neural tube and GFP-expressing host motor neurons (Figure 3.6). As needed, embryos were embedded in agarose, and

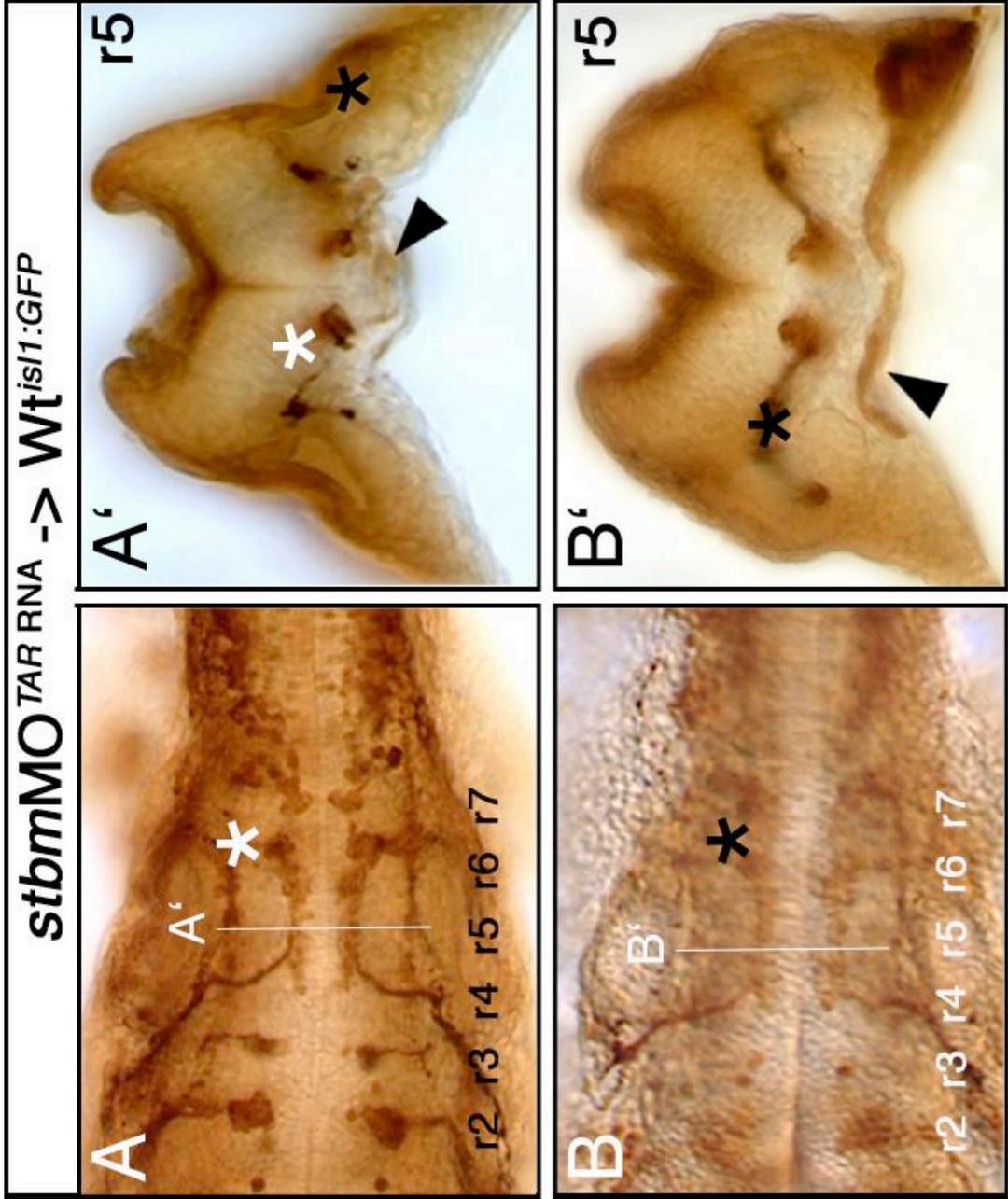


Figure 3.6 *stbm* deficient cells in mesoderm and endoderm do not affect FBMN migration in wild-type embryo. A and B are dorsal view of hindbrain of zebrafish embryos stained with GFP antibody. A' and B' are cross section of embryos in A and B respectively. FBMNs migrate normally in a wild-type embryo (A and B) with *stbm* deficient cells in the mesoderm (A') and endoderm (B'). *Star* points to migrating FBMNs

sectioned (100 micron thickness) on a vibratome (Figure 3.6). We first show that this technique is effective in targeting donor cells to the mesoderm and endoderm of host embryos (Figure 3.6). In three independent experiments, nearly 100% of host embryos contained donor-derived cells in the mesoderm, endoderm or both (39/40). We could reliably and rapidly identify embryos with contributions to the cranial mesoderm because these embryos also contained donor-derived muscle fibers and notochord cells in the trunk (18/40 embryos). Embryos with donor-derived endoderm were identified by the presence of labeled cells in the gut, adjacent to the yolk tube or overlying the yolk cell (21/40 embryos).

After establishing the technique, we transplanted *stbm* MO-injected cells into wild-type embryos to obtain wild-type host with *stbm* deficient mesoderm (64%) and conversely, transplanted wild-type cells into *stbm* morphants and *tri*^{-/-} mutants to obtain morphant or mutant embryos with wild-type mesoderm (65%). We have numerous examples of donor cells in paraxial mesoderm (Figure 3.7A and B) and endoderm (Figure 3.7C and D) that failed to affect migration of host FBMNs in the predicted fashion. However, we had several embryos where the transplanted donor cells present in the ventral neural tube affected the neuronal migration. These results suggest that the function of *stbm* is rather required in the neural tube than in the mesoderm or endoderm.

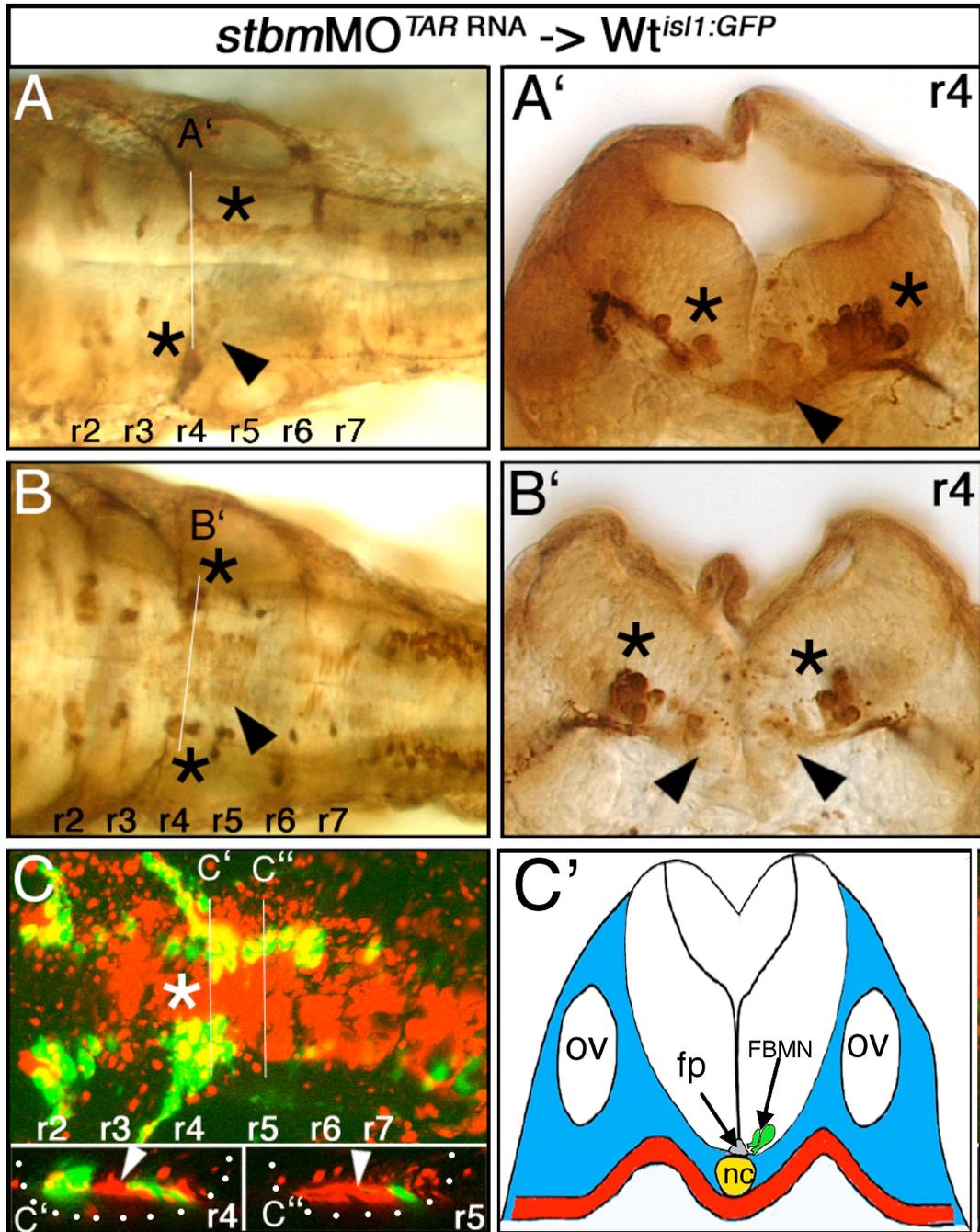


Figure 3.7 Donor derived *stbm* deficient neuroepithelial and floorplate cells block the migration of FBMNs in zebrafish

A and B are GFP antibody labeled, while C and D are confocal images. A, B, C and D are dorsal views of hindbrain of zebrafish with anrojections. A' and B' are cross sections of embryos in A and B respectively, while C', C'', D' and D'' are optical cross sections of embryos in C and D respectively. *Stbm* deficient neuroepithelial and floorplate cells adjacent to FBMNS in a wild-type hindbrain block their migration (A, B, C and D). Wild-type embryos showing unilateral migration defect (A, black star) and bilateral migration defect (B, black star) have *stbm* deficient donor cells within the hindbrain (A, B, A' and B' black arrow heads). Confocal imaging reveals the presence *stbm* deficient donor cells (red in C and D, white arrow heads in C', C'', D' and D'') adjacent to FBMNs and block their migration unilaterally in C and D (white stars, C and D).

3.2.5 *Stbm* functions in the floorplate and neuroepithelial cells to mediate FBMN migration

In our experiments, since we used very low amount of *tar* RNA, we believe that in some donor embryos, the *tar* RNA was not active or extremely low and it caused the donor cells to form the cells in the ventral neural tube rather than the mesoderm of host embryos. These donor derived cells that formed the ventral neural tube gave us some important observations. First, we have been able to block the migration of FBMNs in wild-type host embryos by transplanting *stbm* MO-injected cells into the ventral neural tube (Table 3.1A; Figure 3.8). When the donor derived *stbm* deficient cells form the floorplate (Figure 3.8A and A') and neuroepithelial cells neighbouring the FBMNs (Figure 3.8B and B'), the FBMNs fail to migrate (7%) (Figure 3.8 A and B). We took confocal optical cross sections to examine the nature of donor derived cells in live mosaic embryos (Figure 3.8 C, C', C'', D, D' and D''). Optical cross sections reveal that donor derived (red cells) mostly formed the floorplate and neuroepithelial cells of r4 and r5 (Figure 3.8 C', C'', D' and D''), though some donor derived FBMNs could not be ruled out. Likewise, donor derived wild-type floorplate and neuroepithelial cells rescue the migration of FBMNs in *tri*^{-/-} or *stbm* MO morphants (14%) (Figure 3.9 B, B', C, C', C'', D, D' and D''), but the cells in dorsal neural tube were not able to rescue the migration (Figure 3.9A and A'). Optical sections show that the donor derived cells predominantly formed the floorplate cells of r4 and r5

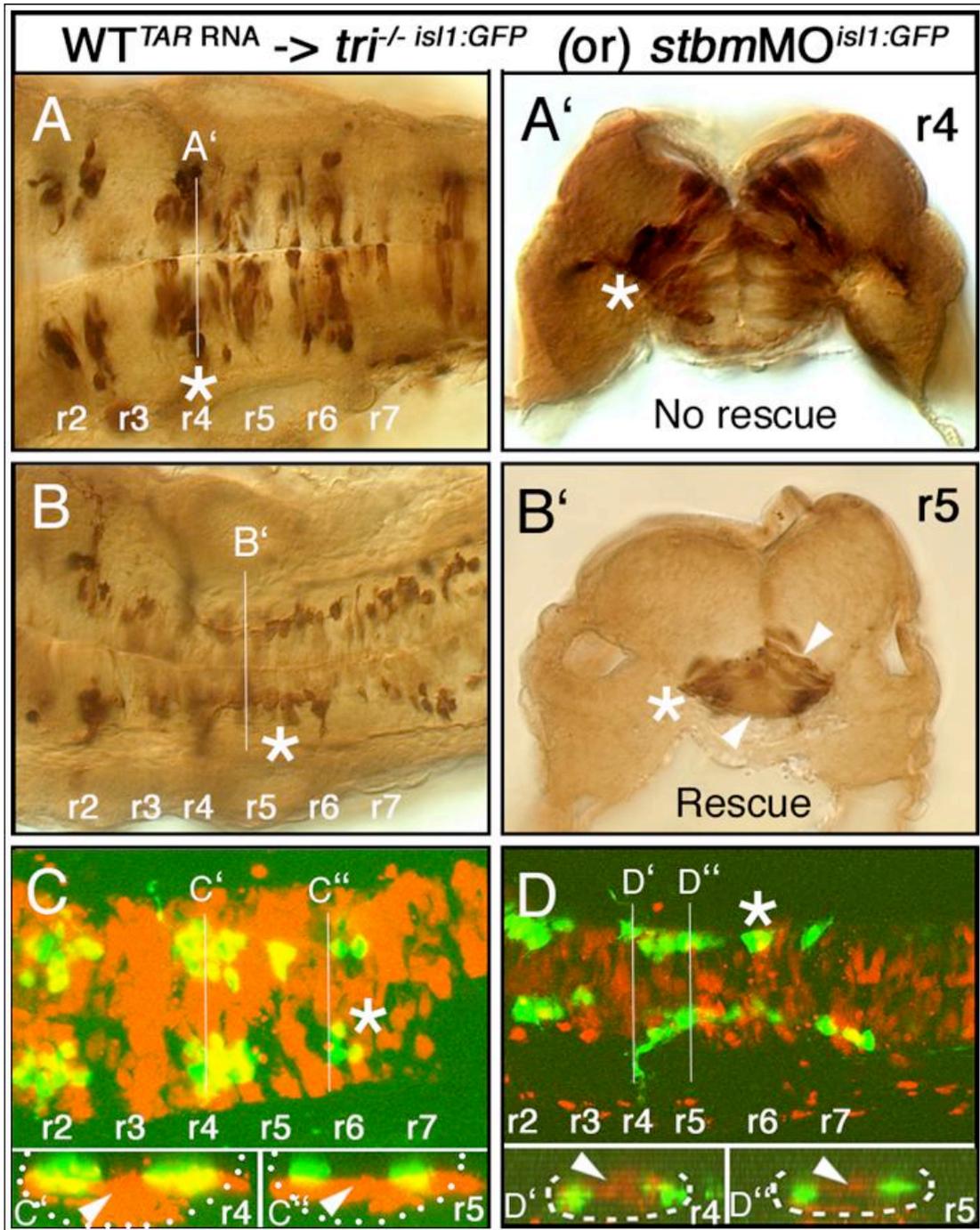


Figure 3.8 Donor derived wild-type neuroepithelial and floorplate cells rescue the migration of FBMNs in *trilobite*^{-/-} / *stbm* MO embryos. A, B, C and D are dorsal views of hindbrain of zebrafish with anterior to the left. A and B are GFP antibody labeled, while C and D are confocal projections. A' and B' are cross sections of embryos in A and B respectively, while C', C'', D' and D'' are optical cross sections of embryos in C and D respectively. Donor derived wild-type neuroepithelial and floorplate cells (B', C', C'', D' and D'', white arrow heads) adjacent to FBMNs in mutant hindbrain rescue neuronal migration (B, C, D). Donor derived wild-type cells when present in the dorsal neural tube away from the FBMNs, were not able to rescue migration in mutant hindbrain (A and A'). White stars point to rescued FBMNs migration.

(Figure 3.9C', C'', D' and D''), though some donor derived FBMNs could not be excluded. However, both of these experiments suggest that *stbm* function is necessary and sufficient in the ventral neural tube especially those forming the floorplate including FBMNs themselves rather than in the mesoderm.

3.3 Discussion

Genetic interaction between *stbm* and *pk1a* to mediate FBMN migration

Stbm and *pk1a* are integral members of non-canonical Wnt signaling pathway that mediates planar cell polarity in a frizzled/disheveled dependent manner in drosophila (reviewd by Strutt, 2003; Klein and Mlodzik, 2005), convergence and extension movements during gastrulation in zebrafish (Carriera-Barbosa et al., 2003; Jessen et al., 2002; Park and Moon., 2001; Veeman et al., 2003) and gastrulation and neural tube closure in mouse and humans (Kibar et al., 2007; Torban et al., 2008; Murdoch et al., 2001). Previous studies from our lab and others have shown that *stbm* and *pk1a* are necessary to mediate FBMN migration in the zebrafish hindbrain and it functions independently of non-canonical wnt signaling pathway (Bingham et al., 2002; Jessen et al., 2002; Carrierra-Barbosa et al., 2003). Several studies on planar polarity signaling in drosophila eye and wings have shown that *Stbm* and *Pk* physically interact and that is physiologically

important (Jenny et al., 2003; Bastock et al., 2003). *Stbm* and *pk1a* are also known to function together in mediating convergent extension movements and neuralation morphogenesis in zebrafish (Carriera-Barbosa et al., 2003; Ciruna et al., 2006; Tawk et al., 2007). In this study, we show that *stbm* and *pk1a* are genetically interacting to mediate FBMN migration in zebrafish. Carriera-barbosa et al have previously shown that *pk1a* is required for FBMN migration and it genetically interacts with *stbm*. But, in our hands *pk1a* knockdown using morpholino partially disrupts, rather than fully blocking FBMN migration (data not shown). Also, they used *trr^{m209}* allele, which is haplo-insufficient. Therefore, we co-injected sub-optimal doses of *stbm* and *pk1a* MO and show that these genes do function together. *Stbm* functions non cell-autonomously (Jessen et al., 2002) to mediate neuronal migration and identity of the cell-types where *stbm* function is not well understood because of the ubiquitous expression of *stbm*. Taken together, this genetic interaction has given us a platform to identify the cell-types, by looking at the expression of *pk1a*.

***stbm* functions in the floorplate neuroepithelial cells to mediate neuronal migration**

Detailed expression analyses showed that *stbm* and *pk1a* have overlapping expression pattern in mesoderm or endoderm not inside the neural tube. This suggested that *stbm* could function in the

mesoderm and endoderm to mediate neuronal migration inside the neural tube. But, our targeted mosaic analysis have shown that *stbm* does not function in the mesoderm or endoderm, rather it is required within the ventral neural tube in the floorplate neuroepithelial cells surrounding the migrating FBMNs. To examine whether floorplate is necessary for FBMN migration, we checked FBMN migration in the mouse *gli2* mutants, which lacks floorplate, but still able to specify ventral motor neurons in the hindbrain (Matisse et al., 1998; Ding et al., 1998). Zebrafish, *gli2* mutants could not be used, because ventral motor neurons are not specified due to the absence of sonic hedgehog signaling (Vanderlaan et al., 2005). FBMNs in mouse *gli2* mutants fail to migrate out of r4 (data not shown), strongly suggesting that floorplate cells are required for neuronal migration. Interestingly, Mouse looptail (*Lp/Lp*; *Vangl2*) mutant which encodes a non-functional strabismus protein also have FBMN migration defect (data not shown) and these mutants exhibit an abnormal broadening and flattening of ventral midline (floorplate) when compared with their heterozygous and wild-type littermates (Greene et al., 1998). Floorplates of *Lp/Lp* mutant embryos also have a broad domain of *shh* (sonic hedgehog) and *netrin1* expression, compared with their heterozygous and wild-type littermates (Greene et al., 1998). Expression analysis of *Lp/Vangl2* in mouse embryos have revealed that *Lp/Vangl2* expression is absent in the floorplate at E9.5 and E10.5 (ages at which FBMNs specify and

start to migrate) and it also is negatively regulated by *shh* expression in floorplate (Murdoch et al., 2001) suggesting that the normal function of *Lp/Vangl2* gene may be to restrict the lateral extent of floorplate differentiation (Murdoch et al., 2001). Moreover, the floorplate of zebrafish *MZtri* (maternal zygotic trilobite) mutant embryos are broader than in wild-type (Ciruna et al., 2006). Taken together, these studies strongly suggests that floorplate cells play a vital role in FBMN migration in zebrafish and further experiments to characterize the floorplate development in *stbm*/trilobite mutants is absolutely important. Also, it is important to check the expression of *stbm* more carefully in the floorplate of zebrafish embryos.

Novel cellular roles for *stbm* in neuronal migration

PCP signaling molecules such as *fz3a* and *celsr2* have been shown to function in the neuroepithelium to mediate neuronal migration (Wada et al., 2006). While *Pk1a* is expressed mainly in the mesoderm and endoderm and is more likely to mediate neuronal migration from outside the neural tube, newly identified *pk1b* is expressed in the FBMNs to mediate their migration. But, *stbm* appears to have a novel role by functioning in the floorplate cells. Remarkably, mouse *Lp/Lp* mutants have a expanded expression of molecules like netrin1, which is a known chemorepulsive molecule in cerebellar interneuron migration (Alcantara et al., 2000; Guijarro et al., 2006). It will be exciting to investigate the role of netrin1 in FBMN migration. *Stbm* could be

mediating contact dependent / cell adhesion based effect on the FBMN migration especially because it is known to genetically interact with *TAG-1* and *Lama1* molecules (discussed in chapter 5).

Stbm may also be functioning in the neighbouring FBMNs and the interaction between the facial neurons may facilitate migration termed as 'community effect' (Gurdon et al., 1993; Cooper et al., 2003). Our data are consistent with this underlying the possibility of donor derived non-transgenic FBMNs guiding or blocking the migration of the GFP positive host FBMNs. Therefore, interactions between the migrating motor neurons could be an important factor mediating migration and needs more research.

CHAPTER FOUR

Role of Strabismus Domains in Mediating FBMN

Migration in Zebrafish Hindbrain

Unpublished: Sittaramane, V., and Chandrasekhar, A., (2008).
(Manuscript in preparation)

4.1 Introduction

Cell migration is a fundamental process that defines the development of an embryo. Early developmental processes such as gastrulation and late developmental processes such as tissue formation require organized cell migrations in a meticulous direction to a specific location. Central nervous development involves extensive cell migration and it facilitates designing a distinct cyto-architecture for the brain. The function of the nervous system is completely dependent on the highly intricate pattern of connections between neurons. Neurons migrate from their birthplace and arrive at precise destinations to form viable circuit through synapses. Errors during these processes may lead to severe disturbances including mental retardation and motor dysfunction. Thus, understanding the mechanisms that regulate neuronal migration would aid in developing novel therapeutic strategies. Developing brain is characterized by the migration of several different neurons to their final destinations. Facial motor neurons are a subset of branchiomotor

neurons found in the hindbrain that undergoes a simple and elegant tangential migration caudally from rhombomere 4 (r4) to r6 and r7 in zebrafish (Chandrasekhar et al., 1997; Bingham et al., 2002). In zebrafish trilobite mutants, facial branchiomotor neurons (FBMNs) fail to migrate from r4 (Bingham et al., 2002; Jessen et al., 2002). Thus, *Stbm* is required for the migration of facial motor neurons, but the molecular events mediating the migration remains to be investigated.

Trilobite encodes Strabismus (*Stbm*), an important member of the wnt/PCP pathway which regulates the convergent and extension cell movements during gastrulation (Jessen et al., 2002). Strabismus has been well studied for its role as a component of the wingless/Wnt signaling pathway in mediating polarized cellular behaviors and patterning events in an epithelial cell layer (planar cell polarity/PCP) in flies and vertebrates. The drosophila Wingless protein and its vertebrate counterparts (Wnts) are secreted glycoproteins that play major roles in development (Veeman et al., 2003a; Logan and Nusse, 2004; Klein and Mlodzik, 2005). In general, binding of specific Wnts to particular Frizzled (Fz) receptors activates one of two signaling cascades, a canonical pathway involving Rho kinases, Jun kinases and calcium transients, and leading to changes in the cytoskeleton and cell polarity (Veeman et al., 2003a; Klein and Mmlodzik, 2005). Many components of the non-canonical pathway, epitomized by Strabismus/Van gogh (*Stbm/Vang*), regulate polarity of cell in epithelia

(i.e. planar cell polarity) such as wing bristle cells and ommatidial cell in the fly (Taylor et al., 1998; Wolf and Rubin, 1998; Keifer, 2005), and inner ear hair cells and neural tube cells in mammals (Kibar et al., 2001; Murdoch et al., 2001a; Torban et al., 2004a; Doudney and Stainer, 2005). Furthermore, Wnt/PCP components also regulate convergent extension (CE) cell movements during vertebrate gastrulation (reviewed in Veeman et al., 2003a), and the tangential migration of FBMNs (Bingham et al., 2002; Jessen et al., 2002; Carreira-Barbosa et al., 2003; Wada et al., 2006 and Wada et al., 2007).

Strabismus is transmembrane protein that is a component of the non-canonical Wnt/PCP pathway (Veeman et al., 2003a; Torban et al., 2004a). The role of the Wnt/PCP components like *Stbm* in regulating CE cell movements during vertebrate gastrulation is well established. However, there are multiple lines of evidence suggesting that the role of *Stbm* in FBMN migration is independent of its function in the Wnt/PCP pathway. (1) Several *trilobite* alleles (*tc240a*, *vu46*, *b626*) generate only mild CE defects, whereas FBMN migration is completely blocked (Jessen and Solnica-Krezel, personal communication). (2) *Stbm* functions in the environment during FBMN migration, but in the migrating cells during CE movements (Jessen et al., 2002). (3) Overexpression or knockdown of *stbm* leads to similar CE movement defects (a characteristic property of Wnt/PCP components), whereas FBMNs migrate normally following *stbm* overexpression (Figure 4.3).

(4) Disruption of wnt/PCP signaling by inhibiting Wnt5a, Wnt11, Dishevelled, or Glypican function severely affects CE movements, but not FBMN migration (Bingham et al., 2002; Jessen et al., 2002). These observations suggest strongly that Stbm may function through novel, Wnt/PCP –independent cellular and molecular mechanisms to mediate FBMN migration. Therefore, it is important to understand the structural basis of Stbm’s role in FBMN migration. In this study, we investigate the role of N- and C- terminal domains of Stbm to mediate FBMN migration.

4.2 Results

4.2.1 Stbm/Trilobite/Vangl2 is a four-pass transmembrane protein

Zebrafish *stbm* has 75%, 61% and 76% identity with Xenopus, mouse and human orthologues, respectively (Park and Moon, 2002). Amino-acid sequence analysis predicts the presence of four potential transmembrane domains close to the N-terminus and a putative PDZ-domain binding motif at the C-terminus (Park and Moon, 2002). While the C-terminal region of Stbm interacts with the cytosolic Disheveled protein (Park and Moon, 2002; Torban et al., 2004b), the orientation of the N-terminal domain is uncertain since the four transmembrane regions are predictions of analysis software. To solidify these predictions, Stbm sequence was analyzed using an extended suite of sequence analysis software (Sequence analysis: **Psi-Blast, MotifScan,**

Motis; Protein structure prediction: Psi-Pred, mGenTHreader, Sp3, SPARKS2; Membrane protein segment and orientation predictions: THUMBUP, SOSUI, TMHMM; Disordered region prediction: DisEMBL. Analysis was done by Dr. Dong Xu, Computer Sciences, University of Missouri). These analysis predict with high reliability that Stbm contains exactly four transmembrane domains, which given the cytosolic location of the C-terminal region definitively places the N-terminal region also in the cytosol. Further, the analyses indicate that the N-terminal region has a disordered tertiary structure, in contrast to the C-terminal region, which contains defined elements (Figure 4.1A). To check if the Stbm protein is localized in the membrane, wild-type embryos injected with myc epitope- tagged *stbm* RNA were stained with anti-myc antibodies. Myc tagged recombinant Stbm protein is correctly targeted to the membrane (Figure 4.1B). These data suggests that Stbm indeed is localized in the membrane.

To study the roles of different regions of Stbm in FBMN migration, we generated the myc epitope-tagged Stbm Full-length, Stbm Δ C (1-111 amino-acids) and Stbm Δ N (240-526 amino-acids) cDNA (Figure 4.1C). Further, we checked their expression by injecting their RNA into wild-type embryos and processed them for western-blot with anti-myc antibody (Figure 4.1D). Western-blot analysis revealed that Stbm regions of appropriate sizes are expressed upon injection of RNAs (Figure 4.1D).

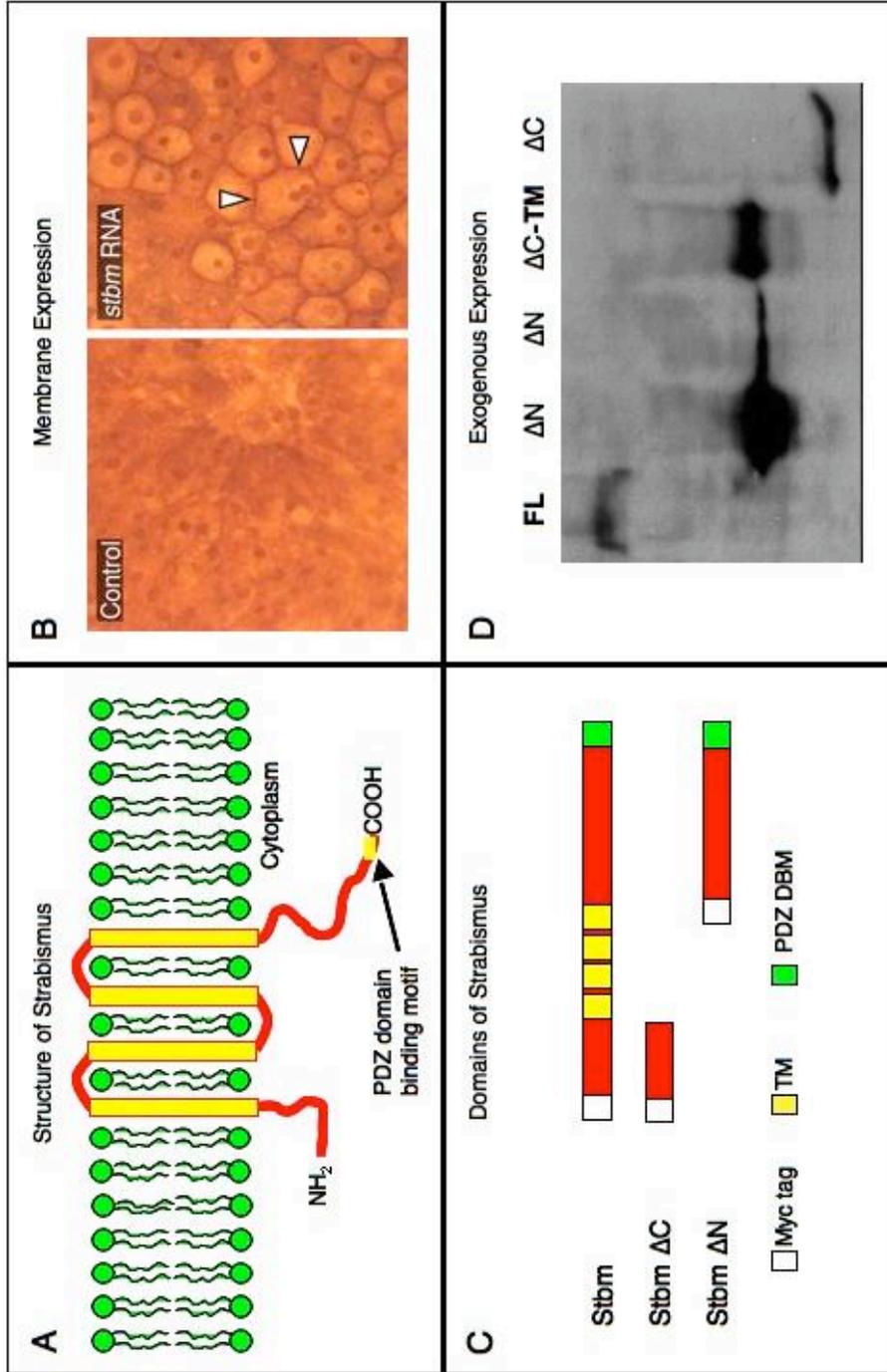


Figure 4.1 Strabismus domains and their expression A.

Schematic of the four pass transmembrane protein Strabismus with both N- and C-terminal in the cytoplasm. C-terminal has a known PDZ-domain binding motif, while the N-terminal has no known domains. B. Control or RNA-injected embryos were fixed at 80% epiboly, and stained with anti-HA antibody. Arrowheads point to location of Stbm in membrane. C. Schematic of Myc-epitope tagged Stbm full-length, Stbm N-terminal and Stbm C-terminal constructs prepared. D. Western blot with anti-Myc antibody (30 μ g/lane) of proteins isolated from wild-type embryos injected with synthetic mRNA. (FL) Full-length Stbm RNA, (Δ N) Stbm C-terminal, (Δ C) Stbm N-terminal, (Δ C-TM) RNA for Stbm N-terminal region with TMs.

4.2.2 Developing an FBMN migration rescue assay using wild-type embryos

We showed previously that wild-type *Stbm* is able to rescue defective FBMN migration in *tri* mutant embryos (Jessen et al., 2002). The rescued mutant embryos (exhibiting wild-type like FBMN distribution) were identified by genotyping using allele-specific primers. Indeed, we initially used this assay to demonstrate that full-strength *Stbm*, but not truncated *Stbm* encoded by *tri*^{m209} allele, can rescue FBMN migration in *tri*^{k50f} mutant embryos (data not shown; mutant genotyped using z17411 marker). However, this rescue assay is cumbersome for a structure-function analysis of *Stbm* because the number of embryos to be scored and genotyped becomes very large since only 25% of embryos obtained from *tri*^{+/-} parents would be *tri* mutants. This problem is exacerbated if the rescuing abilities of two *Stbm* variants are similar, necessitating even larger sample sizes. To overcome this problem, we developed a rescue assay involving the expression of *Stbm* constructs in wild-type embryos where endogenous *stbm* function has been knocked down using *stbm* morpholinos. The advantages of this assay are: (1) large sample sizes are easily obtained since only wild-type embryos are used, and (2) there is no need to genotype embryos. Below, we first describe a sensitive index for FBMN migration in a collection of embryos, followed by the implementation of the rescue assay.

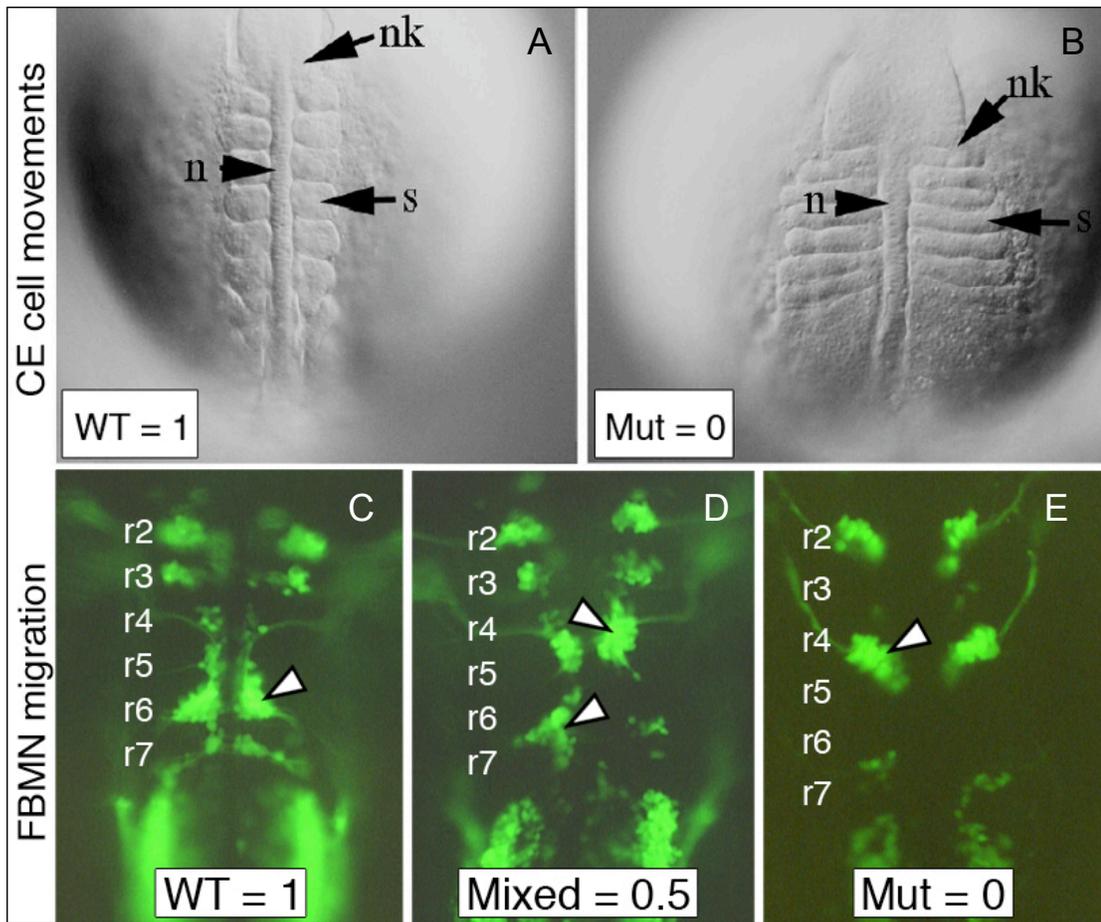


Figure 4.2 FBMN Migration indices.

The CE phenotype is scored at the 8-15 somite stage. Wild-type CE phenotype is assigned an index value of 1, while a reduced CE (mutant) phenotype is assigned a value of 0. Similarly, embryos in which FBMNs have migrated on both sides into r5-r7 are assigned an index value of 1, and embryos with complete migration block a value of 0. Embryos with intermediate migration phenotypes are assigned a value of 0.5. n, notochord; nk, neural keel; s, somite.

4.2.3 The FBMN migration index - A sensitive measure of neuronal migration in a population of embryos

To assay the ability of *Stbm* (or other) constructs to regulate CE cell movements and FBMN migration, we separate a collection of embryos into two groups for CE phenotypes at the 8-15 somite stage (wild-type and mutant; Figure 4.2A), and three groups for FBMN migration phenotypes at 36 hpf (wild-type, mutant and mixed; Figure 4.2A). The CE and FBMN migration indices are weighted averages of the distribution of embryos between the different phenotypic classes. For example, FBMN migration index = $[(N_0 \cdot 0) + (N_{0.5} \cdot 0.5) + (N_1 \cdot 1)]$ divided by $(N_0 + N_{0.5} + N_1 = \text{total number of embryos})$. For a completely wild-type collection, the index equals 1.0, and for a completely mutant population (where each embryo exhibits total loss of FBMN migration), the index equals 0. The CE movement index is similarly calculated. Together, these indices provide sensitive measures for the status of CE and FBMN movements in a collection of embryos, as demonstrated below.

4.2.4 FBMN rescue assay using *stbm* morphant embryos

We generated a dose-response curve (Figure 4.3) to determine the optimal concentration of antisense *stbm* morpholino to use in the rescue experiments. Following expression of full-length *Stbm*, FBMN migration was only poorly rescued in 4ng *stbm* MO-injected embryos,

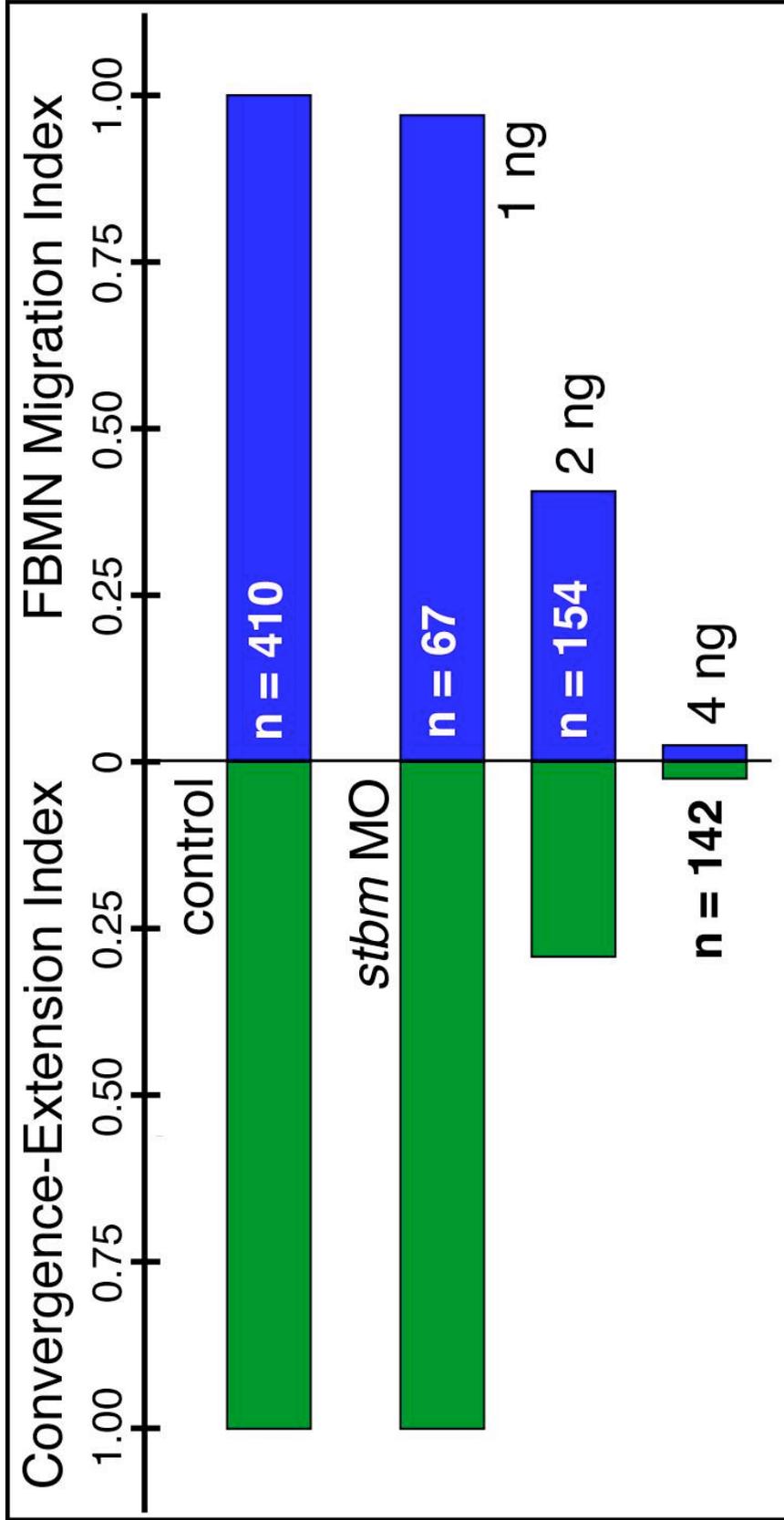


Figure 4.3 Convergent-extension and FBMN migration indices in normal and *stbm* morphant embryos Different doses of *stbm* morpholino (MO) were injected per embryo, and migration indices were calculated for each collection of embryos (n= number of embryos injected and scored).

perhaps due to complete loss of endogenous *Stbm* (data not shown). By contrast, rescue of the morphant phenotype was significant and consistent in embryos co-injected with 2 ng *stbm* MO and 0.4-0.48 ng *stbm* mRNA (Figure 4.4). The rescue of FBMN migration is not an artifact of titration of MO binding between the endogenous and injected *stbm* RNAs because the injected synthetic mRNA lacks the morpholino-binding site due to a deletion of the 5'UTR (Δ 5'UTR). We also know the injected RNA generates functional *Stbm* protein since increasing doses of RNA from 0.3-0.48 ng/embryo lowers the CE index (i.e., *stbm* gain-of-function mimics the *stbm* loss-of-function phenotype; Figure 4.4), and co-injection of *stbm* RNA and *stbm* MO has additive effects on reducing CE movements (Figure 4.4).

4.2.5 Stbm C- and N-terminal domains can independently rescue FBMN migration

To define the roles of different regions of *Stbm* in FBMN migration, we tested whether the cytosolic N- and C-terminal domains (Figure 4.1C) could rescue FBMN migration in *stbm* MO-injected embryos. Injection of the *Stbm* N-terminal or C-terminal RNAs alone caused reduced CE movements (Figure 4.5), indicating that truncated proteins are present (Figure 4.1D), and interfere with gastrulation

movements. Importantly, overexpression of neither construct affected FBMN migration. We found that the *Stbm* C-terminal region, and unexpectedly the *Stbm* N-terminal region, rescued FBMN migration in morphants, although the C-terminal appears to be more effective at rescue (Figure 4.5). The rescuing ability of the C-terminal region is expected because this fragment binds PDZ domain proteins like Disheveled (Park and Moon, 2002), and since FBMN migration is eliminated in trilobite alleles that encode C-terminally truncated proteins (Jessen et al., 2002). In contrast, the rescuing ability of the N-terminal region is very surprising, but reproducible. This suggests that the N-terminal and C-terminal regions of *Stbm* may independently facilitate the formation of a cytoplasmic complex that mediates FBMN rescue.

4.2.6 Development of heat shock inducible *stbm* transgenic lines

Stbm N- and C-terminal domains by themselves cause reduced convergent extension movements like the full-length *Stbm* and *stbm* morpholino. Thus, co-injection of *stbm* MO and *stbm* N- or C-terminal domains cause severely reduced convergent extension movements potentially affecting the survivability of the injected embryos available for the assay at 36 hpf. To overcome this difficulty, we designed to develop transgenic fish which would express myc epitope tagged full-length *Stbm* or *Stbm* N-terminal or *Stbm* C-terminal under the heat

shock promoter using sleeping beauty transposase cassette as shown in schematic (Figure 4.6A). Myc epitope tagged *Stbm* full-length or

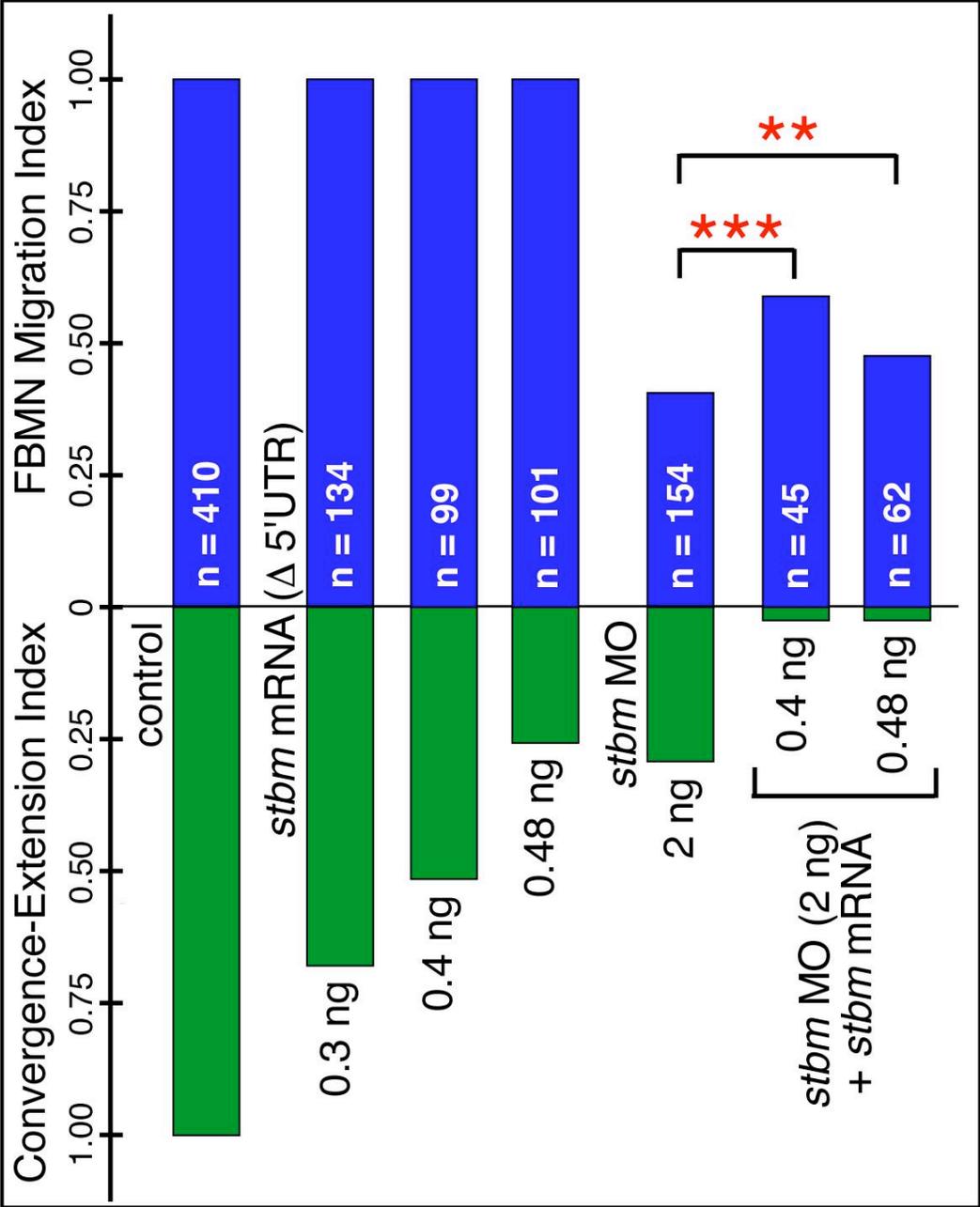


Figure 4.4 Full length and Δ 5' UTR *stbm* RNA can rescue defective FBMN migration in *stbm* morphants.

Injection of increasing amounts of *stbm* mRNA generated larger fractions of embryos with reduced CE movements (green), whereas FBMN migration remained completely normal (blue). Co-injection of *stbm* mRNA and *stbm* MO greatly exacerbated the CE phenotype (left side bracket), while the migration defects of *stbm* morphants were significantly rescued (right side brackets).

Stbm domain under heat shock promoter is subcloned into sleeping beauty vector containing lens specific γ -crystallin GFP as reporter (Figure 4.6A). The constructs were injected with sleeping beauty transposase RNA into *Tg(islet1:GFP)* embryos and the embryos showing the expression of GFP in the lens were selected and grown as founder fish (F_0). F_0 fishes were screened for stable germline insertion of transgene after 12 weeks by out crossing them into wild-type *Tg(islet1:GFP)* fish. F_0 with stable germline insertion produced offsprings with lens GFP (F_1). F_1 fish were grown for another 12 weeks and checked by out crossing them with wild-type *Tg(islet1:GFP)* fish to produce F_2 . These F_2 embryos were heat shocked at 30 hpf and the embryos were processed for western-blot analysis with anti-myc antibody to check for heat shock induced production of Stbm proteins. We made the transgene cassette for Stbm full-length, Stbm N- and C-terminal domains and injected them into *Tg(islet1:GFP)* embryos and were successfully able to produce lens GFP positive F_2 offsprings for Stbm N- and C-terminal transgenic fish. We are still screening for a lens positive F_1 for Stbm full-length transgenic fish. We were also able to do successful initial heat shock experiments to check for their heat shock inducibility using Stbm N-terminal transgenic fish (Figure 4.6B). We are conducting further experiments using Stbm N- and C-terminal transgenic fish.

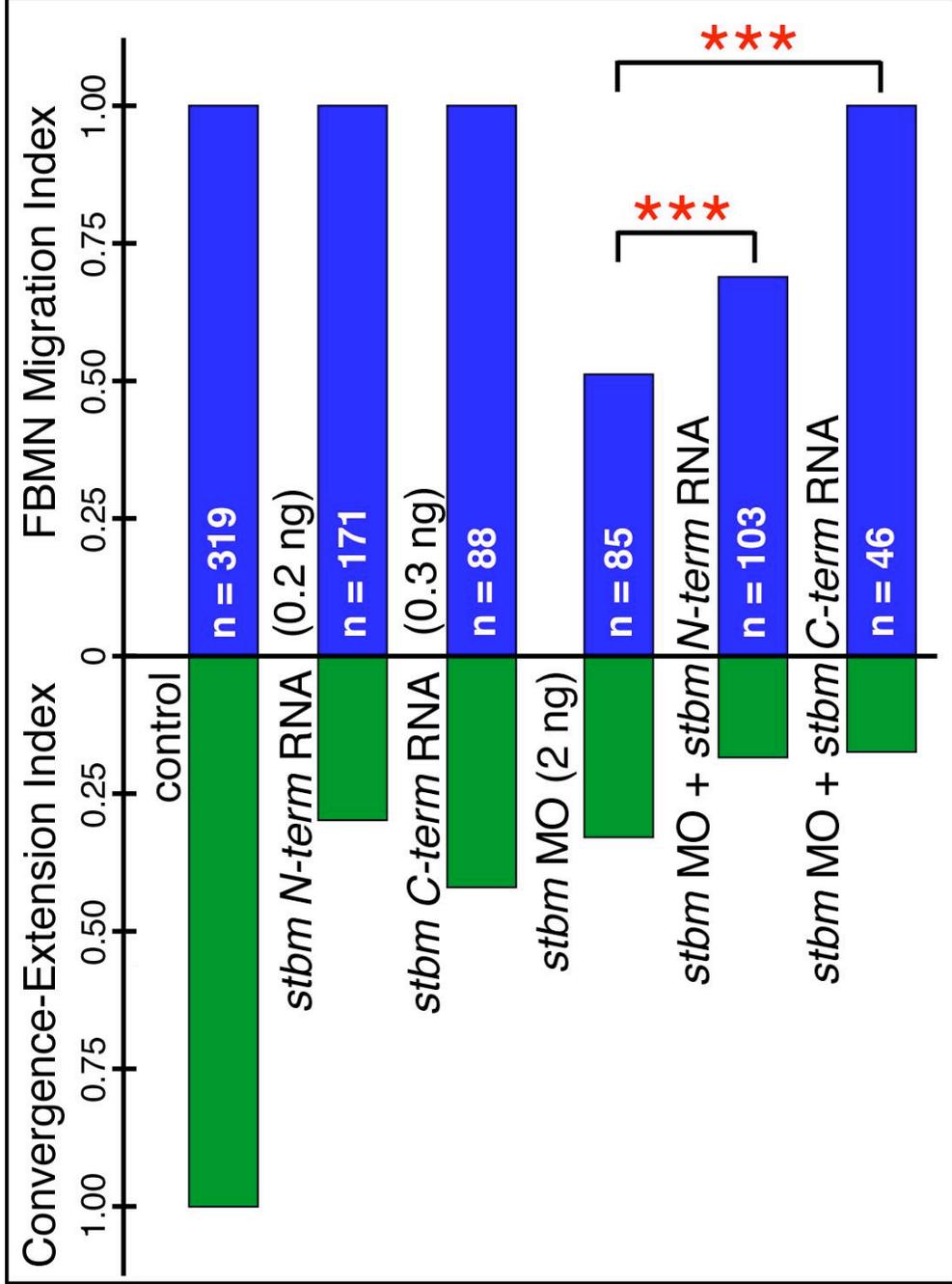


Figure 4.5 *stbm* N- and C- terminal domains can rescue defective FBMN migration in *stbm* morphant embryos.

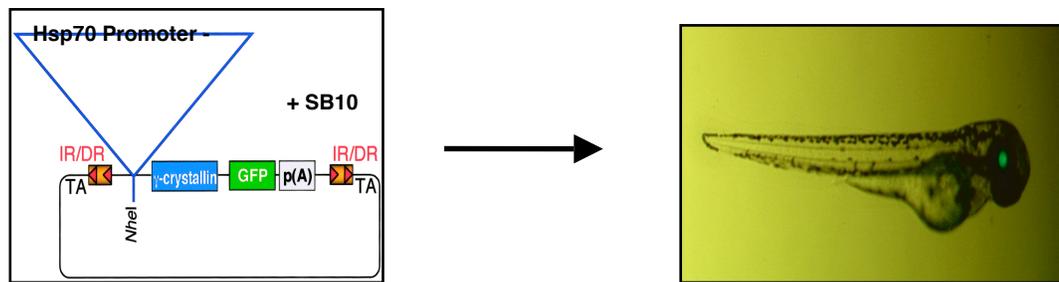
Injection of *stbm* N-terminal or C-terminal RNAs alone causes reduced CE movements, but has no effect on FBMN migration. Co-injection of RNA and *stbm* MO exacerbates the CE defect, but significantly rescues the defective FBMN phenotype of *stbm* morphants.

4.3 Discussion

Strabismus is an integral member of the Wnt/PCP pathway and its role in PCP signaling has been studied extensively. Planar cell polarity is the coordinated organization of cells within the plane of the epithelium. This polarity is perpendicular to the apical-basal polarity and is seen in many tissues in flies and human. In drosophila wing and eye, the polarity is largely influenced by the cellular localization of the core PCP proteins. The core proteins are initially distributed uniformly along the apical cortex of the cell, but over time they become localized to distal (Frizzled (Fz) and Dsh), proximal (Prickle (Pk) and Stbm), or both membranes (Flamingo (Fmi), Diego (Dgo)) (Usui et al., 1999; Axelrod, 2001; Feiguin et al., 2001; Shimada et al., 2001; Strut, 2001; Tree et al., 2002b; Bastock et al., 2003; Wu et al., 2004), suggesting that they may form a multiprotein complex that positions one another asymmetrically in the cell (Keifer et al., 2005). There is abundant evidence for direct interactions between the PCP proteins: for example, Dsh binds Pk (Katanev et al., 2005), Dgo binds Pk and Stbm (Das et al., 2004) and Pk binds Stbm (Jenny et al., 2003). At the level of Dsh, two independent and parallel pathways lead downstream to the activation of the small GTPases RHO and RAC (Eaton et al., 1996; Fanto et al., 2000; Habbas et al., 2003; Strutt et al., 1997; Tahinci and Symes, 2003). The RHO pathway activates RHO-associated kinase ROCK,

which mediates cytoskeletal re-organization (Kim and Han, 2005; Marlow et al., 2002; Veeman et al., 2003; Winter et al., 2001), while the RAC pathway stimulates JNK activity (Boutros et al., 1998; Habas et al., 2003; Li et al., 1999b; Yamanaka et al., 2002; Wallingford and Habbas, 2005). In vertebrates, PCP signaling is studied extensively in convergent extension movements during gastrulation (Heisenberg et al., 2000; Wallingford et al., 2000) and morphogenetic movements during neural tube closure (Heisenberg et al., 2000; Wallingford and Harland, 2002). Homologs of Dsh, Pk, Fmi and Stbm have been identified and shown to mediate vertebrate PCP (Sumanas et al., 2000; Tada and Smith, 2000; Wallingford et al., 2000; Park and Moon, 2002; Carriera-Barbosa et al., 2003; Takeuchi et al., 2003; Veeman et al., 2003). As in flies, Stbm is likely to signal through Dsh, with direct interaction between the C-terminal domain of Stbm and PDZ-domain of Dsh. In Zebrafish FBMN migration, Stbm functions in a Wnt/PCP independent pathway, but still involves other PCP molecules such as Pk1a (Carriera-Barbosa et al., 2003), Fmi (Wada et al., 2006); Fzd3a (Wada et al., 2006), and Scrb1 (Wada et al., 2005). *stbm* genetically interacts with at least *pk1a* to mediate FBMN migration. Though, the mechanism by which these molecules facilitate neuronal migration is not clear, our data with the Stbm domain analysis suggests that both the N-terminal and the C-terminal domains of Stbm could cooperate to

assemble a multiprotein signaling complex at the cell membrane to stimulate downstream events. Since *stbm* is ubiquitously expressed,



(Modified from Davidson *et al.*, 2003.

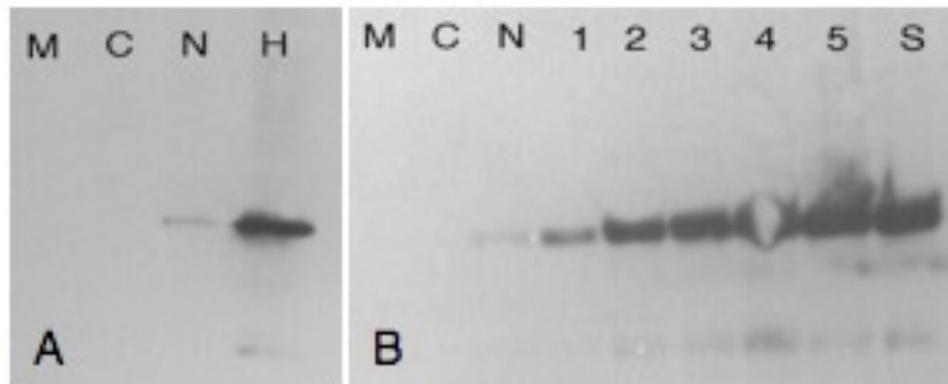


Figure 4.6 Development of heat shock inducible transgenic lines. A. Schematic for the transgene construct that is injected with sleeping beauty transposase (SB10) mRNA to produce lens GFP positive F₀ offspring. B. Western blot analysis of lens GFP positive Stbm N-terminal F₂ embryos heat shocked at 30 hpf using anti-myc antibody (12 embryos/lane). (M) Marker, (C) Control Lens GFP negative, (N) Control Lens GFP positive not heat shocked (H, 1) Lens GFP positive heat shocked and incubated for 1 hour, (2) 2 hours, (3) 3 hours, (4) 4 hours, (5) 5 hours and (s) Heat shocked for the second time at 5 hours after first heat shock and incubated for 2 hours.

signaling through this pathway may be restricted to those cells that also express other components, such as *Pk*, *Scrb* or *Fmi*, and/or in response to putative signals that bind Stbm extracellularly (Tag1, Laminin α 1). Furthermore, since Stbm is constitutively present, signaling may be activated by the onset expression of other components of the complex. Our data indicate that expression of either the Stbm N-or the C-terminal domains in the cytosol is sufficient to rescue FBMN migration in *stbm* morphants. Interestingly, overexpression of these domains also severely reduces convergence extension movements, a property shared with full-length Stbm (Jessen et al., 2002). The Stbm N-terminal domain is 111 amino acids long, and has a disordered structure with no apparent motifs within. The Stbm C-terminal domain is 286 amino acids long, and has an ordered structure, with the PBM motif at the C-terminus. Further deletion analysis of the N- and C-terminal domains may identify specific regions within each domain that are sufficient to rescue defective FBMN migration. Within the N-terminal domain, amino acids 1-50 may be especially important since an in-frame 13 amino acid insertion after 21 amino acid generates a mutant allele (*trilobite*^{tc240a}; Jessen et al., 2002) that has mild gastrulation defects, but is completely defective in FBMN migration (Bingham et al., 2002). Within the Stbm C-terminal domain, the PBM motif appears to be necessary, since it is deleted in the *trilobite*^{m209} (Jessen et al., 2002) that exhibits severe

defects in CE movements and FBMN migration (Marlow et al., 1998; Bingham et al., 2002).

CHAPTER FIVE

The cell adhesion molecule Tag1, transmembrane protein Stbm/Vangl2, and Laminin α 1 exhibit genetic interactions during migration of facial branchiomotor neurons in zebrafish

In Press: Sittaramane, V., Sawant, A., Wolman, MA., Maves, L., Halloran, MC and Chandrasekhar, A., *Developmental Biology*. 2008, Nov 5.

5.1 Abstract

Interactions between a neuron and its environment play a major role in neuronal migration. We show here that the GPI-linked cell adhesion molecule Tag1 is necessary for the migration of the facial branchiomotor neurons (FBMNs) in the zebrafish hindbrain. In *tag1* morphant embryos, FBMN migration is specifically blocked, with no effect on organization or patterning of other hindbrain neurons. Furthermore, using suboptimal morpholino doses and genetic mutants, we found that *tag1*, *laminin- α 1* and *stbm*, which encodes a transmembrane protein Vangl2, exhibit pairwise genetic interactions for FBMN migration. Using time-lapse analyses, we found that while FBMNs are unable to migrate caudally in all three single morphant

embryos, they exhibit distinct differences in dynamic behaviors. These data suggest that *tag1*, *laminin- α 1* and *vangl2* may define a novel mechanism that integrates signaling between the FBMN and its environment to regulate migration.

5.2 Introduction

Cell migration is an essential process in the development of an embryo. Migration of immature or new born neurons from the site of birth to their final position is a vital step in the development of the nervous system. Disturbances in this process can lead to severe impairments including mental retardation, epilepsy and severe learning disabilities (Marin and Rubenstein., 2003). Neuronal migration is largely dependent on the ability of the migrating neurons to interact with adjacent cells to perceive the signals that guide them during migration. Cell migration involves the protrusion of a leading edge and the formation of new adhesions at the front while simultaneously contracting and releasing the adhesions at the rear end (Porcionatto, 2006). These cell adhesions are provided by cell surface and extracellular matrix (ECM) molecules collectively termed as cell adhesion molecules (CAMs). CAMs critically mediate cell-cell binding, tissue patterning and other developmental processes including axon pathfinding and neuronal migration (Sobeih and Corfas., 2002). CAMs have demonstrated roles in neuronal migration and axon pathfinding.

Transient axonal glycoprotein-1 (*tag-1*) is implicated in the tangential migration of neurons in caudal medulla (Denaxa et al., 2005), neocortex (Denaxa et al., 2001), superficial migratory stream that produce lateral reticular and external cuneate nuclei (LRN/ECN; Kyriakopoulou et al., 2002) and growth cone guidance (Wolman et al., 2008). TAG1 is a glycoposphatidyl-inositol anchored glycoprotein that belongs to the Immunoglobulin superfamily (Furley et al., 1990) with six immunoglobulin (Ig) domains followed by four fibronectin (FN) III domains (Freigang et al., 2000). Tag1 is also expressed in other migrating neurons like FBMNs in mouse and zebrafish hindbrain (Garel et al., 2000; Warren et al., 1999); however, the requirements of TAG1 for the tangential migration of FBMNs have not been studied yet.

Many ECM molecules have also been investigated for potential roles in cell motility. Interactions between the neurons and extracellular matrix are fundamental for their normal migration. Laminin and fibronectin are known to provide support to neuronal precursor migration in cerebellum, while other molecules such as tenascin and netrin orient their migration (Porcionatto, 2006). Other ECM molecules involved in the neuronal migration include reelin, integrins, HSPGs and anosmin-1 (Sobeih and Corfas, 2002). Laminins are major components of the basement membranes and function as a permissive substrate and directional cue for axon outgrowth and cell migration (Paulus and Halloran., 2006). Laminins are heterotrimeric with combinations of α , β ,

and γ subunits (Miner and Yurchenco, 2004; Pollard et al., 2006). Recent studies in zebrafish have shown that laminin α -1 is required for nucMLF axon growth cone guidance (Wolman et al., 2008) and retinal ganglion cell axon pathfinding and migration of FBMNs (Paulus and Halloran., 2006).

Branchiomotor neurons are born in specific rhombomeres within the hindbrain and innervate muscles differentiating in the pharyngeal arches (Noden, 1983; Lumsden and Keynes, 1989). In zebrafish the facial (FBMNs) and the glossopharyngeal (nIX) motor neurons migrate tangentially to their final positions after inductions in anterior hindbrain (Chandrasekhar et al., 1997; Higashijima et al., 2000). FBMNs are born in rhombomere 4 (r4) at 17-18 hours post fertilization (hpf) and migrate tangentially over the next 18 hours such that by 36 hpf most of the FBMNs reach r6 and r7 (Bingham et al., 2002). While several molecules have been identified as necessary for FBMN migration, there is a dearth of knowledge on how these molecules interact with others and the environment to enable the migrating cells to reach their final position. Here, in this study, we report that transient axonal glycoprotein-1 (*tag1*), which is expressed in the FBMNs is necessary for their migration. We also show that cell surface molecule *tag1* interacts with *vangl2* which encodes for transmembrane protein strabismus and *lama1* which encodes the extracellular matrix protein laminin α -1.

5.3 Materials and Methods

5.3.1 Animals

Zebrafish (*Danio rerio*) were maintained following standard protocols and university ACUC guidelines as described previously (Westerfield, 1995; Bingham et al., 2002). For analysis of facial branchiomotor neuron (FBMN) migration, *Tg(isl1:gfp)* fish, which express GFP in branchiomotor neurons (Higashijima et al., 2000), were crossed into mutant backgrounds. The following mutant lines were employed in these studies: *trilobite* (*tri*^{tc240a}, Hammerschmidt et al., 1996; *tri*^{m209}, Solnica-Krezel et al., 1996); *bashful* (*bal*^{b765}, L.M., unpublished data; *bal*^{uw1}, Paulus and Halloran, 2006). Embryos were developed at 28.5°C and staged by hours post fertilization (hpf) (Kimmel et al., 1995).

5.3.2 Immunohistochemistry and in Situ Hybridization

Immunohistochemistry was performed according to standard protocols described previously (Chandrasekhar et al., 1997; Bingham et al., 2002) using anti-acetylated α -tubulin antibody (Chitnis and Kuwada, 1990; Sigma, 1:500 dilution), zn5 antibody (Trevarrow et al., 1990, Developmental Studies Hybridoma Bank (DSHB), 1:10 dilution), Tyrosine hydroxylase antibody (Guo et al., 1999; Chemicon/Millipore, 1:500 dilution), GFP antibody (Vanderlaan et al., 2005; Invitrogen,

1:1000 for DAB reaction and 1:4000 for FITC labeling), 3A10 antibody (Hatta, 1992; DSHB, 1:500 dilution) and TAG-1 antibody (Lang et al., 2001; 1:500 dilution). Fluorescent immunolabeling were performed using RITC-conjugated secondary antibody (for zn5, α -tubulin and TAG-1 antibodies; Jackson Immunochemicals, 1:500), and FITC-conjugated secondary antibody (for GFP antibody; Invitrogen, 1:500). Synthesis of digoxigenin labeled probes and whole mount in situ hybridization were carried out using procedures described previously (Chandrasekhar et al., 1997; Vanderlaan et al., 2005). Stained embryos were deyolked and mounted in glycerol, and imaged using DIC optics on an Olympus BX60 microscope. At least 10 wild-type and 10 mutant embryos were examined for all comparisons. For confocal imaging, embryos were mounted in glycerol and imaged using an Olympus IX70 microscope equipped with a BioRad Radiance 2000 confocal laser system. Images were processed in Adobe Photoshop to adjust brightness and contrast only.

5.3.3 Morpholino and mRNA Injections

Morpholinos targeting *tag1* (MO1; Liu and Halloran, 2005), *stbm/vangl2* (Jessen et al., 2002) and *lama1* (MO1; Pollard et al., 2006) were obtained from Gene Tools (Corvallis, OR) or Open Biosystems (Huntsville, AL). For each MO, we performed at least two dose-response experiments to determine the doses that either resulted in a

majority of embryos with normal or intermediate FBMN migration phenotypes (suboptimal dose; Figs. 2B, D) or completely blocked FBMN migration (optimal dose; Figs. 2C, D). We estimated the dose per embryo based upon the concentration of the MO solution, and the diameter (volume) of the injection bolus in the yolk cell. We typically injected 3-4 nl per embryo. The following doses (suboptimal, optimal) were used: *tag1* MO (6 ng; 12 ng); *stbm* MO (2 ng, 4 ng); *lama1* MO (1 ng, 2 ng). For the rescue experiments with *tag1* RNA (Fig. 3), a dose of 9 ng *tag1* MO was used. For the genetic interaction experiments (Figs. 5-8), we co-injected two MOs at the sub-optimal doses. For single MO experiments, controls were either uninjected embryos or embryos injected with a standard control MO (7-10 ng) from Gene Tools (5'-CCTCTTACCTCA-GTTACAATTTATA). Since the control MO did not affect FBMN migration (Fig. 8), many experiments included only uninjected embryos as controls. For the double MO experiments, controls included injection of single MOs with an appropriate amount of the control MO to match the total MO dose of the double MO-injected embryos. Embryos injected with a suboptimal dose of one MO alone or co-injected with control MO exhibited identical FBMN phenotypes (data not shown), indicating that the enhancement of FBMN migration defects seen in double MO-injected embryos (Fig. 8) is not a non-specific effect of increasing MO dose.

Since we observed increased cell death in *tag1* morphants at the optimal (12 ng) but not suboptimal (6 ng) dose, *p53* MO was coinjected with *tag1* MO in a 1.5:1 ratio to block p53-induced apoptosis (Robu et al., 2007). The FBMN migration defect was similar between *p53 + tag1* MO-injected and *tag1* MO-injected embryos (data not shown), indicating that the migration defect is not a non-specific effect of the *tag1* MO dose. Data shown in Figures 2 and 4 are from embryos injected with *tag1* MO alone and *tag1 + p53* MOs, respectively (see Figure legends).

Capped *tag1* mRNA was synthesized using the mMessage mMachine Kit (Ambion) from a template lacking the first 20 nucleotides of the 25 nt morpholino binding site in the 5'UTR. The mRNA was checked for purity and size by gel electrophoresis and estimated by UV spectrometry, and ~600 pg was injected into 1-2 cell stage embryos as described previously (Vanderlaan et al., 2005).

5.3.4 In vivo time-lapse analysis of gfp-expressing migrating motor neurons

At 16-17 hpf, *Tg(isl1:gfp)* embryos were mounted dorsally in 1.2% agarose, bathed in E3 medium containing 0.002% tricaine (Sigma) to anesthetize the embryo, and supplemented with 10mM HEPES to buffer the pH around the embryo during extended time-lapse observations. The embryos were aligned such that the r4-r5 (caudal)

direction was always pointing to 3 o'clock. Gfp-expressing motor neurons in rhombomere 4 were selected for imaging in all cases, so that the behavior of FBMNs in wild-type embryos could be compared to the behavior of FBMNs that fail to migrate out of r4 in *tag1*, *stbm*, and *lama1* morphant embryos. Images were acquired at two-minute intervals using Cytos (ASI, Eugene, OR) on an Olympus BX60 microscope equipped with shutters in the fluorescence and bright-field paths. Recordings were performed at ~28°C, the health and FBMN migration phenotype of embryos were checked at 36 hpf, and data from sickly embryos and those with weakly penetrant migration phenotypes (e.g., Fig. 2B) were excluded from analysis. FBMN behaviors were analyzed and motility parameters were computed using DIAS software (Solltech, Iowa City, IA). The speed, length-width ratio (LWR), and Rate of Area Change (RAC) for each cell were computed for every two-minute interval, and the mean values over the entire observation period (typically 40-60 min) were pooled for 15 cells within every treatment condition. RAC is defined as the total area of protrusion and retraction of a cell divided by time interval between frames (2 min), and is a measure of dynamic changes in cell area (i.e., cell activity). Caudal directionality is the ratio of the distance traveled by the cell in the caudal direction to the total distance traveled. Caudal speed is the product of caudal directionality and cell speed, and is a measure of the cell's movement toward r5. Rate of Direction Change was calculated

manually by calculating the number of 90° changes in centroid direction (Fig. 9) per 10 min during the observation period.

5.4 RESULTS

5.4.1 Transient Axonal Glycoprotein-1 (Tag1) is expressed in the Facial Branchiomotor Neurons (FBMNs)

Tag1 encodes a GPI-linked cell adhesion molecule that is expressed transiently in a variety of neurons, and may regulate cell-cell or cell-matrix interactions affecting intracellular signaling (Brummendorf and Rathjen, 1996; Warren et al., 1999). Expression of *tag1* in facial branchiomotor neurons (FBMNs) was previously reported in zebrafish and mouse (Warren et al., 1999; Garel et al., 2000). We examined *tag1* expression in detail in the zebrafish hindbrain, and found that putative FBMNs expressing *tag1* are located in rhombomeres 5 and 6 (r5-r6) at 18-19 hpf (Figure 5.1A). At 24 hpf, most of the expressing cells are found in r5-r6, coinciding with the period of extensive FBMN migration (Figure 5.1B and 5.1C). By 30 hpf, all *tag1*-expressing FBMNs are found in r6 and r7 (Figure 5.1E). Interestingly, labeling with anti-Tag1 antibody (Claudia Becker paper) shows that while FBMN axons express Tag1 along their entire length inside the hindbrain, only a few FBMN cell bodies in r6 and r7 express Tag1 (Figure 5.1D), suggesting that protein expression on cell bodies may be limited to the earliest motor neurons to migrate out of r4.

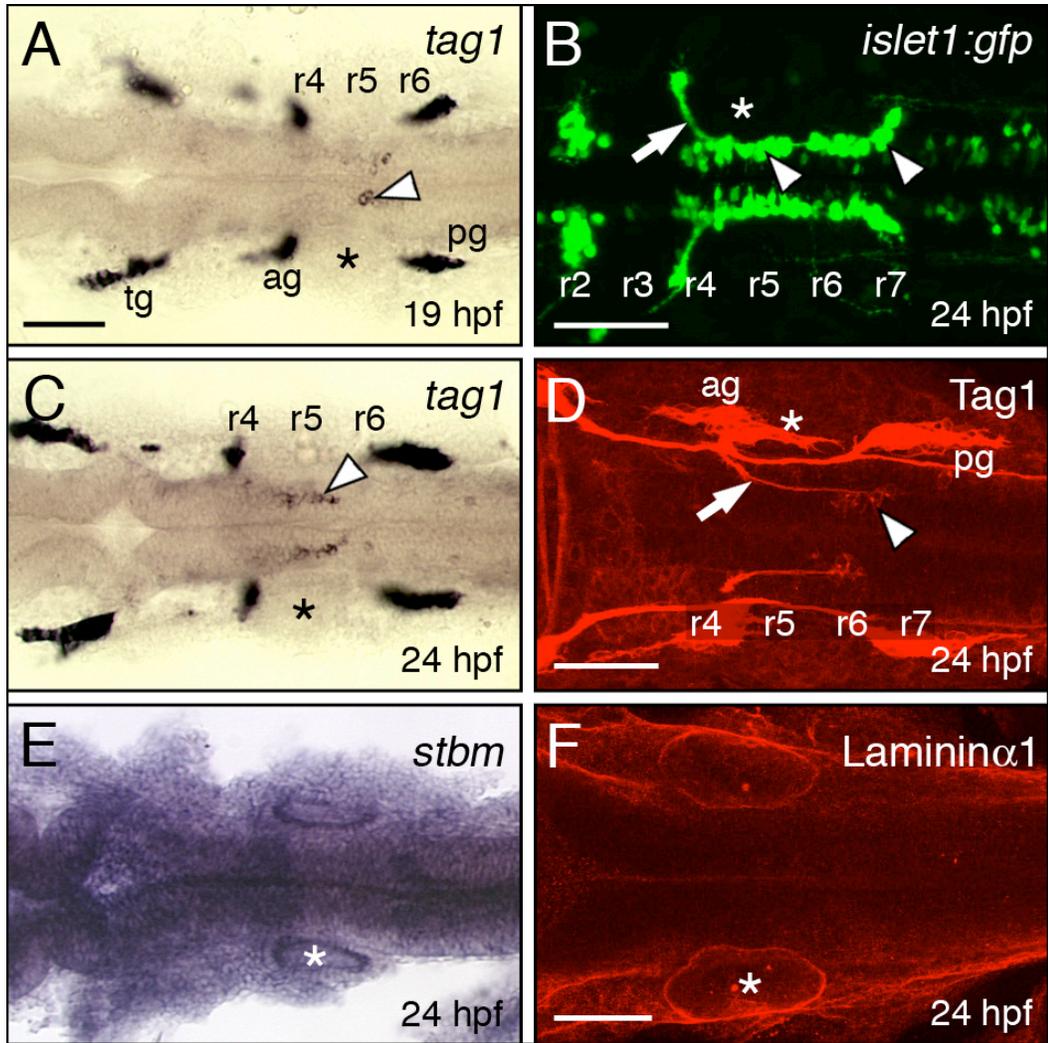


Figure 5.1 Expression patterns of *tag1*, *stbm*, and *lama1* in the hindbrain during FBMN migration.

All panels show dorsal views of the hindbrain with anterior to the left. Asterisks mark the otic vesicle in each panel. (A, C) *tag1* is expressed in an increasing number of migrating FBMNs (arrowheads) between 19 hpf (A) and 24 hpf (C). Strongest expression is initially found in cells located in r5/r6 (A), and later in cells spanning r5 and r6 (C). (B) In a 24 hpf *Tg(isl1:gfp)* embryo, FBMNs (arrowheads) are found throughout the migratory pathway from r4 to r7, with their axons (arrow) exiting the hindbrain in r4. (D) At 24 hpf, Tag1 immunostaining labels only cell bodies of FBMNs located in r6 and r7 (arrowhead), and their axons (arrow). (E) *stbm* is ubiquitously expressed in the neural tube, and in surrounding non-neural tissues. (F) Laminin immunostaining reveals ubiquitous expression of *lama1* in ventral neural tube and adjacent non-neural tissues. tg, trigeminal ganglion; ag, acoustic ganglion; pg, posterior lateral line ganglion. Scale bar in A (75 μ m for A, C, E); in B, D, F (75 μ m).

5.4.2 *Tag1* is necessary for the tangential migration of FBMNs in zebrafish

Since *tag1* is expressed in migrating FBMNs, we tested whether *tag1* is essential for this process by knocking down its expression using *tag1* antisense oligonucleotide morpholinos (MO) (Liu and Halloran, 2005; Wolman et al., 2008). Injection of *tag1* MO (6-15 ng/embryo) causes a dose dependent loss of FBMN migration (Figure 5.2D). At a moderate dose (9-12 ng), FBMN migration is impaired but not blocked (Figure 5.2B), whereas at high MO dose (15 ng), FBMNs mostly fail to migrate (Figure 5.2C). To test whether the *tag1* morphant phenotype results from the specific loss of *tag1* expression, we attempted to rescue the FBMN phenotype by expressing full-length *tag1* mRNA in MO-injected embryos. Expression of synthetic *tag1* mRNA lacking the MO-binding site does not have any effect on FBMN migration (Figure 5.3C, 5.3E). Co-injection of *tag1* mRNA and high dose of *tag1* MO leads to a significant reduction in the number of embryos with blocked FBMN migration (Figure 5.3B, D, and E), demonstrating the specificity of the *tag1* morphant phenotype.

5.4.3 Neuronal development in *tag1* morphants

There is appreciably more cell death in the *tag1* morphant hindbrain compared to wild-type embryos (Figure 5.4C, D), even after co-injection of p53 MO to reduce non-specific effects (Ekker 2005

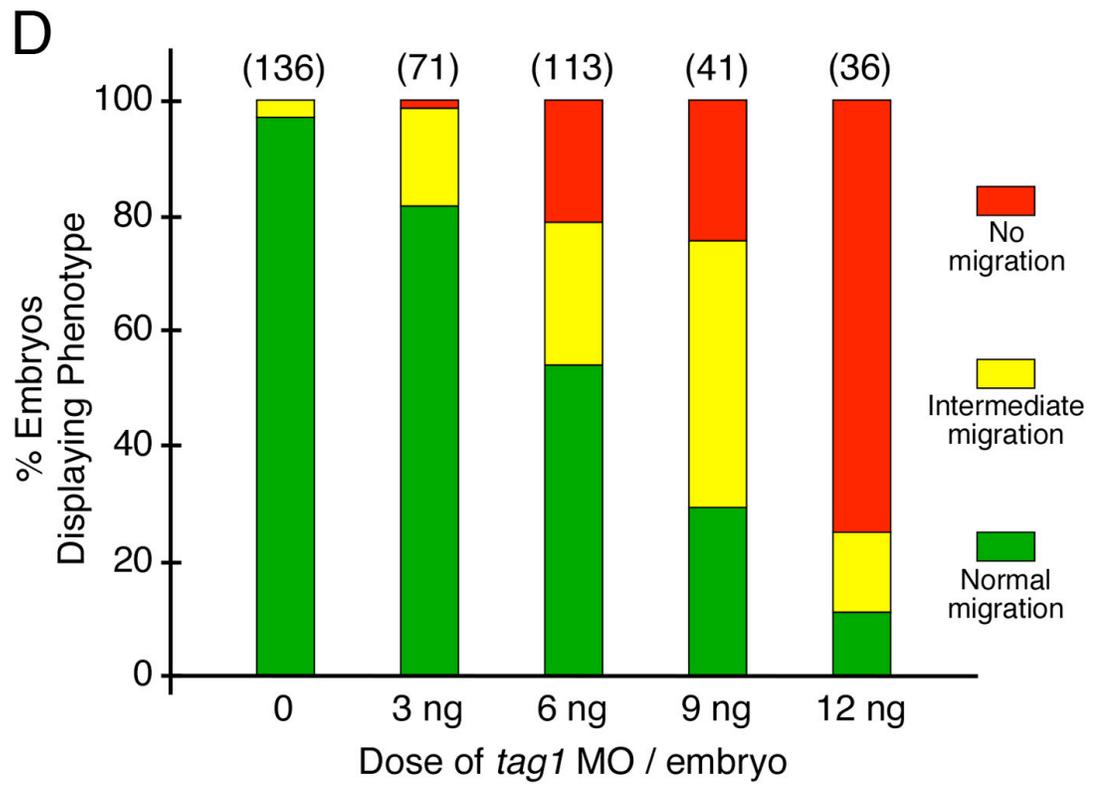
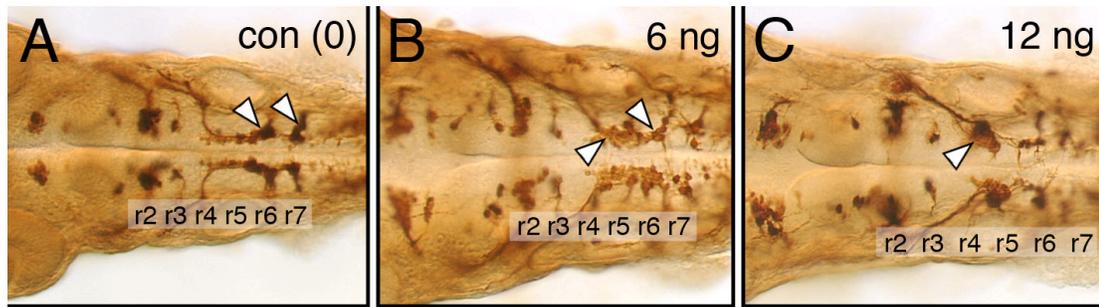


Figure 5.2 FBMN migration is affected in *tag1* morphants.

Top panels show dorsal views of the hindbrain with anterior to the left. (A) In a 36 hpf control (uninjected) embryo, FBMNs (arrowheads) migrate normally into r6 and r7. (B) An embryo injected with a suboptimal dose (6 ng) of *tag1* MO exhibits an intermediate phenotype, with many FBMNs (arrowheads) remaining in r4 and others migrating into r6 and r7. (C) In an embryo injected with an optimum dose (12 ng), most FBMNs (arrowhead) fail to migrate tangentially out of r4, but many appear to be displaced into r5. (D) Quantification of the *tag1* MO dose-response effect. The green, yellow, and red phenotypic classes correspond to the FBMN migration patterns depicted in panels A-C, respectively. Data from 2-3 experiments; number in parenthesis denotes number of embryos. Scale bar in A (75 μm for A-C).

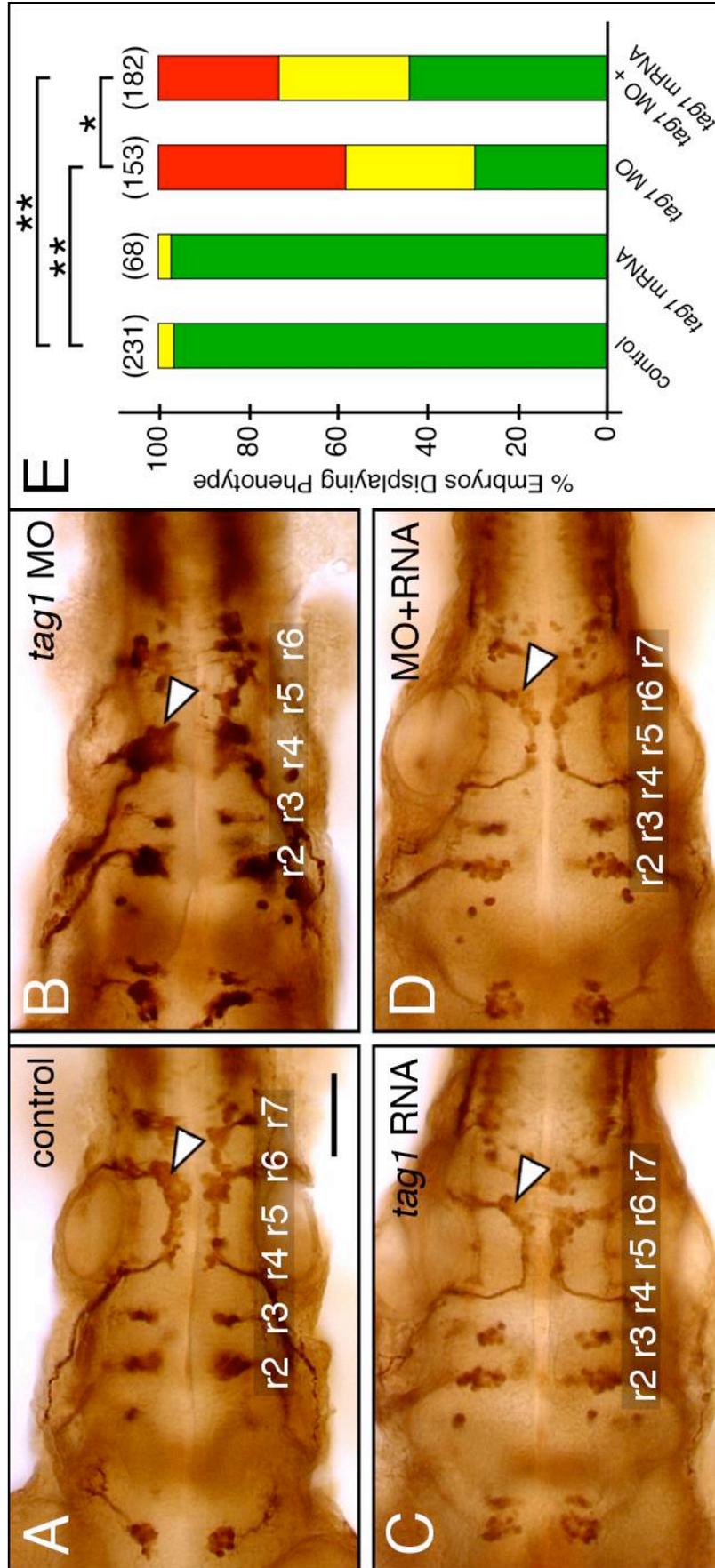


Figure 5.3 Rescue of the *tag1* morphant phenotype.

Panels A-D show dorsal views of the hindbrain with anterior to the left. Arrowheads indicate FBMNs. (A) FBMNs migrate normally in an uninjected control embryo. (B) FBMNs mostly fail to migrate in a *tag1* morphant embryo. (C) FBMNs migrate normally in a *tag1* mRNA injected embryo. (D) FBMN migration is mostly rescued in an embryo co-injected with *tag1* MO and *tag1* mRNA. (E) Quantification of the rescue data. The distribution of different phenotypes among the various treatments was analyzed by Pearson's Chi-Square statistics. The differences in the phenotypic distributions between the indicated pairs of samples were highly significant (*, $P < 0.01$; **, $P < 0.001$). Data from 4 experiments. Number in parenthesis denotes number of embryos. Scale bar in A (75 μm for A-D).

paper), indicating that the high *tag1* MO doses used (12-16 ng per embryo) may be slightly toxic. Nevertheless, hindbrain patterning and development are unaffected in morphant embryos. Hindbrain commissural neurons and their axons, labeled with the zn5 antibody (Trevarrow et al., 1990), are located at rhombomere boundaries and develop normally in *tag1* morphants (n=38) in a similar fashion to wild-type embryos (n=41) (Figure 5.4A, B). *Krox20* (Oxtoby and Jowett, 1993) expression in r3 and r5 is similar in wild-type (n=30) and morphant embryos (n=26) (Figure 5.4I, J). The ventrocaudal migration of noradrenergic locus coeruleus neurons from the cerebellum into r1, assayed by anti-tyrosine hydroxylase (TH) antibody (Guo et al., 1999) occurs normally in *tag1* morphants (n=60), as in wild-type embryos (n=54) (Figure 5.4K, L). These data suggest strongly that the *tag1* morphant hindbrain develops normally, with specific effects on FBMN migration.

Since *tag1* is expressed in cells such as the nucMLF neurons, the trigeminal sensory neurons, and the anterior and posterior lateral line ganglion neurons, in addition to the FBMNs (Warren et al., 1999), we examined their development in *tag1* morphants by tubulin immunostaining. The longitudinal fascicles (DLF and MLF; Chitnis and Kuwada, 1990) pioneered by the trigeminal sensory and nucMLF neurons are consistently more fluorescent, and apparently thicker, in *tag1* morphants (Figure 5.4F, H) compared to wild-type embryos

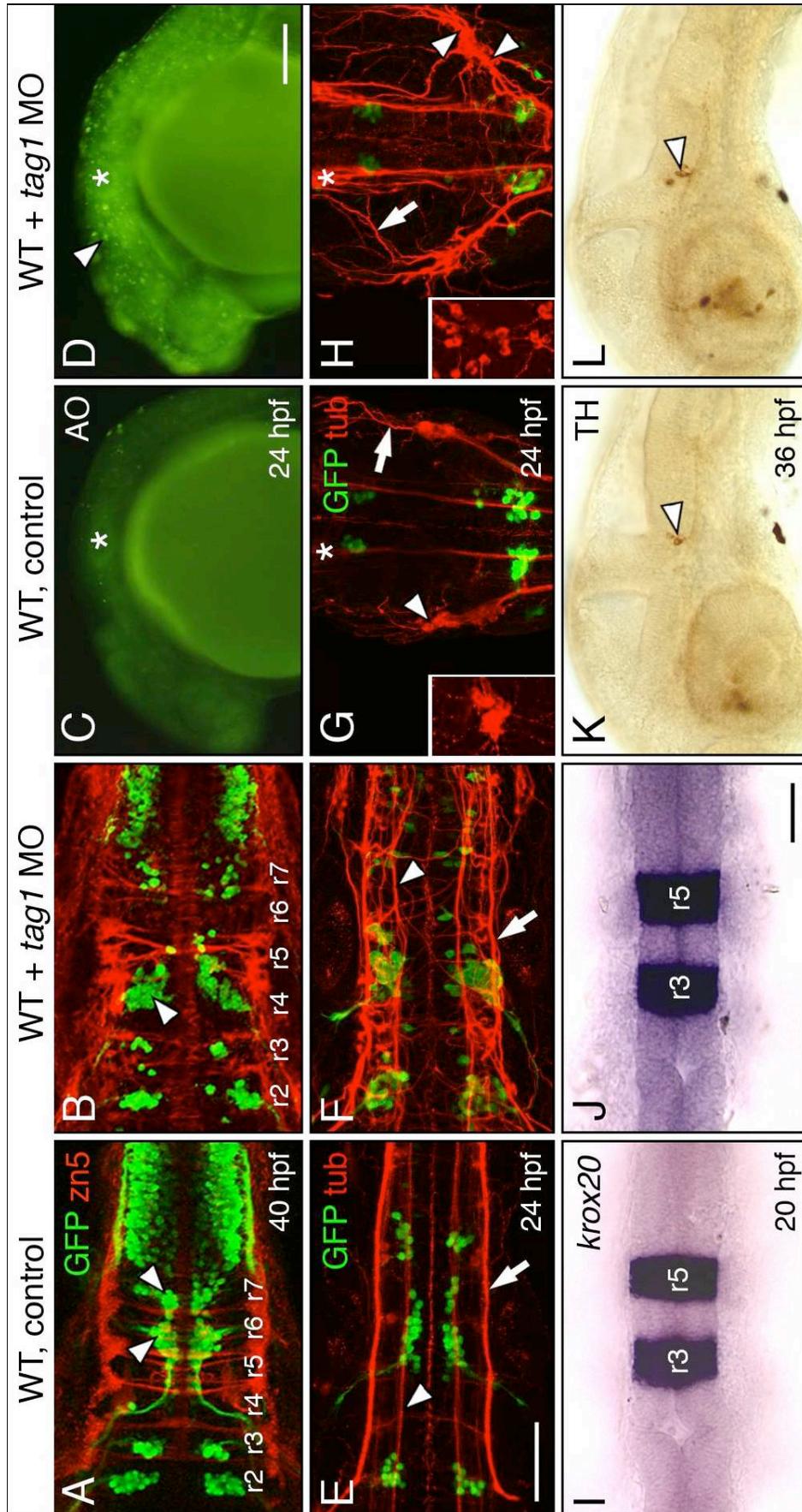


Figure 5.4 Neuronal defects in *tag1* morphants.

Panels A, B, E-J show dorsal views of the head with anterior to the left (anterior at top in G, H). Panels C, D, K and L show lateral views of the head with anterior to the left. *Tag1* morphants (D, F, H) were co-injected with *p53* MO to minimize non-specific apoptosis (Robu et al., 2007). WT embryos (controls) either uninjected or injected with *p53* MO alone exhibited identical phenotypes in the tissues examined. (A, B) Migration of FBMNs (arrowheads) into r6 and r7 (A) is mostly eliminated in a *tag1* MO-injected embryo (B). Zn5-labeled commissural neurons at rhombomere boundaries develop normally in morphants. (C, D) While acridine orange (AO) labeling reveals very few dying cells in a control embryo (C), there are many more dying cells (arrowhead) in a *tag1* morphant (D). Asterisk marks otic vesicle. (E) In a control embryo, FBMNs migrate in close proximity to the medial longitudinal fascicle (MLF, arrowhead). Arrow indicates the dorsal longitudinal fascicle (DLF) containing the central (afferent) axons of the trigeminal sensory neurons. (F) In a *tag1* morphant, the MLF (arrowhead) and DLF (arrow) appear brighter, but develop normally. (G, H) The trigeminal sensory ganglion (arrowhead) in a control embryo (G) is compact (inset shows lateral view), with a few prominent peripheral axons (arrowhead). In contrast, the trigeminal ganglion in a *tag1* morphant (H) is composed of loosely organized cells (arrowheads, and inset showing lateral view), with a large number of peripheral axons

(arrow). Asterisks indicate the nucleus of the MLF, with brightly-labeled projections in the morphant, compared to the control embryo. (I, J) Expression of *krox20* in r3 and r5 is similar between control and *tag1* morphant embryos. (K, L) Ventrocaudal migration of tyrosine hydrolase (TH)-positive locus coeruleus neurons (arrowhead) into r1 is similar between control and *tag1* morphant embryos. Scale bar in D (150 μm for C, D); in E (75 μm for A, B, E-H); in J (75 μm for I-L).

(Figure 5.4E, G). NucMLF neurons exhibit pronounced axon guidance defects following *tag1* knockdown (Figure 5.4G, H; Wolman et al., 2008). Mauthner cells, which are located in r4 and do not express *tag1*, developed normally with decussating axons (data not shown). The trigeminal sensory ganglion was dramatically affected in *tag1* morphants. The wild-type ganglion (Figure 5.4G) is compact, with 2-3 prominent dendrites extending into the ophthalmic and mandibular regions. By contrast, the cell bodies are greatly scattered in *tag1* morphants, with 5-10 prominent dendrites extending all over the head (Figure 5.4H) (data not shown). These data indicate that *tag1* knockdown leads to axon guidance, fasciculation, and adhesion defects that are limited to *tag1*-expressing neurons. Together with the effects on FBMN migration in *tag1* morphants, our data suggest strongly that *tag1* functions cell autonomously in these dynamic processes.

5.4.4 *Tag1*, *stbm* (*vangl2*) and *laminina1* genetically interact with each other to mediate FBMN migration

Migrating neurons likely regulate their behavior by interacting with cues found on neighboring cells and the extracellular matrix (ECM). The transmembrane protein *Stbm* (*Vangl2*) is expressed ubiquitously (Figure 5.1F), and functions non-cell autonomously during FBMN migration (Jessen et al., 2002), likely in floor plate cells (Chapter III). An ubiquitously expressed ECM molecule, Laminin α 1 (*Lama1*),

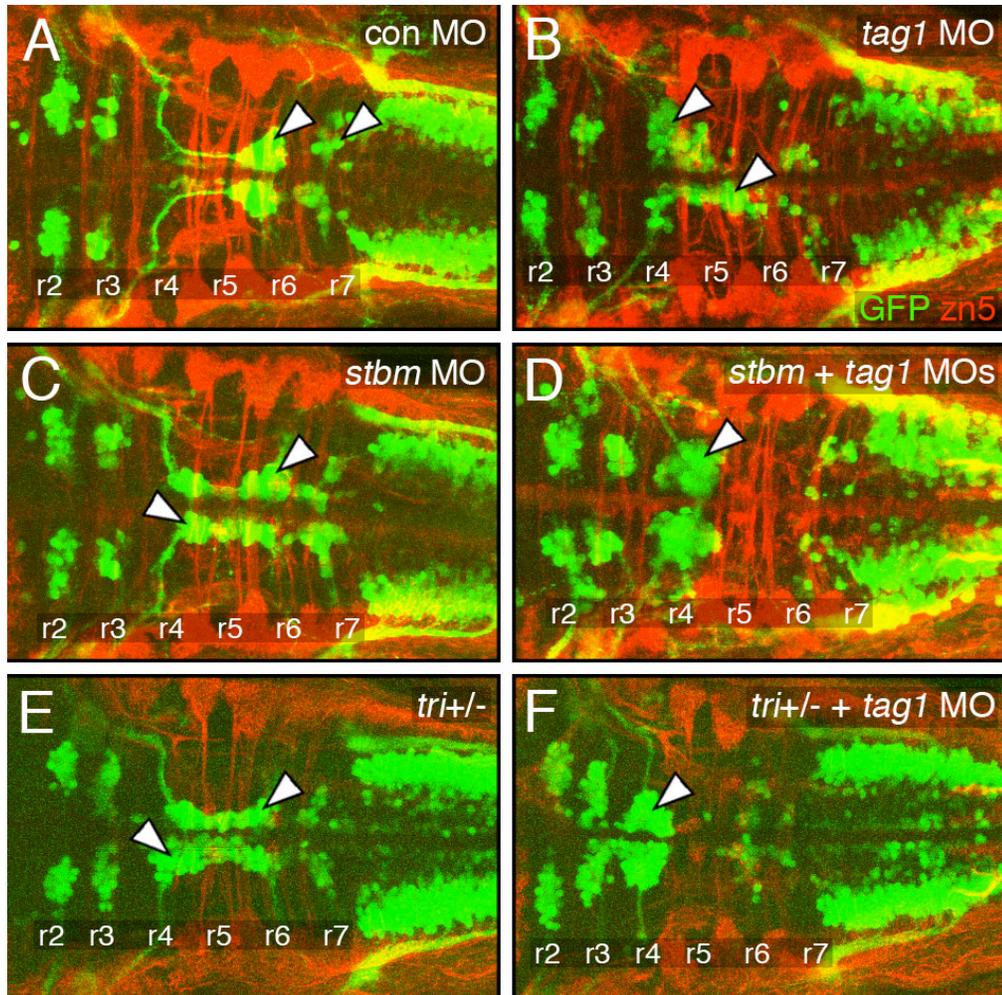


Figure 5.5 Genetic interactions between *tag1* and *stbm*.

All panels show dorsal views of the hindbrain with anterior to the left. *Tg(isl1:gfp)* embryos were fixed at 48 hpf, and processed for immunohistochemistry with zn5 antibody (red) to label commissural axons at rhombomere boundaries, and anti-GFP antibody (green) to label FBMNs (arrowheads). (A) FBMNs migrate normally in a control embryo. (B, C) Partial loss of FBMN migration in embryos injected with suboptimal dose of *tag1* MO (B) or *stbm* MO (C). (D) Complete loss of FBMN migration in an embryo injected with suboptimal doses of *tag1* and *stbm* MOs. (E) Partial loss of FBMN migration in a *trilobite*^{tc240a} (*tri*) heterozygous (*stbm*^{+/-}) embryo. (F) Complete loss of FBMN migration in a trilobite heterozygote injected with suboptimal dose of *tag1* MO. Scale bar in F (75 μm for A-F).

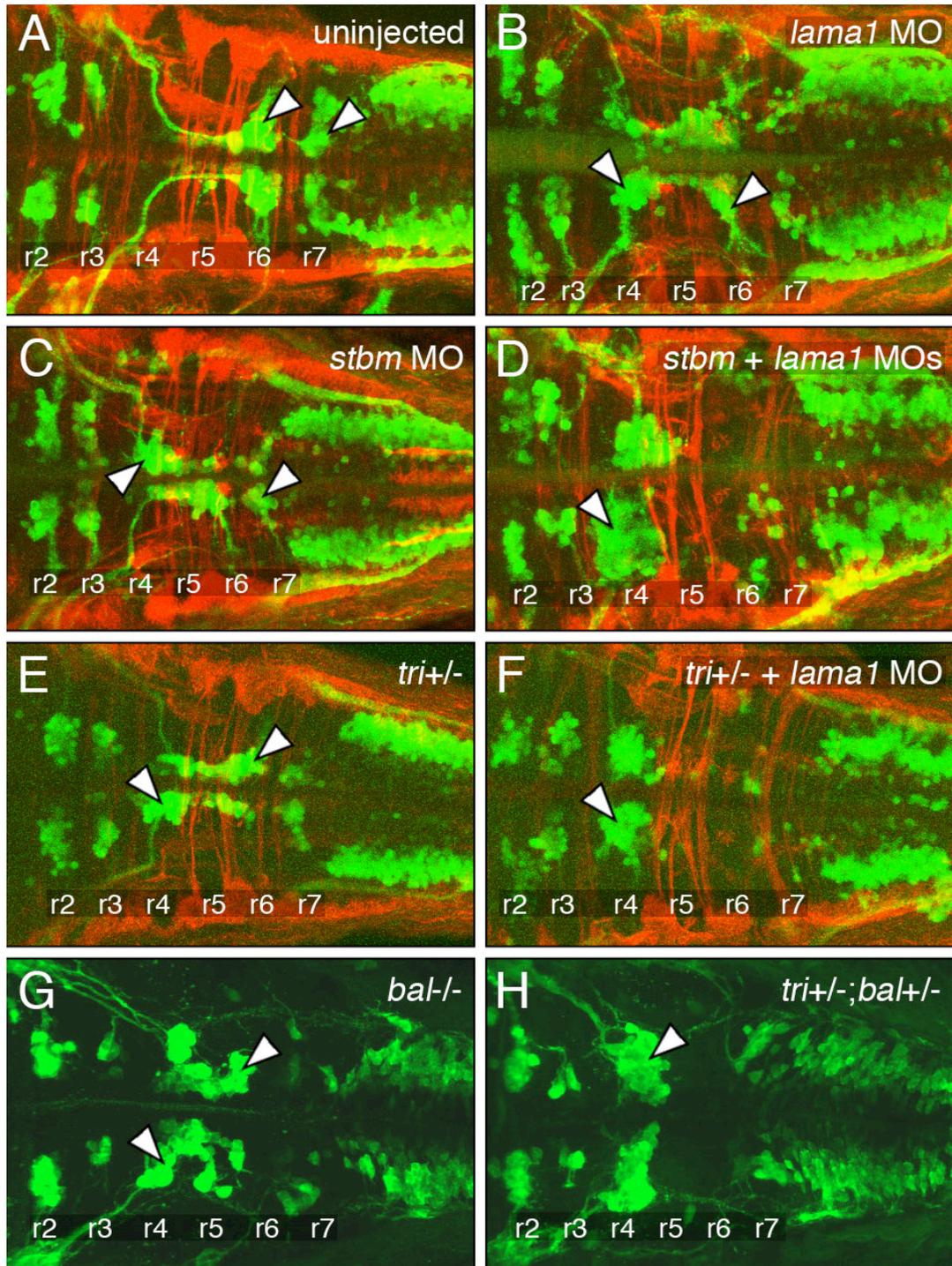


Figure 5.6 Genetic interactions between *stbm* and *lama1*.

All panels show dorsal views of the hindbrain with anterior to the left. *Tg(isl1:gfp)* embryos were fixed at 48 hpf, and processed for immunohistochemistry with zn5 antibody (red) to label commissural axons at rhombomere boundaries (A-F), and anti-GFP antibody (green) to label FBMNs (A-H; arrowheads). (A) FBMNs migrate normally in a control embryo. (B, C) Partial loss of FBMN migration in embryos injected with suboptimal dose of *lama1* MO (B) or *stbm* MO (C). (D) Complete loss of FBMN migration in an embryo injected with suboptimal doses of *lama1* and *stbm* MOs. (E) Partial loss of FBMN migration in a trilobite^{tc240a} (tri) heterozygous (*stbm*^{+/-}) embryo. (F) Complete loss of FBMN migration in a *trilobite* heterozygote injected with suboptimal dose of *lama1* MO. (G) Greatly reduced FBMN migration in a *bashful*^{b765} homozygous (*lama1*^{-/-}) embryo. (H) Complete loss of FBMN migration in a *trilobite*; *bashful* double heterozygote. Scale bar in H (75 μm for A-H).

also plays a role in FBMN migration (Paulus and Halloran, 2006). Therefore, we tested whether *stbm* and *lama1* exhibited genetic interactions with *tag1* for FBMN migration.

irst, we performed extensive dose-response analysis to identify the optimum and suboptimal doses for *tag1*, *stbm*, and *lama1* MOs that would cause complete and partial loss of FBMN migration, respectively. The optimum MO doses were 15 ng for *tag1* (Figure 5.2D) and 3 ng for *stbm* and *lama1* (data not shown), and the suboptimal doses were 9 ng for *tag1* (Figures 5.2B, 5.5B and 5.7C) and 1.5 ng for *stbm* (Figs. 5C and 6C) and *lama1* (Figs. 6B and 7B). Nearly all uninjected wild-type and control MO-injected (7 ng and 11 ng) embryos exhibited normal FBMN migration (Figures 5.5A, 5.6A, 5.7A and 5.8). Co-injection of suboptimal doses of *tag1* and *stbm* MOs has a synergistic effect, leading to complete loss of FBMN migration in a majority of embryos (Figures 5.5D and 5.8). To test further, we injected a suboptimal dose of *tag1* MO into embryos from crosses between wild-type and *tri*^{-/-} fish carrying the *isl1-GFP* transgene (generating 100% heterozygous embryos). While most uninjected *tri*^{+/-} embryos exhibited intermediate migration defects (Figures 5.5E and 5.8), over 60% of *tag1* MO-injected heterozygotes showed complete loss of FBMN migration (Figures 5.5F and 5.8). These data suggest strongly that *tag1* and *stbm* function together to mediate FBMN migration.

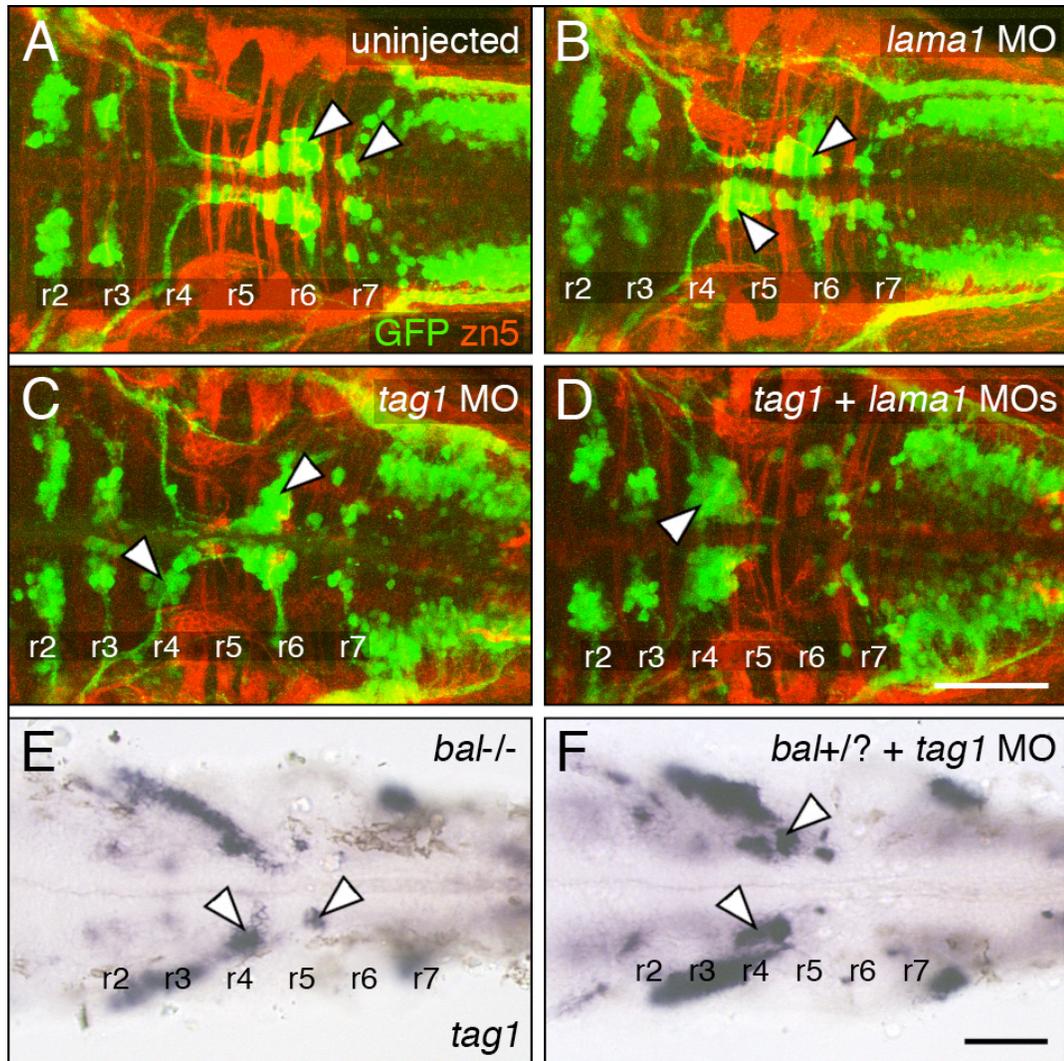


Figure 5.7 Genetic interactions between *tag1* and *lama1*.

All panels show dorsal views of the hindbrain with anterior to the left. *Tg(isl1:gfp)* embryos (A-D) were fixed at 48 hpf, and processed for immunohistochemistry with zn5 antibody (red) to label commissural axons at rhombomere boundaries, and anti-GFP antibody (green) to label FBMNs (arrowheads). Non-transgenic embryos (E, F) were fixed at 30 hpf, and processed for *tag1* in situ hybridization to label FBMNs (arrowheads). (A) FBMNs migrate normally in a control embryo. (B, C) Partial loss of FBMN migration in embryos injected with suboptimal dose of *lama1* MO (B) or *tag1* MO (C). (D) Complete loss of FBMN migration in an embryo injected with suboptimal doses of *tag1* and *lama1* MOs. (E) Greatly reduced FBMN migration in a *bashful*^{uw1} homozygous (*lama1*^{-/-}) embryo. (H) Severe, nearly complete loss of FBMN migration in a putative *bashful* heterozygote injected with suboptimal dose of *tag1* MO. Scale bar in D (75 μm for A-D); in F (75 μm for E, F).

In control experiments, we co-injected suboptimal doses of *stbm* or *tag1* MO with control MO to match the MO dose of *stbm* + *tag1* MO injections. In these experiments, the control MO did not exacerbate the intermediate FBMN phenotype generated by injection of suboptimal doses of *stbm* or *tag1* MO alone (data not shown), indicating that the synergistic effect of *stbm* + *tag1* MO co-injection is not an artifact of the amount of MO injected. Co-injection of suboptimal doses of *stbm* and *lama1* MOs also results in complete loss of FBMN migration (Figures 5.6D and 5.8). Next, injection of suboptimal dose of *lama1* MO into *tri*^{+/-} embryos, which show intermediate FBMN phenotype (Figures 5.6E), also leads to elimination of FBMN migration (Figures 5.6F and 5.8). Finally, we examined embryos from a *bal (lama1)* ^{+/-}; *tri (stbm)* *Tg(isl1:gfp)* incross. The embryos were sorted on the basis of trunk (*tri* phenotype) and hindbrain (*bal* phenotype) morphology. The *bal* mutant embryos display nearly complete loss of FBMN migration (Figure 5.6G; n=3) as described previously (Paulus and Halloran, 2006). Importantly, putative double heterozygous embryos are morphologically wild-type, but exhibit complete loss of FBMN migration (Figure 5.6H; n=7). These results suggest strongly that *stbm* and *lama1* genetically interact during FBMN migration.

Co-injection of suboptimal doses of *lama1* and *tag1* MOs also results in complete loss of FBMN migration (Figures 5.7D and 5.8). Next, we injected a suboptimal dose of *tag1* MO into embryos from

a *bal*^{+/-} incross, and assayed FBMN migration at 30 hpf using *tag1* in situ. While FBMN migration was largely blocked in *bal* mutants as expected (Figure 5.7E), migration was also mostly eliminated in putative *bal*^{+/-} heterozygotes (Figure 5.7F), suggesting strongly that *tag1* and *lama1* interact genetically during FBMN migration.

5.4.5 *Tag1*, *stbm*, and *lama1* regulate persistent movement of FBMNs

The genetic interaction data suggest that *tag1*, *stbm*, and *lama1* participate in the same pathway to regulate FBMN migration. Therefore, we examined whether knockdown of function of these genes affected dynamic cellular behavior in similar fashion. Since FBMNs fail to move out of r4 in morphant embryos, we restricted our behavioral analyses to motor neurons located in r4. GFP-expressing FBMNs in control and morphant embryos (injected with optimum dose) were imaged at 2 min intervals beginning at 18-19 hpf, and several motility parameters were calculated from the processed time-lapse movies (Table 5.2; see Materials and Methods). Control and morphant embryos have similar length-to-width ratios, move at comparable speeds within r4, and display similar amounts of protrusive activity (rate of area change). However, as expected, FBMNs in morphant embryos move very slowly along the rostrocaudal axis toward r5 (caudal speed) compared to control FBMNs due to their inability to maintain a

persistent direction (caudal directionality), although *tag1* morphant FBMNs appear to be less affected. This defect results from the inability of morphant FBMNs to generate protrusions in a directed (polarized) fashion compared to control embryos (rate of direction change; Figure 5.8). Difference images show that whereas control cells preferentially form protrusions in the caudal direction, with few direction changes (Figure 5.8A), morphant embryos generated protrusions in random directions leading to significant direction changes and little net progress toward r5 (Figure 5.8B-D). We also examined FBMN behaviors in *tri*[±] embryos injected with suboptimal doses of *tag1* or *lama1* MOs. These data demonstrate that knockdown of *tag1*, *stbm*, and *lama1* have similar effects in the dynamic behavior of FBMNs, suggesting that the three molecules may regulate the same cellular process involved in the generation of persistent protrusive activity.

DISCUSSION

Transiently expressed Axonal Glycoprotein 1 (Tag1) is a well-studied member of immunoglobulin (Ig) superfamily, and is involved in variety of developmental processes such as cell adhesion, neurite outgrowth, axon pathfinding and neuronal migration. The role of Tag1 in each of these processes is complex and can vary in different cellular contexts. Tag1 can mediate cell-cell contacts through homophilic

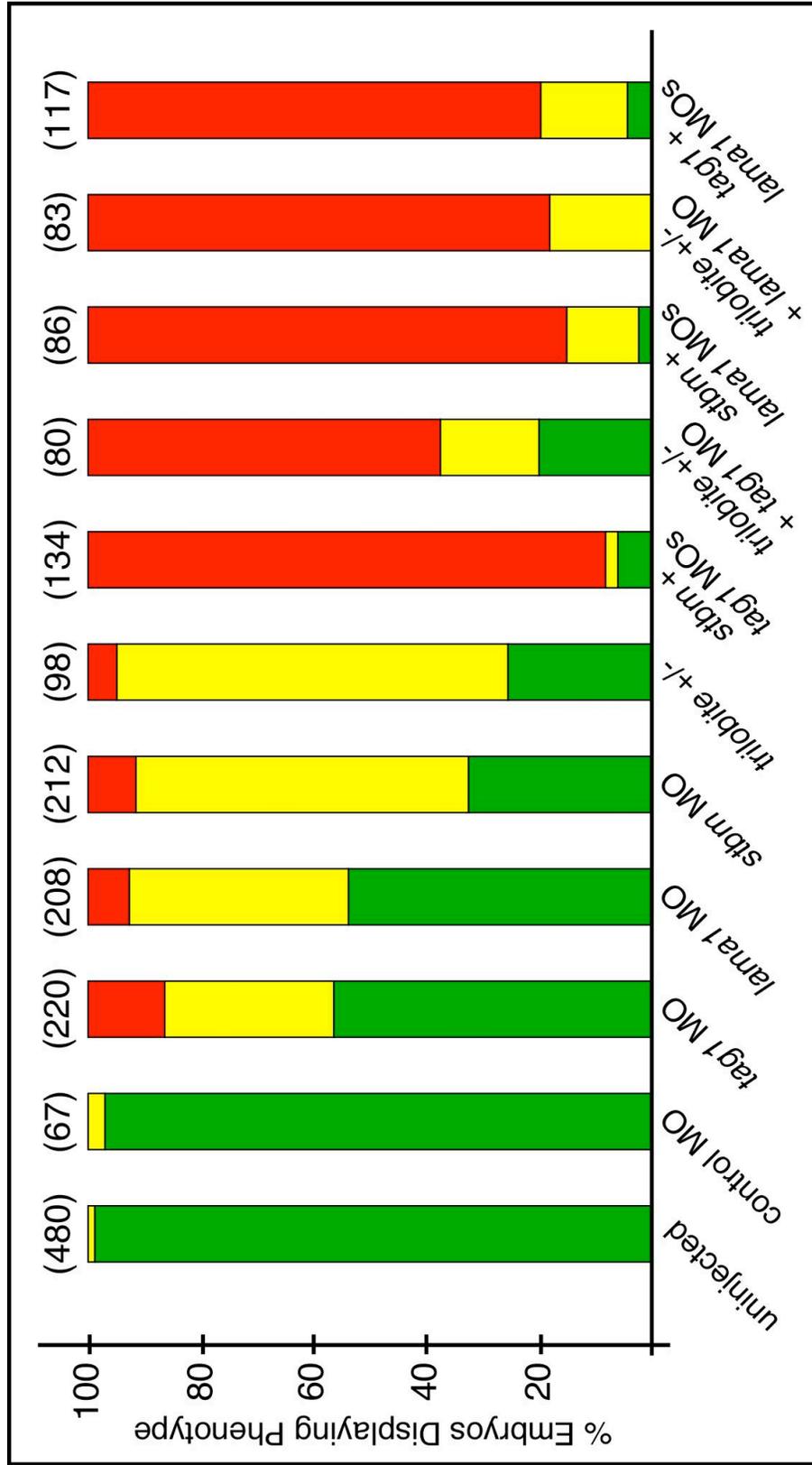


Figure 5.8 Quantification of genetic interaction data.

Pairwise comparisons were done using Pearson's Chi-square statistics. The differences in the phenotypic distributions between pairs of samples were either not significant (NS), or highly significant (*, $P < 0.01$; **, $P < 0.001$). Data from 2-6 experiments; number in parenthesis denotes number of embryos.

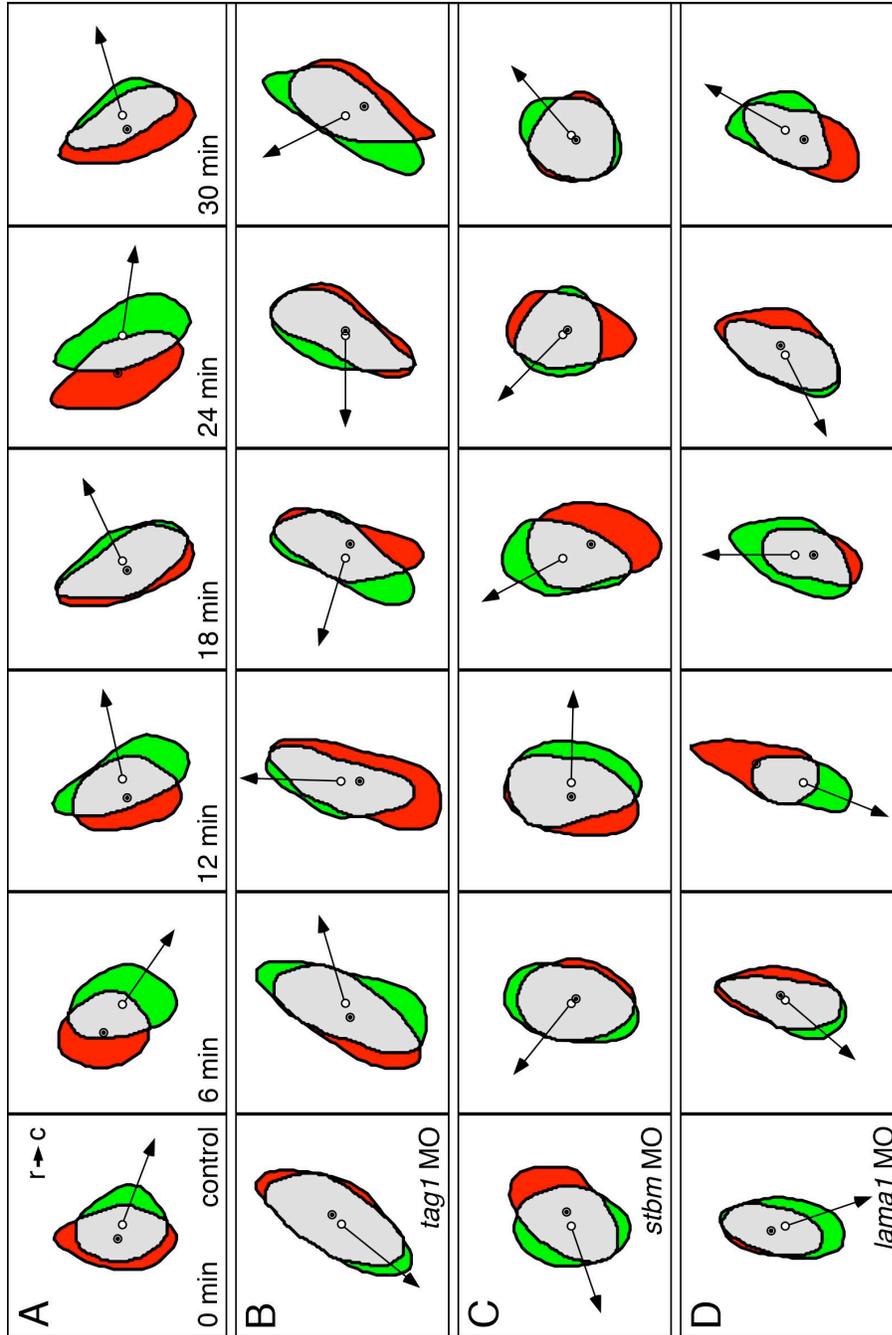


Figure 5.9 FBMNs deficient in *tag1*, *stbm* or *lama1* function exhibit non-polarized protrusive activity.

Panels show difference images at 6-minute intervals of motor neurons located in r4. Red indicates area of retraction from previous cell position, and green indicates area of protrusion in current cell position. The filled and open circles mark the centroids in the previous and current cell positions, respectively. Arrows point in the direction of cell movement. (A) An FBMN in a control embryo generates protrusions that are biased toward the caudal (c) direction, and retractions that are biased toward the rostral (r) direction, resulting in net caudal translocation of the cell. (B-D) In a *tag1* MO- (B), *stbm* MO- (C), or *lama1* MO- (D) injected embryo, protrusion and retraction areas form in relatively random directions around the periphery of the FBMN. Consequently, the neurons switch directions frequently, resulting in little or no caudal translocation. At least 6 motor neurons were examined by shape analysis for each condition.

Table 5.1: Genetic interactions during FBMN migration between *trilobite* (*stbm*⁻), *bashful* (*lama1*⁻), and *tag1* morphant embryos

| | Control (15 cells) | <i>Stbm</i> MO (15 cells) | <i>Tag1</i> MO (15 cells) | <i>Lama1</i> MO (15 cells) |
|---|--------------------------|------------------------------------|------------------------------------|-------------------------------------|
| Speed (µm/hr) | 19.40 ± 6.72 | 24.55 ± 8.88 | 24.05 ± 5.34 | 22.76 ± 5.46 |
| Length to Width ratio | 2.03 ± 0.33 | 2.07 ± 0.67 | 1.85 ± 0.38 | 1.97 ± 0.39 |
| Directionality | 0.37 ± 0.16 | 0.46 ± 0.20 | 0.47 ± 0.26 | 0.44 ± 0.19 |
| Caudal speed (µm/hr) | 8.35 ± 6.48 | 0.96 ± 5.46* | 2.70 ± 5.94* | 0.90 ± 4.80* |
| Caudal directionality | 0.27 ± 0.20 | 0.01 ± 0.33* | 0.16 ± 0.32 | 0.05 ± 0.27* |
| Rate of Direction Change (# of 90° changes/10 min) | 1.18 ± 0.51 | 1.75 ± 0.56* | 1.74 ± 0.45* | 1.39 ± 0.56 |
| Rate of Area Change (µm ² /min) | 13.42 ± 1.99 | 12.18 ± 3.59 | 12.53 ± 3.67 | 12.47 ± 2.80 |

See Methods section for definition of parameters and their calculation
*, Highly significant with $p < 0.05$

Table 5.2: Differences in dynamic behaviors between FBMNs located in r4 of morphant embryos

| | Control (15 cells) | <i>tag1</i> MO (15 cells) | <i>Stbm</i> MO (15 cells) | <i>lama1</i> MO (15 cells) |
|---|-----------------------|------------------------------|------------------------------|-------------------------------|
| Speed ($\mu\text{m/hr}$) | 19.40 \pm 6.72 | 24.05 \pm 5.34 | 24.55 \pm 8.88 | 22.76 \pm 5.46 |
| Length to Width Ratio (LWR) | 2.03 \pm 0.33 | 1.85 \pm 0.38 | 2.07 \pm 0.67 | 1.97 \pm 0.39 |
| Rate of Area Change ($\mu\text{m}^2/\text{min}$) | 13.42 \pm 1.99 | 12.53 \pm 3.67 | 12.18 \pm 3.59 | 12.47 \pm 2.80 |
| Caudal speed ($\mu\text{m/hr}$) | 8.35 \pm 6.48 | 2.70 \pm 5.94* | 0.96 \pm 5.46* | 0.90 \pm 4.80* |
| Caudal directionality | 0.27 \pm 0.20 | 0.16 \pm 0.32 | 0.01 \pm 0.33* | 0.05 \pm 0.27* |
| Rate of Direction Change (# of 90° changes/10 min) | 1.74 \pm 0.60 | 2.89 \pm 0.56* | 2.77 \pm 0.53* | 2.77 \pm 0.46* |

See Methods section for definition of parameters and their calculation
*, Highly significant with $p < 0.05$

binding on apposed membranes (trans interaction) (Rader et al., 1993; Felsenfeld et al., 1994) and also by heterophilic interactions with other cell adhesion molecules like L1/NgCAM (Kuhn et al., 1991), NrCAM (Suter et al., 1995), NCAM (Milev et al., 1996), proteoglycans like neurcan and phosphacan and extracellular matrix molecules like tenascinC (Milev et al., 1996). In addition, *tag1* is expressed in the migrating cells of superficial migratory stream of the caudal medulla, and is required for their migration (Kyriakopoulou et al., 2002; Denexa et al., 2005). Interestingly, while Tag1 is a GPI-anchored membrane protein, it may be able to regulate intracellular signaling indirectly through its extracellular interactions with transmembrane proteins like L1/NgCAM (Lemmon et al., 1992; Zisch et al., 1995; Brummendorf and Rathjen, 1996; Law et al., 2008).

We show here that zebrafish *tag1* (Warren et al., 1999) is necessary for FBMN migration. In 24 hpf embryos, Tag1 protein is detected only on the axons and cell bodies of a subset of FBMNs located in r6 and r7, which are likely to be the earliest motor neurons to have migrated out of r4. While FBMNs located in r4 and r5 express *tag1* mRNA, these neurons do not express Tag1 protein implicating post-transcriptional regulation of *tag1* expression, which has not been reported previously. Interestingly, migration of all FBMNs is blocked in *tag1* morphants, suggesting that *tag1* knockdown blocks migration of the earliest-migrating ("pioneer") FBMNs (expressing Tag1 protein),

which in turn may regulate the migration of later-migrating ("follower") FBMNs (not expressing Tag1 protein). This putative non-autonomous effect on "follower" FBMNs could be mediated by heterophilic interactions of Tag1 with other cell adhesion molecules like NrCAM or L1/NgCAM (Brummendorf and Rathjen, 1996) or Contactin1 (Fujita and Nagata, 2007), or may be independent of Tag1 function.

We observed significant but incomplete rescue of FBMN migration defects in *tag1* morphants injected with full-length wild-type *tag1* mRNA. Since the FN and Ig domains are both necessary for Tag1 homophilic interactions (Tsiotra et al., 1996; Kunz et al., 2002; Pavlou et al., 2002), the rescuing abilities of variants lacking these domains will reveal the importance of homophilic interactions in Tag1-mediated FBMN migration. Since GPI-anchored proteins like Tag1 can be released into the extracellular matrix, it would be instructive to test the abilities of secreted and membrane-bound forms of Tag1 to rescue FBMN migration given that these forms of Tag1 exhibit different activities in aggregation assays (Pavlou et al., 2002).

In *tag1* morphants, Tg sensory neurons fail to cluster and are mostly found as isolated cells, whereas these neurons are tightly clustered in wild-type embryos. These data suggest that Tag1 may help maintain the integrity of the ganglion, which is consistent with its potential to interact homophilically and heterophilically with other cell adhesion molecules (Brummendorf and Rathjen, 1996). Tg afferent

axons are defasciculated following ectopic Slit or neurotrophin expression (Yeo et al., 2004; Ozdinler et al., 2004), and Tg peripheral axons are defasciculated following contactin1 knockdown (Fujita and Nagata, 2007), but our observations are the first report of disruption of Tg cell body clustering. Other cell types expressing *tag1* such as the nucMLF in the midbrain and Rohon-Beard sensory neurons in the spinal cord also exhibit specific defects in axon outgrowth in *tag1* morphants (Liu and Halloran, 2005; Wolman et al., 2008). We have not yet carefully examined in *tag1* morphants the development of other *tag1*-expressing cell types such as retinal ganglion cells, cerebellar neurons, and trunk neural crest cells (Warren et al., 1999).

We have identified strong pairwise genetic interactions between *tag1*, *stbm*, and *lama1* during FBMN migration. Other studies have documented genetic interactions of *stbm* with *pk1a* (encoding a cytoplasmic Stbm-interacting protein; Carreira-Barbosa et al., 2003), *celsr2* (encoding an atypical Cadherin; Wada et al., 2006), and *hdac1* (encoding histone deacetylase 1; Nambiar et al., 2007) for neuronal migration. One caveat of these studies is that co-injecting suboptimal doses of morpholinos against any two genes may generate non-specific artifacts, with FBMN migration being especially sensitive to these effects. However, we believe this is unlikely for two reasons. First, all of the pairwise interactions have also been observed when MO targeted against one gene was injected into embryos heterozygous for

hypomorphic or null mutations in the second gene. Second, co-injection of control mismatch MOs with a suboptimal dose of a gene-targeting MO does not exacerbate FBMN migration defects generated by the gene-specific MO alone.

The connection between the identified genetic interactions and the underlying molecular mechanisms is unclear. The parsimonious explanation is that *stbm*, *tag1*, and *lama1* participate in a common mechanism mediating FBMN migration. Moreover, analysis of single cell behaviors by time-lapse imaging indicates that knocking down the expression of any of the three genes leads to similar deficits in the ability of FBMNs to generate protrusions in a specific direction, suggesting again that these genes regulate a singular mechanism underlying a specific cell behavior. It is unlikely that *Stbm* interacts directly with either *Tag1* or *Lama1* since the two predicted extracellular loops *Stbm* are only 15-18 amino acids long, with little secondary structure (Dr. Dong Xu, Department of Computer Science, University of Missouri, personal communication). Importantly, *Stbm* functions non-cell autonomously in neuroepithelial cells in the ventral neural tube, including floor plate cells (V.S. and A.C., manuscript in preparation), whereas *Tag1* may function cell autonomously on FBMNs; hence, *Stbm* and *Tag1* likely do not interact either in cis or in trans to regulate FBMN migration. Interestingly, other molecules discussed below may provide

a link between these disparate but functionally associated membrane proteins.

The cytoplasmic protein Scrb1, which is the zebrafish ortholog of the *Drosophila* apicobasal polarity protein Scribble, binds Stbm, is required for FBMN migration, and functions non-cell autonomously for this process (Wada et al., 2005). In *Drosophila*, scribble interacts genetically with α PS3 integrin, a member of the α -integrin gene family, for cell cycle entry (Brumby et al., 2004), raising the possibility that vertebrate scrb1 may genetically interact with integrin genes during FBMN migration. Importantly, Tag1 and other Ig superfamily members like L1 physically interact with each other in cis, and L1 physically interacts with β 1 Integrins (Brummendorf and Rathjen, 1996; Malhotra et al., 1998; Thelen et al., 2002). Furthermore, Tag1-mediated migratory events in cultured neurons require L1 and β 1 Integrin functions (Felsenfeld et al., 1994). These studies suggest that the genetic interactions that we have described between *stbm*, *tag1*, and *lama1* may reflect a fundamental role for β 1 Integrins in FBMN migration. Experiments testing this hypothesis are in progress.

CHAPTER SIX

Expression of Unconventional Myosin Genes During Neuronal Development in Zebrafish

Published: Sittaramane, V and Chandrasekhar, A., Gene Expression Patterns. 2008. Feb; 8 (3): 161-70.

6.1 Abstract

Neuronal migration and growth cone motility are essential aspects of the development and maturation of the nervous system. These cellular events result from dynamic changes in the organization and function of the cytoskeleton, in part due to the activity of cytoskeletal motor proteins such as myosins. Although specific myosins such as myosin 2 (also known as conventional or muscle myosin), myosin 1, and myosin 5 have been well characterized for roles in cell motility, the roles of the majority of unconventional (other than myosin 2) myosins in cell motility events have not been investigated. To address this issue, we have undertaken an analysis of the unconventional myosins in zebrafish, a premier model for studying cellular and growth cone motility in the vertebrate nervous system. Here, we report the characterization and expression patterns of several members of the unconventional myosin gene family. Based on

available genomic sequence data, we have identified 17 unconventional myosin- and 4 myosin 2-related genes in the zebrafish genome in addition to previously characterized myosin (-1, -2, -5, -6, -7) genes. Phylogenetic analyses indicate that these genes can be grouped into existing classifications for unconventional myosins from mouse and man. In situ hybridization analyses using EST probes for 15 of the 21 identified genes indicate that 11/15 genes are expressed in a restricted fashion in the zebrafish embryo. Specific myosins are expressed in particular neuronal or neuroepithelial cell types in the developing zebrafish nervous system, consistent with potential roles in neuronal migration and/or growth cone motility.

6.2 Introduction

During embryogenesis, neuronal cell bodies and growth cones migrate extensively to establish precisely connected networks with target tissues. The functional properties of neural networks underlying physiology and behavior are critically dependent upon accurate positioning of neuronal cell bodies, and their axonal and dendritic processes. Not surprisingly, a number of brain disorders result from the loss of or aberrant migration of neurons and defective axon guidance (Copp and Harding, 1999; Gleeson and Walsh, 2000; Oster and Sretavan, 2003; ten Donkelaar et al., 2004). A large number of extracellular cues and their receptors have been intensively studied,

and demonstrated to play essential roles in regulating the migration of neuronal growth cones and cell bodies (Chilton, 2006). Furthermore, the biochemical and molecular interactions between the signal transduction cascades initiated by these guidance cues and the cytoskeletal machinery that controls dynamic cellular and growth cone behaviors are being elucidated (Guan and Rao, 2003; Kalil and Dent, 2005). Nevertheless, the roles of specific components of the actin and microtubule cytoskeletons in generating particular responses to extracellular cues remain obscure. We are interested in characterizing the functions of the unconventional, non-muscle myosins in neuronal migration and axon guidance, and in elucidating whether these activities are regulated by guidance cues in the developing nervous system.

Unconventional non-muscle myosins are actin-binding motor proteins that lack the tail domain of conventional muscle myosin (myosin 2), and function in numerous processes including cell migration in lower eukaryotes, intracellular motility and trafficking, and sensory transduction (Libby and Steel, 2000; Tuxworth and Titus, 2000; Wu et al., 2000; Soldati, 2003; Hirokawa and Takemura, 2003). Furthermore, unconventional myosins have been localized to neuronal growth cones and regulate growth cone motility in vitro (Wang et al., 1996; Evans et al., 1997; Suter et al., 2000; Deifenbach et al., 2002; De La Cruz et al., 2004; Sousa et al., 2006). Phylogenetic analysis of the catalytic head

domain (containing the ATP-binding site) of all available myosin heavy chain sequences shows that 18 families of myosins exist, including conventional (muscle) myosin 2, and the plant-specific myosin 8 (Sellers, 2000; Berg et al., 2001; Volkmann et al., 2003). In addition to differences in the catalytic head domain, unconventional myosins belonging to various families differ in the presence and arrangement of specific domains and motifs (Figure 6.1) that likely confer unique functions on each class of proteins (Wu et al., 2000; De La Cruz and Ostap, 2004). Whereas only 4-6 unconventional myosin families have been identified in unicellular organisms and invertebrates like *Caenorhabditis*, comprehensive phylogenetic analyses have identified over 10 unconventional myosin families in *Drosophila*, and 16 unconventional myosins (except myosin 8) in mammals (Berg et al., 2001).

There has been no systematic characterization of unconventional myosins in zebrafish. Mutations generating defects in sensory neuron development and function have led to the cloning of members of the myosin 6 and 7 families (Ernest et al., 2000; Kappler et al., 2004; Seiler et al., 2004; Coffin et al., 2007). Since the zebrafish embryo is an excellent model for studying cell migration and axon guidance (Kuwada, 1995; Hutson and Chien, 2002), the potential roles of unconventional myosins in these dynamic cellular processes can be readily investigated. Therefore, we have carried out an extensive

characterization of the expression of unconventional myosin genes in the developing zebrafish nervous system. Our results demonstrate that several myosin genes have restricted expression patterns during nervous system development, consistent with roles in neuronal migration and axon guidance.

6.3 Results and Discussion

6.3.1 Phylogenetic analysis of zebrafish unconventional myosins

Exhaustive search of the zebrafish genome assembly (Zv6, March 2006 and Zv7, July 2007) identified a total of 21 myosin genes representing classes 1, 2, 5, 9, 10, 15, 16 and 18 (myosins 6 and 7 were excluded from searches). In order to group the newly identified zebrafish myosins into appropriate classes, we constructed a phylogenetic tree with human (Hs) and mouse (Mm) orthologs using amino acid sequences of the highly conserved core motor domains of various myosin classes, equivalent to 88-780 residues of chicken skeletal myosin II (Hodge and Cope, 2000; Berg et al., 2001). Alignment of core domains was performed in Megalign using Clustal-W method (Reddy and Day, 2001; see Methods for additional details). An unrooted rectangular tree (Figure 6.2) for the aligned sequences was generated by maximum parsimony method (Jiang and Ramachandran, 2004; see Methods). The tree identifies the presence of at least two

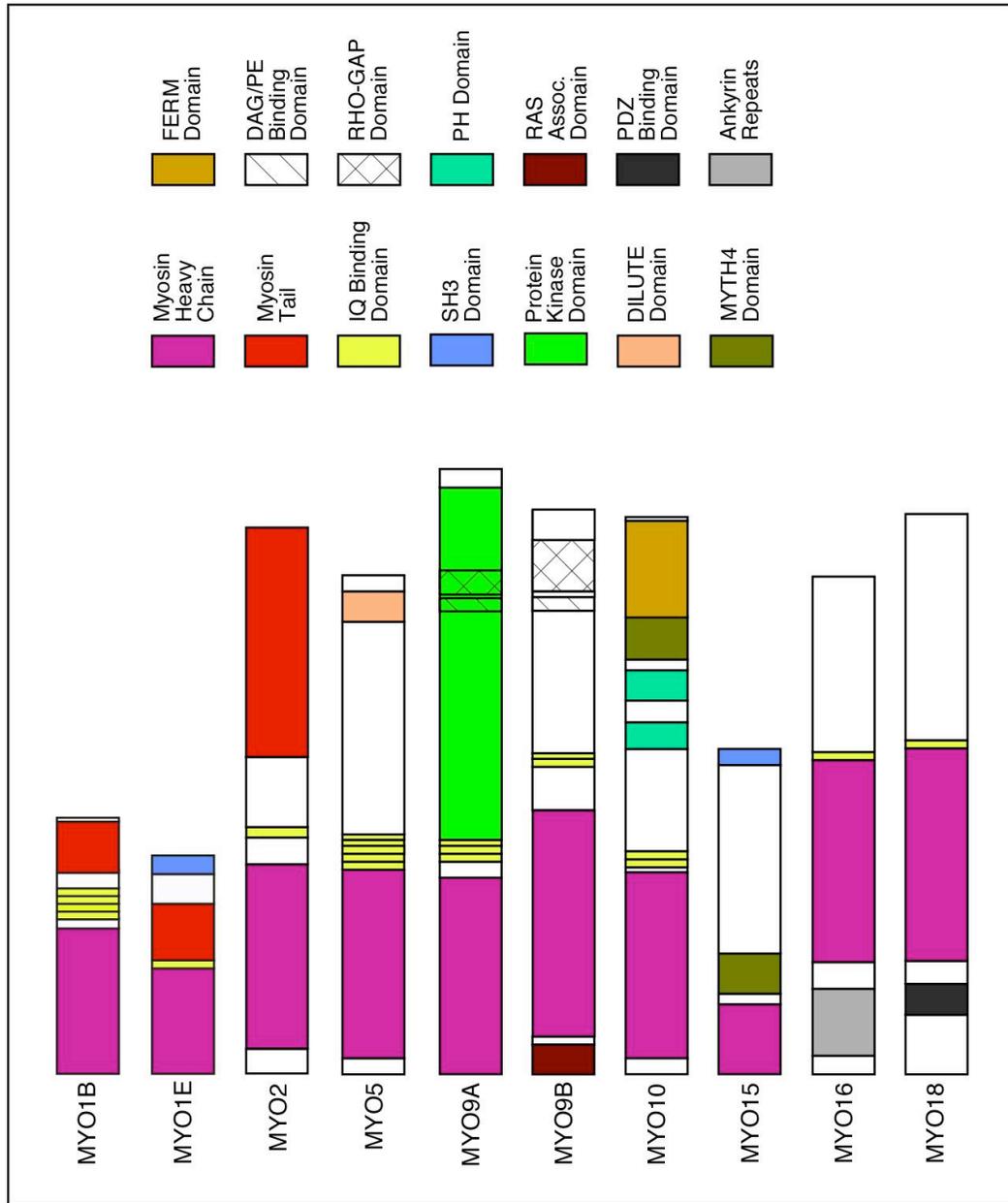


Figure 6.1 Domain organization of myosins examined in this report. Myosins are classified into several families based upon the occurrence and distribution of identified domains and sequence motifs in the heavy chain polypeptide. The nomenclature follows that for human and mouse proteins (Berg et al., 2001). This list contains only those myosins for which ESTs were obtained and expression analyzed in zebrafish embryos. The myosin head domain containing the actin- and ATP-binding sites (purple) is largely conserved, with differences identifying various classes. Other domains and motifs are found in only a subset of the proteins.

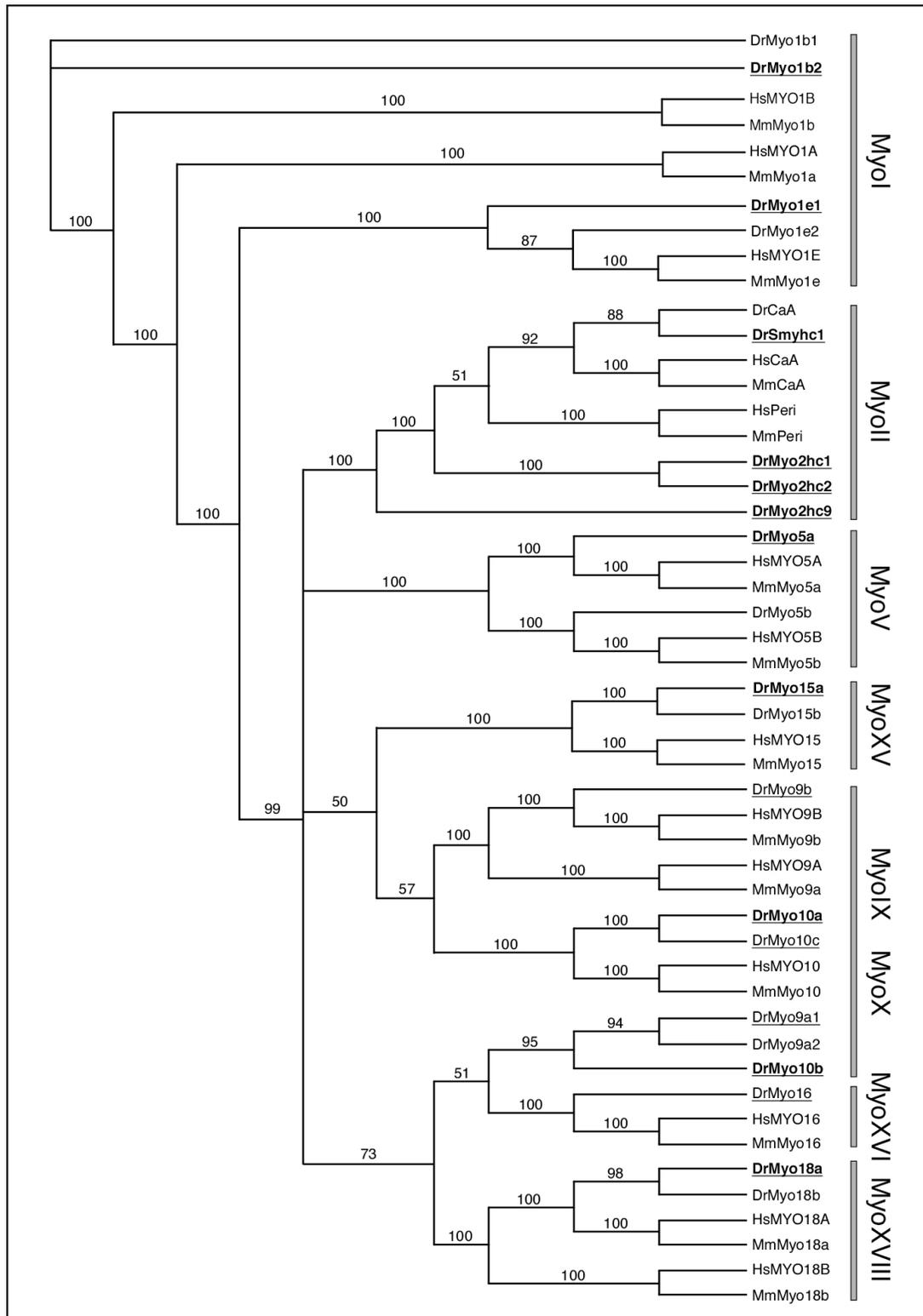


Figure 6.2 Phylogenetic relationship of unconventional myosin family members between zebrafish (*Danio rerio*), mouse (*Mus musculus*), and man (*Homo sapiens*).

Unrooted tree with bootstrap values for myosin family members that were examined in this report (see Methods for details). Myosins for whom ESTs were characterized are identified by underlines. Those myosins among these that were expressed in zebrafish embryos (14-48 hpf) are identified by bold type (Table 1). Zebrafish myosins outside these two categories but included in this phylogenetic tree were identified solely from database searches. Abbreviations: CaA, cardiac myosin A; Peri, Perinatal skeletal myosin (*Myhc8*); *Smyhc*, Slow myosin heavy chain.

genes each in the Myo1b, Myo1e, Myo9a, Myo15 and Myo18 classes and three genes each in the Myo5 (data not shown) and Myo10 classes in the available zebrafish genome. Our study also identifies four conventional myo2 genes corresponding to different heavy chain genes as shown in the tree (Figure 6.2). While most zebrafish myosins identified in this study group with one of the classes of human and mouse myosins with >90% bootstrap value, core motor domain of zebrafish Myo9a1, Myo9a2 and Myo10b group with Myo16 and Myo18 (Fig. 2). However, when full-length sequences are used for analysis, these genes group with their *Myo9a* and *Myo10* orthologs, respectively due to the presence of class specific domains (Figure 6.1).

6.3.2 Expression Analysis of Zebrafish Myosins

We carried out a detailed analysis of the expression patterns of various myosins for which ESTs were available in 2004 (Table 6.1). This includes all zebrafish genes described in Figs. 6.1 and 6.2, except *myo1b1*, *myo1e2*, *myo5b*, *myo15b*, *myo9a2*, and *myo18b* (no ESTs), and *myo6* and *myo7* whose expressions were previously described (Ernest et al., 2000; Seiler et al., 2004; Kappler et al., 2004). We initially examined expression patterns in embryos fixed at 15, 18, 24, 30, 36, and 48 hpf. Expression at earlier stages was not examined since we are primarily interested in potential roles for these molecules in neuronal migration and axon guidance, and older ages were

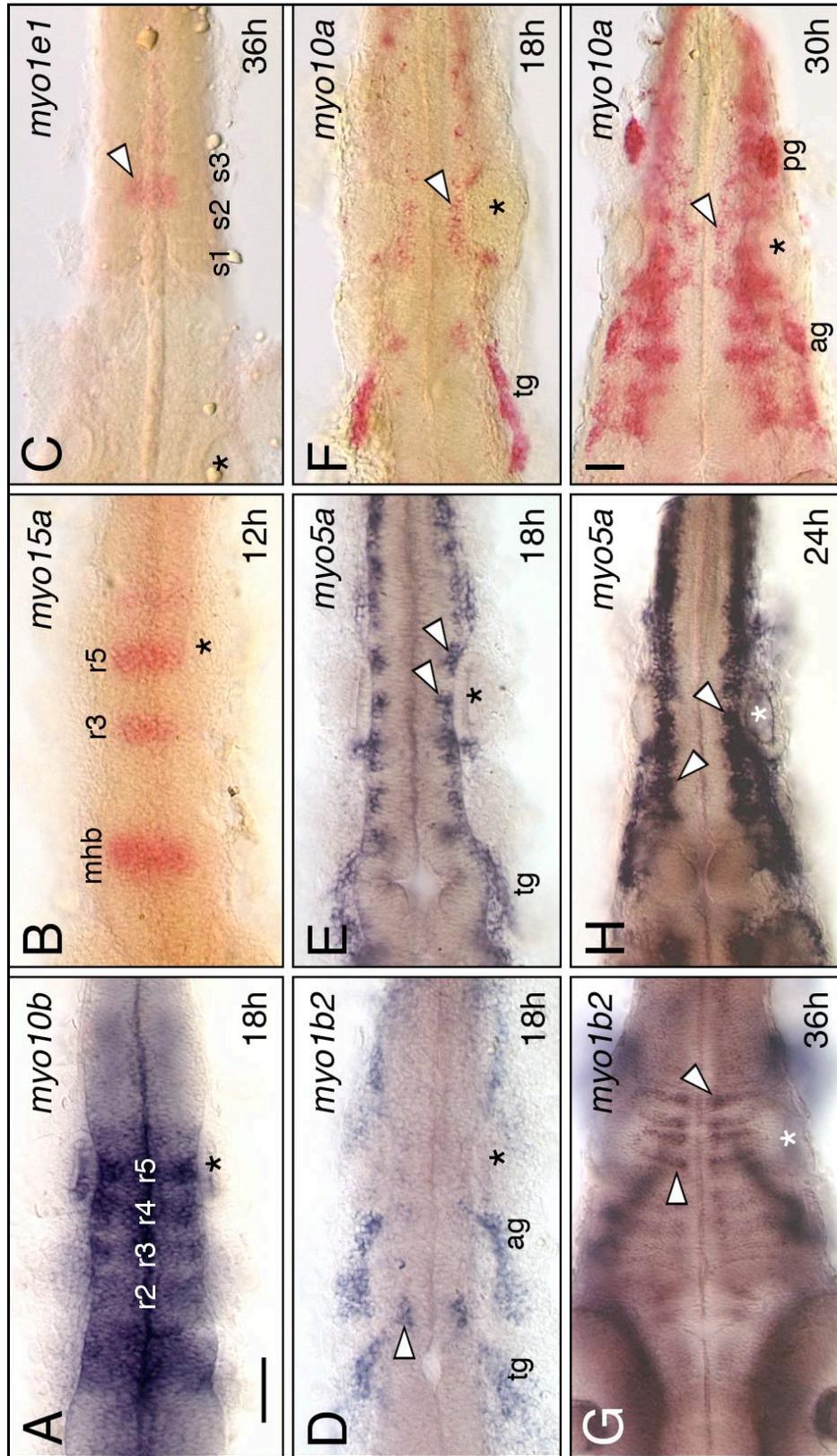


Figure 6.3 Myosins exhibiting restricted expression

patterns in the hindbrain. All panels show dorsal views of the hindbrain with anterior to the left. Asterisks mark the otic vesicle in each panel. (A, B) *myo10b* is expressed at varying levels in rhombomeres 2-5 (A), and *myo15a* is expressed in r3 and r5 (B), with both expressed at the midbrain-hindbrain boundary (mhb). (C) *myo1e1* is weakly but specifically expressed in a mesendodermal domain spanning the 2nd and 3rd somites. (D, G) At 18 hpf, *myo1b2* is expressed in sensory ganglia (tg, ag) and a cluster of cells in r2 (arrowhead, D). By 36 hpf (G), there is prominent expression in cells (arrowheads) at the boundaries of r5 and r6. (E, H) At 18 hpf, *myo5a* is expressed in sensory ganglia, and in differentiating neurons (arrowheads, E) within every rhombomere. By 24 hpf (H), expressing cells form a continuous column along the neural tube (arrowheads). (F, I) At 18 hpf, *myo10a* is expressed in the sensory ganglia (tg), and in the branchiomotor neurons in r2 and r5 (arrowheads, F). By 30 hpf (I), expression persists in the sensory ganglia and migrating motor neurons (arrowhead), and has expanded to large clusters of cells in the anterior hindbrain. tg, trigeminal ganglion, ag/pg, anterior and posterior lateral line ganglion. Scale bar, 75 μ m.

examined as needed. The myosin genes exhibited restricted patterns of expression in various tissues. Only the most salient features of these expression patterns are described below, by focusing on specific tissues in the nervous system.

6.3.2.1 Expression in Hindbrain segments

Two myosins are transiently expressed in a segmented manner in specific rhombomeres. At 18 hpf, *myo10b* is strongly expressed in r5, and more weakly in r2, r3 and r4 (Figure 6.3A). At 12 hpf, *myo15a* is expressed in r3, r5, and at the midbrain-hindbrain boundary (Figure 6.3B), with weaker expression at 18 hpf (data not shown). Thus, these genes are expressed in cells exhibiting sorting behaviors to set up well-defined rhombomere boundaries (Cooke et al., 2005). From 30-36 hpf, *myo1e1* is expressed in a small patch of mesendodermal cells located at the somite 2-3 boundary (Figure 6.3C), either the developing pancreas (Argenton et al., 1999; Stafford and Prince, 2002) or the pronephros (Drummond et al., 1998).

6.3.2.2 Expression in Hindbrain neurons

Three myosins are expressed in specific neuronal populations in the hindbrain. At 18 hpf, *myo1b2* is expressed in a subset of the cranial sensory ganglia, as well as in a small group of unidentified neurons in r2 (Figure 6.3D). Two-color in situ with a motor neuron marker and

analysis in hedgehog pathway mutants indicate that these cells are not cranial motor neurons (data not shown). At 36 hpf, *myo1b2* is expressed by a small number of cells within each rhombomere, with strong expression in cells flanking the boundaries of rhombomeres 5 and 6 (Figure 6.3G). At 18 hpf, *myo5a* is expressed in a subset of the cranial ganglia, and in differentiating neurons in every rhombomere (Figure 6.3E), similar to expression of the neurogenesis marker *huC* (Bingham et al., 2003). By 24 hpf, *myo5a* expression expands into a continuous column, as additional neurons differentiate in these regions (Figure 6.3H). At 18 hpf, *myo10a* is expressed in the trigeminal ganglion, and is also expressed at high levels in the lateral line ganglia by 30 hpf (Figures 6.3F, I). In addition, *myo10a* is expressed weakly by trigeminal and facial branchiomotor neurons from 18-30 hpf, and by other differentiating neurons by 30 hpf (Figure 6.3I). The expression of these myosins in cranial ganglia and in differentiating neurons coincides with axonogenesis or soma migration in these neuronal populations (Trevarrow et al., 1987; Higashijima et al., 2000).

6.3.2.3 Expression in the Forebrain and midbrain

Two myosins, *myo5a* and *myo10a*, are expressed in specific populations of forebrain and midbrain neurons (Figure 6.4). In the forebrain, *myo5a*- and *myo10a*-expressing cells from 18-30 hpf (Figure 6.4A-C; data not shown) appear to correspond to the telencephalic

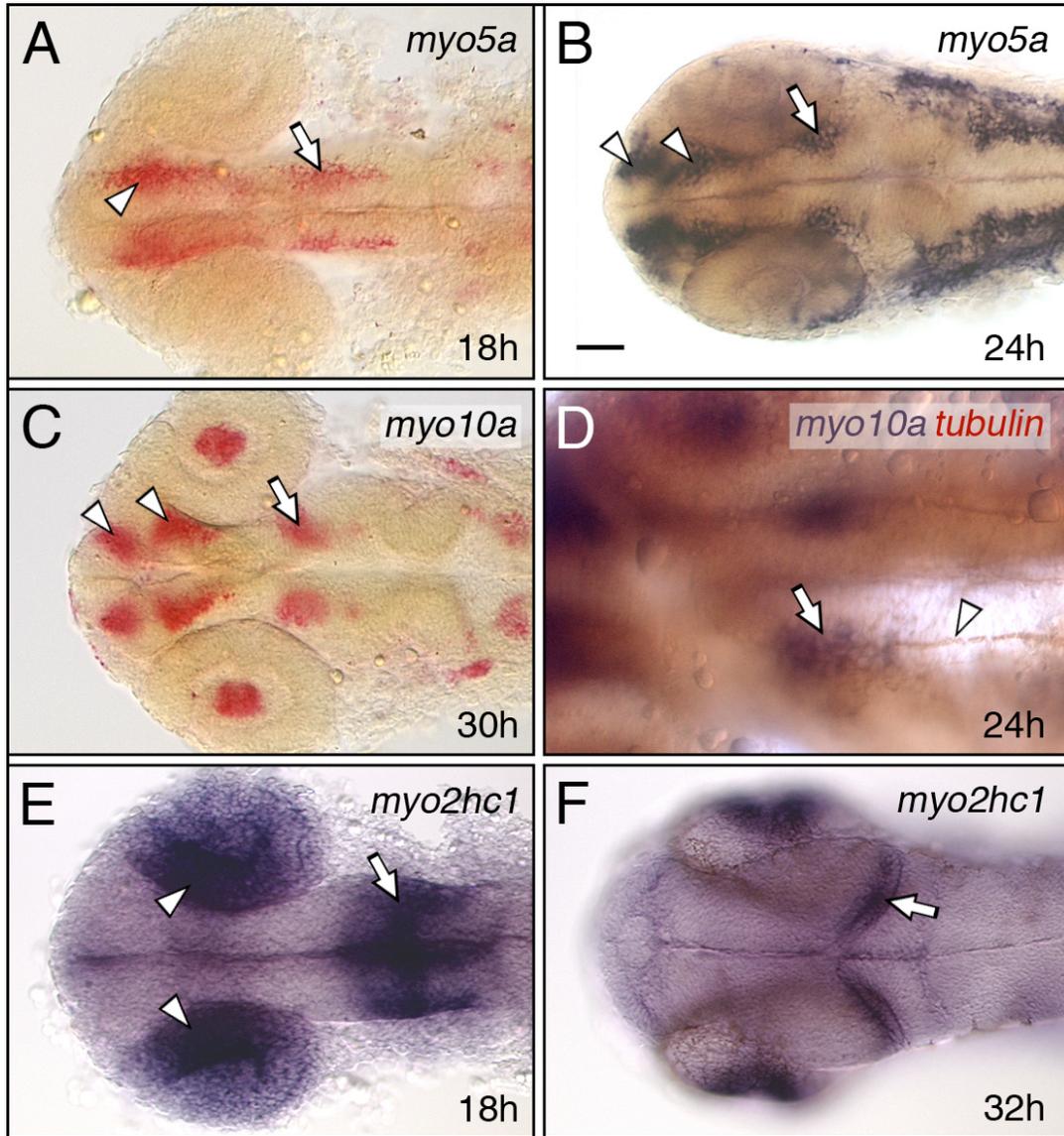


Figure 6.4 Myosin expression in the forebrain and

midbrain. All panels show dorsal views of the head with anterior to the left. (A, B) At 18 hpf, *myo5a* is expressed in nascent neurons (arrowhead, A) in the forebrain, and in the nucMLF neurons (arrow) in the midbrain. By 24 hpf (B), forebrain expression has refined into distinguishable clusters representing the neurons of the anterior and post-optic commissures (arrowheads, B), and is maintained in the nucMLF neurons (arrow). (C) At 30 hpf, *myo10a* is expressed in the neurons of the nucMLF (arrow), and of the anterior and post-optic commissures (arrowheads), and in the lens (see Fig. 6). (D) Double-labeling shows that tubulin antibody-labeled axons (arrowhead) of the MLF arise from the cluster of *myo10a*-expressing neurons (arrow), corresponding to the nucMLF. (E, F) At 18 hpf, *myo2hc1* is expressed in the medial layer of the optic cup (arrowheads), and at the mid-hindbrain boundary (arrow). By 32 hpf (F), expression is restricted to the retinal ganglion layer (see Fig. 6), and to the caudal edge of the developing optic tectum (arrow). Scale bar, 25 μm (D), 50 μm (A-F).

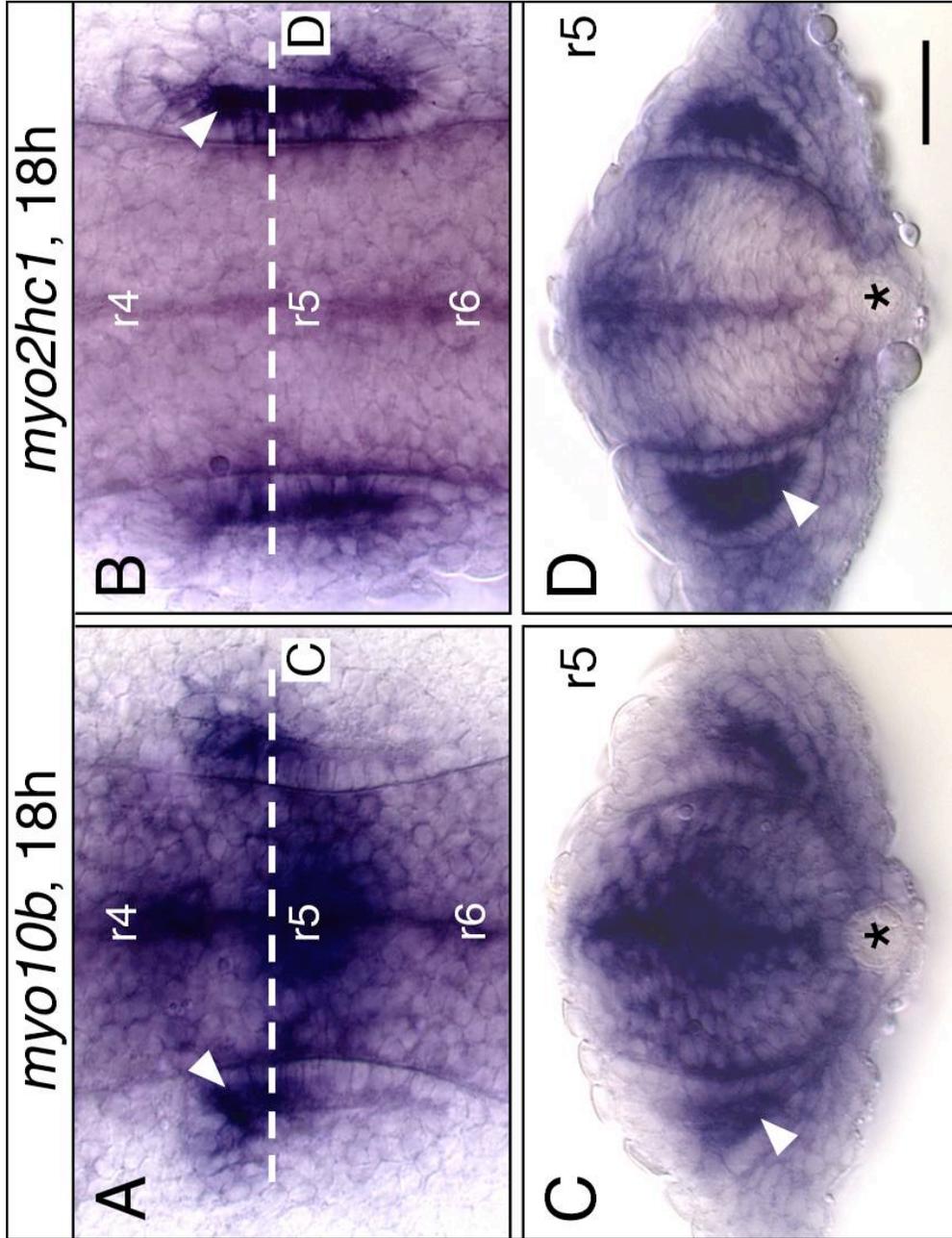


Figure 6.5 Myosin expression in the developing ear.

Upper panels show dorsal views, with anterior at top. Lower panels show cross-sections (dorsal up) at the levels indicated in the upper panels. (A, C) *myo10b* is expressed in epithelial cells (arrowhead) lining the anterior third (A), and the ventral half (C) of the otic vesicle. (B, D) *myo2hc1* is expressed in the epithelial cells of the otic vesicle (arrowheads), adjacent to the hindbrain. Asterisks (C, D) indicate the notochord. Scale bar, 30 μm .

The *myo5a*- and *myo10a*-expressing cells in the midbrain are likely the nucleus of the medial longitudinal fascicle (nucMLF; Chitnis et al., 1990; Figure 6.4A-C), and this was confirmed by anti-tubulin antibody labeling of the MLF in embryos processed for *myo10a* in situ (Figure 6.4D). Myosin gene expression in telencephalic and nucMLF neurons from 18-30 hpf coincides with the period of growth cone motility and axon guidance in these neurons. *Myo2hc1* is strongly expressed at the midbrain-hindbrain boundary at 18 hpf, but becomes restricted to a narrow domain in the caudal optic tectum by 32 hpf (Figure 6.4E, F).

6.3.2.4 Expression in the Otic vesicle

In addition to *myo6b* and *myo7a*, whose expression has been previously described (Ernest et al., 2000; Seiler et al., 2004; Kappler et al., 2004), *myo10b* and *myo2hc1* are also expressed in the otic vesicle. However, their expression is not restricted to the sensory neurons of the epithelium as for *myo6b* and *myo7a*. At 18 hpf, *myo2hc1* transcripts are localized to the apical regions of cells throughout the otic epithelium (Figure 6.5B, D), whereas *myo10b* transcripts are localized to apical regions of cells only in the rostroventral epithelium (Figure 6.5A, C; see also Figure 6.3A). These genes are expressed in the otic vesicle from 15-24 hpf, during morphogenesis of the vesicle (Kimmel et al., 1995).

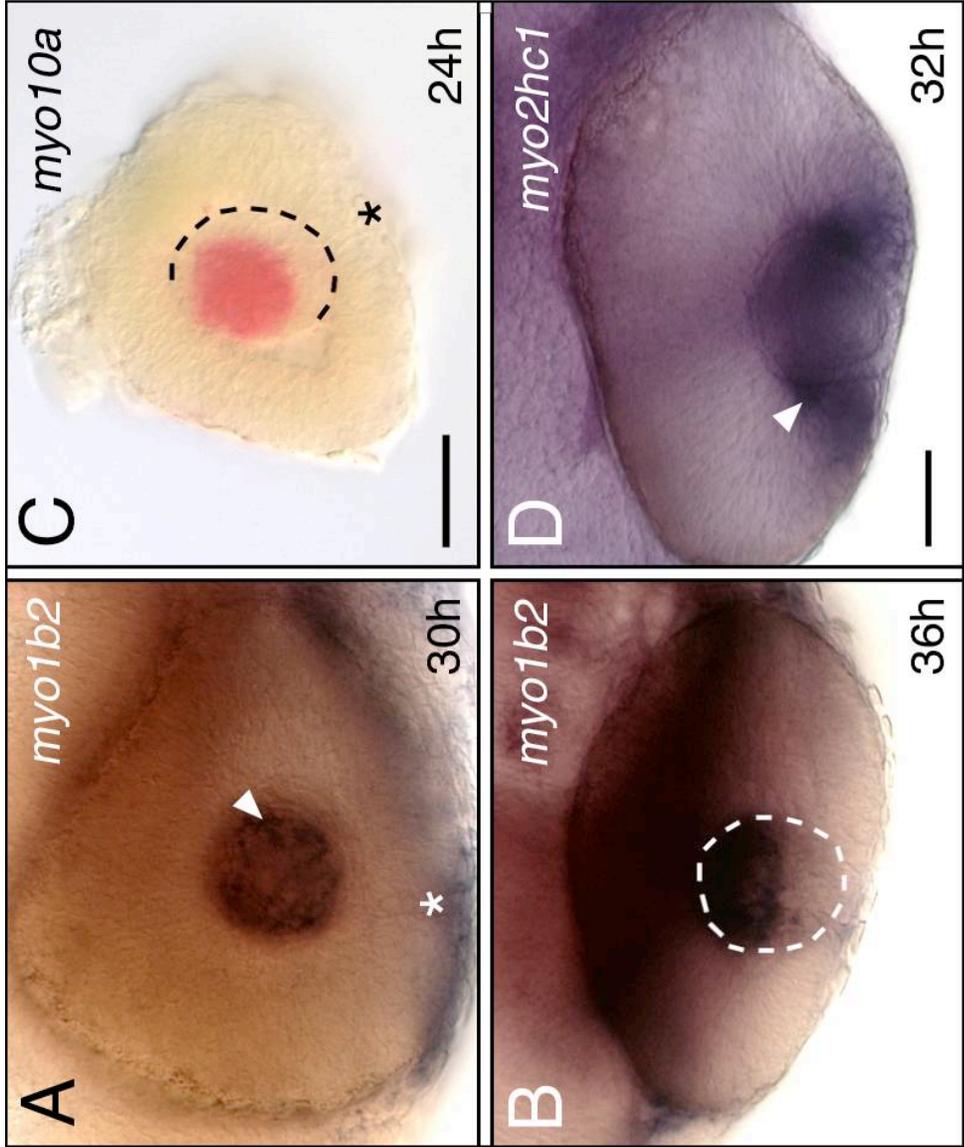


Figure 6.6 Myosin expression in the eye. (A, B) *myo1b2* is expressed in the differentiating lens fibers (arrowhead, A) located in the medial half of the lens (B, dorsal view). (C) *myo10a* is expressed in a subset of lens cells at 24 hpf, and at 30 hpf (see Fig. 4C). (D) *myo2hc1* is expressed in retinal ganglion cells (arrowhead) adjacent to the lens. Asterisks (A, C) indicate the choroid plexus. Scale bar (A, B, D), 40 μm . Scale bar (C), 30 μm .

6.3.2.5 Expression in the Eye

Three myosins are expressed in the eye, two in the developing lens (*myo1b2*, *myo10a*), and one in the retina (*myo2hc1*). Interestingly, *myo1b2* is expressed by cells only in the medial half of the developing lens (Figure 6.6A, B), whereas *myo10a* is expressed only in the dorsal half of the developing lens (Figure 6.6C; see also Figure 6.4C). These localized patterns may reflect the progression of differentiation of lens fibers, or the inability of transcripts to distribute uniformly within differentiating fibers. At 18 hpf, *myo2hc1* is strongly expressed in the medial layer of the optic cup (Figure 6.3E) during the period of eye morphogenesis (Li et al., 2000), and becomes restricted to the ganglion cell layer by 32 hpf (Figures 6.3F and 6.6D), when retinal axons are extending into the brain (Hutson and Chien, 2002).

6.3.2.6 Expression in the Spinal cord and Trunk

As expected, *myo2hc2* is expressed strongly in all muscles (Figures 6.7A and 6.8), and our probe labels expressing tissue more effectively than previously described (Peng et al., 2002). Interestingly, only one other myosin among 18 tested was expressed in the presumptive musculature. At 18 hpf, *myo18a* is expressed throughout caudal (newborn) somites, and becomes restricted to cells at the boundaries between rostral (older) somites (Figure 6.7B). At 18 hpf, *myo1b2* is expressed in the superficial cells of the somites (Figure 6.7C, D),

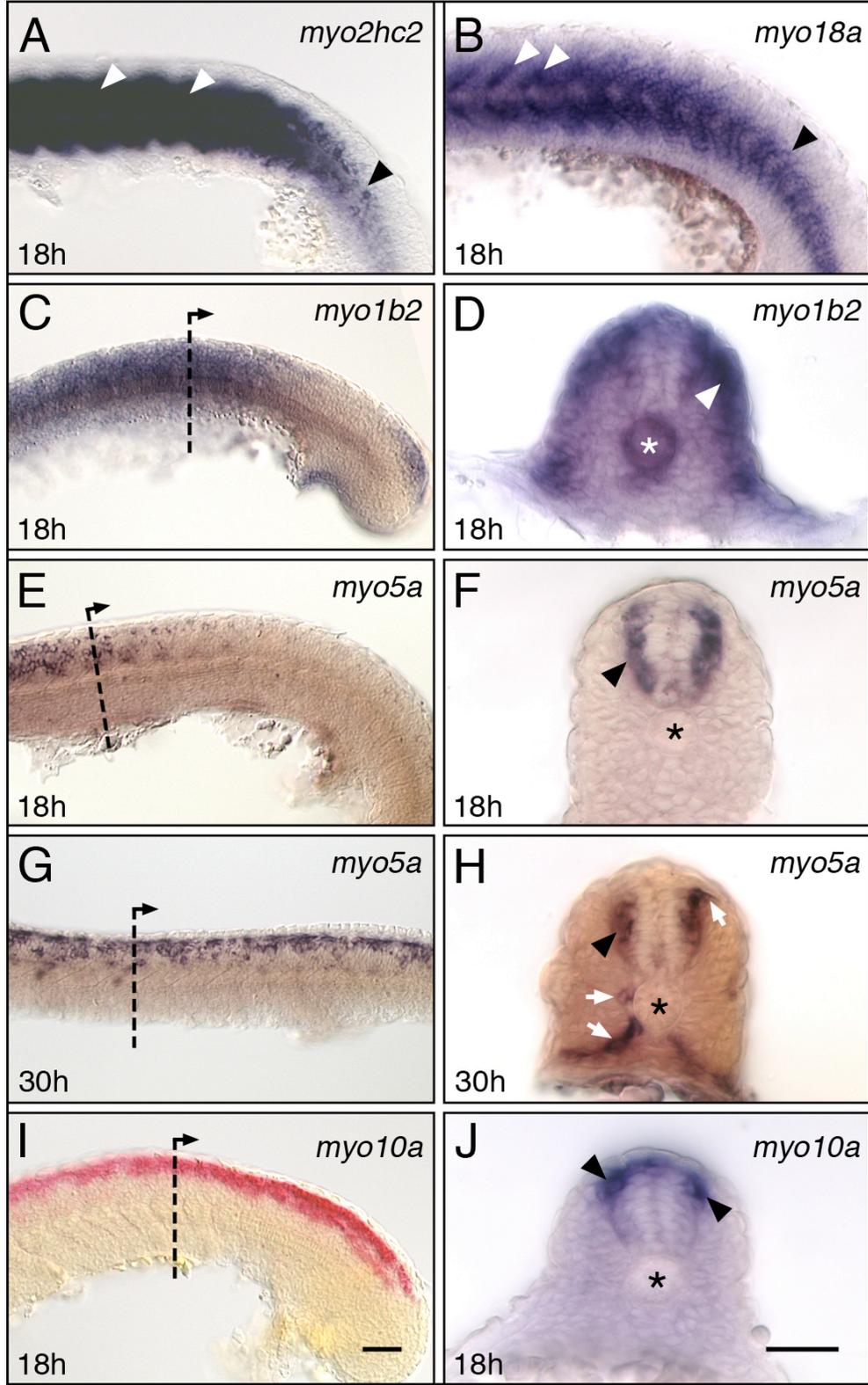


Figure 6.7 Myosin expression in the trunk and spinal cord.

Panels A-C, E, G, I show side views with anterior to left. Panels D, F, H, J show cross-sections at levels indicated in C, E, G, I, respectively. (A) *myo2hc2* is strongly expressed in the differentiating muscles of the somites (white arrowheads), but only weakly in the newly formed somites (black arrowhead). (B) *myo18a* is expressed in the mesenchyme of newly-formed and differentiating somites (black arrowhead), and strongly in the cells at the boundaries of older somites (white arrowheads). (C, D) *myo1b2* is expressed broadly in the trunk, excluding the presomitic mesoderm (C). Expressing cells are located superficially within the somitic mesoderm (arrowhead, D), and in the notochord (asterisk). (E, F) At 18 hpf, *myo5a* expression is restricted to the spinal cord at anterior trunk levels (E), and represents differentiating neurons (arrowhead, F). (G, H) At 30 hpf, *myo5a* is expressed by scattered cells located in the dorsal half of the spinal cord (G). A cross-section in the anterior trunk (H) shows that expressing cells include neurons (arrowhead) and migrating neural crest cells (arrows). (I, J) *myo10a* is expressed in a continuous column of cells in the dorsal half of the spinal cord (I), including neurons (arrowheads, J). Asterisks in D, F, H, J indicate the notochord. Scale bar (I), 50 μm (A-C, E, G, I). Scale bar (J), 50 μm (D, F, H, J).

and weakly expressed in a few cells in the spinal cord, likely neurons. At 18 hpf, *myo5a* is expressed by several presumptive neurons throughout the spinal cord, except in the most dorsal and ventral regions (Figure 6.7E, F). By 30 hpf, *myo5*-expressing cells are located mostly in the dorsal half of the neural tube, with several putative migrating neural crest cells in characteristic locations beside the somites (Figure 6.7G, H). At 18 hpf, *myo10a* is expressed by cells in the dorsal spinal cord in putative neural crest cells (Figure 6.7I, J). These results indicate that specific myosins are expressed in neurons and neural crest cells during the period of cell migration and axon guidance.

6.3.2.7 Expression of *myo2hc2* in cranial muscles

Previous work (Peng et al., 2002) noted weak *myo2hc2* (*myhz2*) expression in two cranial muscles. We found that *myo2hc2* is expressed robustly in all cranial muscles (Figure 6.8). By comparing the expression pattern to that of anti-myosin antibody labeling of cranial muscles (Schilling et al., 1997), we identified most of the muscles in the zebrafish head at 72 hpf. Our *myo2hc2* probe represents an excellent marker for studies of cranial muscle biology.

6.4 Materials and Methods

6.4.1 Animals

Maintenance of zebrafish stocks, and collection and development of embryos in E3 embryo medium were carried out as described previously (Westerfield, 1995; Chandrasekhar et al., 1997; Bingham et al., 2002). Throughout the text, the developmental age of the embryos corresponds to the hours elapsed since fertilization (hours post fertilization, hpf, at 28.5°C).

6.4.2 Cloning and phylogenetic analysis of zebrafish unconventional myosins

We used the nucleotide and amino acid sequences for the various unconventional myosins from human and mouse databases (Reference Review Paper) to search the zebrafish EST databases at Washington University and RZPD for orthologs. Using this information, we obtained EST clones for the various myosins from RZPD (Berlin, Germany), Open Biosystems (Huntsville, AL) and Dr. Jinrong Peng (IMCB, Singapore) (Table 1). The EST clones were verified by sequencing prior to making in situ probes. The EST sequences were used to BLAST the latest assembly of the zebrafish genomic sequence (Zv7, July 2007) using BLASTN to retrieve the most complete annotated cDNA sequences for the various myosin genes. The newly identified zebrafish and previously

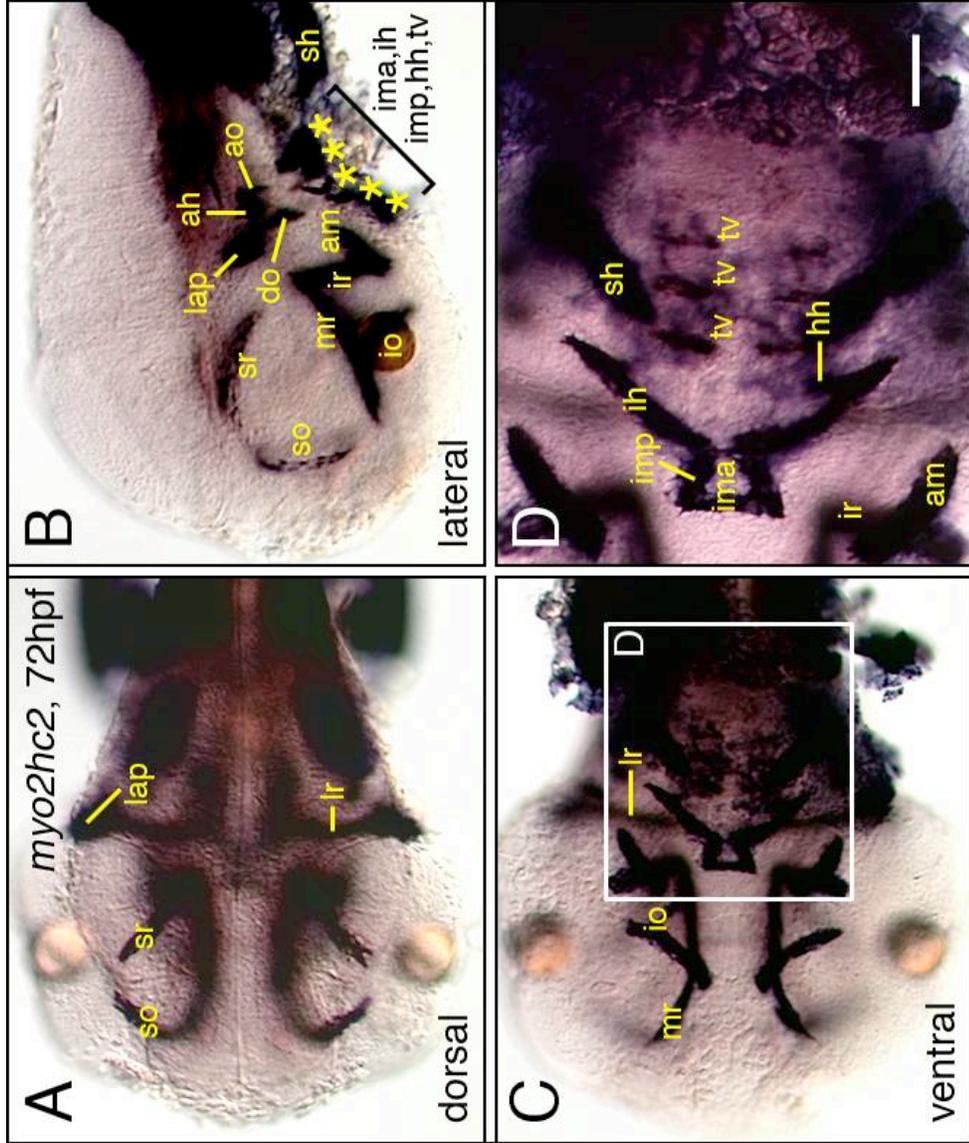


Figure 6.8 *Myosin2* expression in head muscles. (A) In a dorsal view, some eye (so, sr, lr) and jaw (lap) muscles can be identified. (B) In a side view, several eye (so, sr, mr, io, ir, am) and jaw (ah, ao, do, lap) muscles can be distinguished. (C, D) In a ventral view, several eye (am, io, ir, lr, mr), jaw (ima, imp, ih, hh) and gill (tv, sh) muscles can be identified. Scale bar, 100 μm (A-C), 50 μm (D).

described human and mouse myosins were BLASTed against chicken skeletal myosin 2 to delineate the core domain (composed of the catalytic and ATP-binding sites?) corresponding to amino acids 88-780 of the chicken protein. The core domains of zebrafish, human and mouse myosins were aligned using Clustal-W method in Megalign program of LASERGENE (DNASTAR Inc, Madison, WI; Reddy and Day, 2001). The aligned core domains were further analyzed using Mac PAUP 4.0 b10 (<http://paup.csit.fsu.edu/>; Jiang and Ramachandran, 2004) to generate a phylogenetic tree (Fig. 2). The heuristic search option was used in maximum parsimony method to create a tree with strict consensus. Bootstrap analyses were replicated 1000 times to obtain a robust support value at each node which indicates the percent times that the grouping is supported out of 1000 trials (Baker and Titus, 1997; Hodge and Cope, 2000; Sellers, 2000). Bootstrap values of greater than 70 indicate a strongly supported node with 95% probability (Hills and Bull, 1993).

6.4.3 Histological Procedures

The EST clones were verified by sequencing prior to probe synthesis. Synthesis of the digoxigenin-labeled probes, and whole-mount in situ hybridization was carried out as described previously (Bingham et al., 2003). Given the large number of clones and time points, embryos of different ages were pooled for the hybridization step

following protease treatment. Whole-mount immunohistochemistry (tubulin and GFP antibodies) was performed as described previously (Vanderlaan et al., 2005). For combined in situ and antibody labeling, embryos were first processed for in situ before antibody labeling. Embryos were deyolked, mounted in 70% glycerol, and examined with an Olympus BX60 microscope. At least ten embryos were examined for each gene and time point. Images were acquired using an Optronics camera and Scion Imaging Software on a MacOS computer equipped with an LG3 frame grabber. Images were processed in Adobe Photoshop to adjust brightness and contrast only.

Table 6.1: Zebrafish Myosin Genes Characterized in this Report

| Gene Ensembl ID | Chromosome | ESTs (source) *, % | Length of ORF | % Identity to Hs and Mm | Gene Expressed |
|--|------------|--|------------------|-------------------------|----------------|
| <i>Myo1b2</i> ENSDARG00000024694 | 9 | MPMGp609P206Q8 (B) MPMGp609G1826Q8 (B) A1G (A) | Partial (90%) | 81.4 81.5 | Yes |
| <i>Myo1e1</i> ENSDARG00000036179 | 7 | MPMGp609L0725Q8 (B) MPMGp609L0281Q8 (B) MPMGp637H137Q2 (B) IMAGp998P1112400Q3 (B) IMAGp998G1514300Q3 (B) | Full-length | 76.3 76.3 | Yes |
| <i>Smyhc1</i> ENSDARG00000071430 | 24 | MPMGp609B1310Q8 (B) | Full-length | 84.8 84.6 | Yes |
| <i>Myo2hc1 (myhz1)</i> ENSDARG00000067990 | 5 | MPMGp609P1624Q8 (B) | Full-length | 80.8 82.1 | Yes |
| <i>Myo2hc2 (myhz2)</i> ENSDARG00000012944 | 5 | MPMGp609M1825Q8 (B) | Full-length | 80.7 82.1 | Yes |
| <i>Myo2hc9 (myhz9)</i> ENSDARG0000001014 | 3 | IMAGp998D0714289Q3 (B) | Full-length | 84.3 81.9 | Yes |
| <i>Myo5a</i> ENSDARG00000061635 | 18 | 129-E08-02 (S) | Full-length | 79.9 79.9 | Yes |
| <i>Myo6a</i> ENSDARG00000044016 | 20 | IMAGp998H1712050Q3 (B) | Full-length | 80.9 80.6 | No |
| <i>Myo9a1</i> ENSDARG00000019585 | 7 | 46-E08-02 (S) | Partial (90%) | 56.7 56.3 | No |
| <i>Myo9a2</i> ENSDARG00000063639 | 25 | IMAGp998N0912391Q3 (B) | Partial (80%) | 54.8 54.3 | No |
| <i>Myo9b</i> ENSDARG00000062159 | 10 | MPMGp609G0210Q8 (B) | Full-length | 57.3 58.1 | No |
| <i>Myo10a</i> ENSDARG00000062580 | 6 | IMAGp998M2314313Q (B) | Partial (98%) | 61.6 62.1 | Yes |
| <i>Myo10b</i> ENSDARG00000017004 | 2 | MPMGp609N1624Q8 (B) MPMGp609C1781Q8 (B) 88-A02-02 (S) | Partial (84%) | 68.3 67.7 | Yes |
| <i>Myo10c</i> ENSDARG00000063138 | 9 | 112-H11-02 (S) | Full-length | 62.1 62.6 | No |
| <i>Myo15a</i> ENSDARG00000059709 | 3 | 62-G10-02 () | Full-length | 62.2 61.2 | Yes |
| <i>Myo16</i> ENSDARG00000004512 | 9 | 86-H05-02 (S) 100-C07-02 (??) | Full-length | 59.8 57.8 | No |
| <i>Myo18a</i> ENSDARG00000061862 | 15 | DKFZp717N112Q2 (B) | Full-length | 78 76.8 | Yes |
| <i>Myo18b</i> ENSDARG00000061225 | 10 | 54-D04-02 (S) 98-C07-02 (S) | Partial (87%) | 73.7 73.3 | No |

*, Source, B: RZPD, Berlin; S: Dr. Jinrong Peng, IMCB, Singapore; A: Research Genetics (Invitrogen), Alabama.
%, For genes with multiple ESTs, all ESTs were tested, and generated similar in situ results.

REFERENCES

- Alberti, S., S. M. Krause, O. Kretz, U. Philippar, T. Lemberger, E. Casanova, F. F. Wiebel, H. Schwarz, M. Frotscher, G. Schutz, and A. Nordheim. 2005.** Neuronal migration in the murine rostral migratory stream requires serum response factor. *Proc Natl Acad Sci U S A.* 102:6148.
- Alcantara, S., M. Ruiz, F. De Castro, E. Soriano, and C. Sotelo. 2000.** Netrin 1 acts as an attractive or as a repulsive cue for distinct migrating neurons during the development of the cerebellar system. *Development.* 127:1359.
- Allendoerfer, K. L., and C. J. Shatz. 1994.** The subplate, a transient neocortical structure: its role in the development of connections between thalamus and cortex. *Annu Rev Neurosci* 17:185.
- Anderson, S. A., D. D. Eisenstat, L. Shi, and J. L. Rubenstein. 1997.** Interneuron migration from basal forebrain to neocortex: dependence on Dlx genes. *Science.* 278:474.
- Argenton, F., E. Zecchin, and M. Bortolussi. 1999.** Early appearance of pancreatic hormone-expressing cells in the zebrafish embryo. *Mech Dev.* 87:217.
- Arnaud, L., B. A. Ballif, E. Forster, and J. A. Cooper. 2003.** Fyn tyrosine kinase is a critical regulator of disabled-1 during brain development. *Curr Biol.* 13:9.
- Assadi, A. H., G. Zhang, U. Beffert, R. S. McNeil, A. L. Renfro, S. Niu, C. C. Quattrocchi, B. A. Antalffy, M. Sheldon, D. D. Armstrong, A. Wynshaw-Boris, J. Herz, G. D'Arcangelo, and G. D. Clark. 2003.** Interaction of reelin signaling and Lis1 in brain development. *Nat Genet.* 35:270.
- Axelrod, J. D. 2001.** Unipolar membrane association of Dishevelled mediates Frizzled planar cell polarity signaling. *Genes Dev.* 15:1182.
- Ayala, R., T. Shu, and L. H. Tsai. 2007.** Trekking across the brain: the journey of neuronal migration. *Cell.* 128:29.

- Bagri, A., and M. Tessier-Lavigne. 2002.** Neuropilins as Semaphorin receptors: in vivo functions in neuronal cell migration and axon guidance. *Adv Exp Med Biol* 515:13.
- Baker, N. E. 2000.** Notch signaling in the nervous system. Pieces still missing from the puzzle. *Bioessays*. 22:264.
- Bastock, R., H. Strutt, and D. Strutt. 2003.** Strabismus is asymmetrically localised and binds to Prickle and Dishevelled during *Drosophila* planar polarity patterning. *Development*. 130:3007.
- Beffert, U., E. J. Weeber, G. Morfini, J. Ko, S. T. Brady, L. H. Tsai, J. D. Sweatt, and J. Herz. 2004.** Reelin and cyclin-dependent kinase 5-dependent signals cooperate in regulating neuronal migration and synaptic transmission. *J Neurosci*. 24:1897.
- Behar, T. N., M. M. Dugich-Djordjevic, Y. X. Li, W. Ma, R. Somogyi, X. Wen, E. Brown, C. Scott, R. D. McKay, and J. L. Barker. 1997.** Neurotrophins stimulate chemotaxis of embryonic cortical neurons. *Eur J Neurosci*. 9:2561.
- Behar, T. N., S. V. Smith, R. T. Kennedy, J. M. McKenzie, I. Maric, and J. L. Barker. 2001.** GABA(B) receptors mediate motility signals for migrating embryonic cortical cells. *Cereb Cortex*. 11:744.
- Berg, J. S., B. C. Powell, and R. E. Cheney. 2001.** A millennial myosin census. *Mol Biol Cell*. 12:780.
- Bingham, S. 2004.** Cellular and molecular analysis of motor neuron development in the zebrafish hindbrain. Dissertation submitted to the University of Missouri-Columbia.
- Bingham, S., S. Chaudhari, G. Vanderlaan, M. Itoh, A. Chitnis, and A. Chandrasekhar. 2003.** Neurogenic phenotype of mind bomb mutants leads to severe patterning defects in the zebrafish hindbrain. *Dev Dyn*. 228:451.
- Bingham, S., S. Higashijima, H. Okamoto, and A. Chandrasekhar. 2002.** The Zebrafish trilobite gene is essential for tangential migration of branchiomotor neurons. *Dev Biol*. 242:149.
- Birgbauer, E., and S. E. Fraser. 1994.** Violation of cell lineage restriction compartments in the chick hindbrain. *Development*. 120:1347.

- Bock, H. H., and J. Herz. 2003.** Reelin activates SRC family tyrosine kinases in neurons. *Curr Biol.* 13:18.
- Book, K. J., and D. K. Morest. 1990.** Migration of neuroblasts by perikaryal translocation: role of cellular elongation and axonal outgrowth in the acoustic nuclei of the chick embryo medulla. *J Comp Neurol.* 297:55.
- Borghesani, P. R., J. M. Peyrin, R. Klein, J. Rubin, A. R. Carter, P. M. Schwartz, A. Luster, G. Corfas, and R. A. Segal. 2002.** BDNF stimulates migration of cerebellar granule cells. *Development.* 129:1435.
- Bourrat, F., and C. Sotelo. 1988.** Migratory pathways and neuritic differentiation of inferior olivary neurons in the rat embryo. Axonal tracing study using the in vitro slab technique. *Brain Res.* 467:19.
- Boutros, M., N. Paricio, D. I. Strutt, and M. Mlodzik. 1998.** Dishevelled activates JNK and discriminates between JNK pathways in planar polarity and wingless signaling. *Cell.* 94:109.
- Brummendorf, T., and F. G. Rathjen. 1996.** Structure/function relationships of axon-associated adhesion receptors of the immunoglobulin superfamily. *Curr Opin Neurobiol.* 6:584.
- Carpenter, E. M., J. M. Goddard, O. Chisaka, N. R. Manley, and M. R. Capecchi. 1993.** Loss of Hox-A1 (Hox-1.6) function results in the reorganization of the murine hindbrain. *Development.* 118:1063.
- Carreira-Barbosa, F., M. L. Concha, M. Takeuchi, N. Ueno, S. W. Wilson, and M. Tada. 2003.** Prickle 1 regulates cell movements during gastrulation and neuronal migration in zebrafish. *Development.* 130:4037.
- Chandrasekhar, A. 2004.** Turning heads: development of vertebrate branchiomotor neurons. *Dev Dyn.* 229:143.
- Chandrasekhar, A., C. B. Moens, J. T. Warren, Jr., C. B. Kimmel, and J. Y. Kuwada. 1997.** Development of branchiomotor neurons in zebrafish. *Development.* 124:2633.
- Chilton, J. K. 2006.** Molecular mechanisms of axon guidance. *Dev Biol.* 292:13.

- Chitnis, A. B., and J. Y. Kuwada. 1990.** Axonogenesis in the brain of zebrafish embryos. *J Neurosci.* 10:1892.
- Ciruna, B., A. Jenny, D. Lee, M. Mlodzik, and A. F. Schier. 2006.** Planar cell polarity signalling couples cell division and morphogenesis during neurulation. *Nature.* 439:220.
- Clarke, J. D., and A. Lumsden. 1993.** Segmental repetition of neuronal phenotype sets in the chick embryo hindbrain. *Development.* 118:151.
- Coffin, A. B., A. Dabdoub, M. W. Kelley, and A. N. Popper. 2007.** Myosin VI and VIIa distribution among inner ear epithelia in diverse fishes. *Hear Res.* 224:15.
- Conover, J. C., F. Doetsch, J. M. Garcia-Verdugo, N. W. Gale, G. D. Yancopoulos, and A. Alvarez-Buylla. 2000.** Disruption of Eph/ephrin signaling affects migration and proliferation in the adult subventricular zone. *Nat Neurosci.* 3:1091.
- Cooke, J., C. Moens, L. Roth, L. Durbin, K. Shiomi, C. Brennan, C. Kimmel, S. Wilson, and N. Holder. 2001.** Eph signalling functions downstream of Val to regulate cell sorting and boundary formation in the caudal hindbrain. *Development.* 128:571.
- Cooke, J. E., H. A. Kemp, and C. B. Moens. 2005.** EphA4 is required for cell adhesion and rhombomere-boundary formation in the zebrafish. *Curr Biol.* 15:536.
- Cooke, J. E., and C. B. Moens. 2002.** Boundary formation in the hindbrain: Eph only it were simple. *Trends Neurosci.* 25:260.
- Cooper, K. L., J. Armstrong, and C. B. Moens. 2005.** Zebrafish foggy/spt 5 is required for migration of facial branchiomotor neurons but not for their survival. *Dev Dyn.* 234:651.
- Copp, A. J., N. D. Greene, and J. N. Murdoch. 2003.** The genetic basis of mammalian neurulation. *Nat Rev Genet.* 4:784.
- Copp, A. J., and B. N. Harding. 1999.** Neuronal migration disorders in humans and in mouse models--an overview. *Epilepsy Res.* 36:133.

- Coppola, E., A. Pattyn, S. C. Guthrie, C. Goriadis, and M. Studer. 2005.** Reciprocal gene replacements reveal unique functions for Phox2 genes during neural differentiation. *Embo J.* 24:4392.
- Darken, R. S., A. M. Scola, A. S. Rakeman, G. Das, M. Mlodzik, and P. A. Wilson. 2002.** The planar polarity gene strabismus regulates convergent extension movements in *Xenopus*. *Embo J.* 21:976.
- Das, G., A. Jenny, T. J. Klein, S. Eaton, and M. Mlodzik. 2004.** Diego interacts with Prickle and Strabismus/Van Gogh to localize planar cell polarity complexes. *Development.* 131:4467.
- De La Cruz, E. M., and E. M. Ostap. 2004.** Relating biochemistry and function in the myosin superfamily. *Curr Opin Cell Biol.* 16:61.
- Dehmelt, L., and S. Halpain. 2004.** Actin and microtubules in neurite initiation: are MAPs the missing link? *J Neurobiol.* 58:18.
- Del Rio, J. A., C. Gonzalez-Billault, J. M. Urena, E. M. Jimenez, M. J. Barallobre, M. Pascual, L. Pujadas, S. Simo, A. La Torre, F. Wandosell, J. Avila, and E. Soriano. 2004.** MAP1B is required for Netrin 1 signaling in neuronal migration and axonal guidance. *Curr Biol.* 14:840.
- Denaxa, M., C. H. Chan, M. Schachner, J. G. Parnavelas, and D. Karagogeos. 2001.** The adhesion molecule TAG-1 mediates the migration of cortical interneurons from the ganglionic eminence along the corticofugal fiber system. *Development.* 128:4635.
- Denaxa, M., K. Kyriakopoulou, K. Theodorakis, G. Trichas, M. Vidaki, Y. Takeda, K. Watanabe, and D. Karagogeos. 2005.** The adhesion molecule TAG-1 is required for proper migration of the superficial migratory stream in the medulla but not of cortical interneurons. *Dev Biol.* 288:87.
- des Portes, V., J. M. Pinard, P. Billuart, M. C. Vinet, A. Koulakoff, A. Carrie, A. Gelot, E. Dupuis, J. Motte, Y. Berwald-Netter, M. Catala, A. Kahn, C. Beldjord, and J. Chelly. 1998.** A novel CNS gene required for neuronal migration and involved in X-linked subcortical laminar heterotopia and lissencephaly syndrome. *Cell.* 92:51.
- Dhavan, R., and L. H. Tsai. 2001.** A decade of CDK5. *Nat Rev Mol Cell Biol.* 2:749.

- Diefenbach, T. J., V. M. Latham, D. Yimlamai, C. A. Liu, I. M. Herman, and D. G. Jay. 2002.** Myosin 1c and myosin IIB serve opposing roles in lamellipodial dynamics of the neuronal growth cone. *J Cell Biol.* 158:1207.
- Ding, Q., J. Motoyama, S. Gasca, R. Mo, H. Sasaki, J. Rossant, and C. C. Hui. 1998.** Diminished Sonic hedgehog signaling and lack of floor plate differentiation in Gli2 mutant mice. *Development.* 125:2533.
- Djiane, A., J. Riou, M. Umbhauer, J. Boucaut, and D. Shi. 2000.** Role of frizzled 7 in the regulation of convergent extension movements during gastrulation in *Xenopus laevis*. *Development.* 127:3091.
- Doudney, K., and P. Stanier. 2005.** Epithelial cell polarity genes are required for neural tube closure. *Am J Med Genet C Semin Med Genet.* 135C:42.
- Drummond, I. A., A. Majumdar, H. Hentschel, M. Elger, L. Solnica-Krezel, A. F. Schier, S. C. Neuhauss, D. L. Stemple, F. Zwartkuis, Z. Rangini, W. Driever, and M. C. Fishman. 1998.** Early development of the zebrafish pronephros and analysis of mutations affecting pronephric function. *Development.* 125:4655.
- Dulabon, L., E. C. Olson, M. G. Taglienti, S. Eisenhuth, B. McGrath, C. A. Walsh, J. A. Kreidberg, and E. S. Anton. 2000.** Reelin binds alpha3beta1 integrin and inhibits neuronal migration. *Neuron.* 27:33.
- Eaton, S., R. Wepf, and K. Simons. 1996.** Roles for Rac1 and Cdc42 in planar polarization and hair outgrowth in the wing of *Drosophila*. *J Cell Biol.* 135:1277.
- Ernest, S., G. J. Rauch, P. Haffter, R. Geisler, C. Petit, and T. Nicolson. 2000.** Mariner is defective in myosin VIIA: a zebrafish model for human hereditary deafness. *Hum Mol Genet.* 9:2189.
- Evans, L. L., J. Hammer, and P. C. Bridgman. 1997.** Subcellular localization of myosin V in nerve growth cones and outgrowth from dilute-lethal neurons. *J Cell Sci.* 110:439.
- Fanto, M., U. Weber, D. I. Strutt, and M. Mlodzik. 2000.** Nuclear signaling by Rac and Rho GTPases is required in the

establishment of epithelial planar polarity in the *Drosophila* eye. *Curr Biol.* 10:979.

Feiguin, F., M. Hannus, M. Mlodzik, and S. Eaton. 2001. The ankyrin repeat protein Diego mediates Frizzled-dependent planar polarization. *Dev Cell.* 1:93.

Felsenfeld, D. P., M. A. Hynes, K. M. Skoler, A. J. Furley, and T. M. Jessell. 1994. TAG-1 can mediate homophilic binding, but neurite outgrowth on TAG-1 requires an L1-like molecule and beta 1 integrins. *Neuron.* 12:675.

Fox, J. W., E. D. Lamperti, Y. Z. Eksioglu, S. E. Hong, Y. Feng, D. A. Graham, I. E. Scheffer, W. B. Dobyns, B. A. Hirsch, R. A. Radtke, S. F. Berkovic, P. R. Huttenlocher, and C. A. Walsh. 1998. Mutations in filamin 1 prevent migration of cerebral cortical neurons in human periventricular heterotopia. *Neuron.* 21:1315.

Fraser, S. E., and D. H. Perkel. 1990. Competitive and positional cues in the patterning of nerve connections. *J Neurobiol.* 21:51.

Freigang, J., K. Proba, L. Leder, K. Diederichs, P. Sonderegger, and W. Welte. 2000. The crystal structure of the ligand binding module of axonin-1/TAG-1 suggests a zipper mechanism for neural cell adhesion. *Cell.* 101:425.

Fritzsch, B., and F. Hallbook. 1996. A simple and reliable technique to combine oligonucleotide probe in situ hybridization with neuronal tract tracing in vertebrate embryos. *Biotech Histochem.* 71:289.

Furley, A. J., S. B. Morton, D. Manalo, D. Karagogeos, J. Dodd, and T. M. Jessell. 1990. The axonal glycoprotein TAG-1 is an immunoglobulin superfamily member with neurite outgrowth-promoting activity. *Cell.* 61:157.

Gadisseux, J. F., P. Evrard, J. P. Misson, and V. S. Caviness. 1989. Dynamic structure of the radial glial fiber system of the developing murine cerebral wall. An immunocytochemical analysis. *Brain Res Dev Brain Res.* 50:55.

Garel, S., F. Marin, M. G. Mattei, C. Vesque, A. Vincent, and P. Charnay. 1997. Family of Ebf/Olf-1-related genes potentially involved in neuronal differentiation and regional specification in the central nervous system. *Dev Dyn.* 210:191.

- Gavalas, A., C. Ruhrberg, J. Livet, C. E. Henderson, and R. Krumlauf. 2003.** Neuronal defects in the hindbrain of Hoxa1, Hoxb1 and Hoxb2 mutants reflect regulatory interactions among these Hox genes. *Development*. 130:5663.
- Gavalas, A., M. Studer, A. Lumsden, F. M. Rijli, R. Krumlauf, and P. Chambon. 1998.** Hoxa1 and Hoxb1 synergize in patterning the hindbrain, cranial nerves and second pharyngeal arch. *Development*. 125:1123.
- Gilland, E., and R. Baker. 1993.** Conservation of neuroepithelial and mesodermal segments in the embryonic vertebrate head. *Acta Anat* 148:110.
- Gleeson, J. G., K. M. Allen, J. W. Fox, E. D. Lamperti, S. Berkovic, I. Scheffer, E. C. Cooper, W. B. Dobyns, S. R. Minnerath, M. E. Ross, and C. A. Walsh. 1998.** Doublecortin, a brain-specific gene mutated in human X-linked lissencephaly and double cortex syndrome, encodes a putative signaling protein. *Cell*. 92:63.
- Gleeson, J. G., and C. A. Walsh. 2000.** Neuronal migration disorders: from genetic diseases to developmental mechanisms. *Trends Neurosci*. 23:352.
- Glover, J. C. 2001.** Correlated patterns of neuron differentiation and Hox gene expression in the hindbrain: a comparative analysis. *Brain Res Bull*. 55:683.
- Goddard, J. M., M. Rossel, N. R. Manley, and M. R. Capecchi. 1996.** Mice with targeted disruption of Hoxb-1 fail to form the motor nucleus of the VIIth nerve. *Development*. 122:3217.
- Goto, T., and R. Keller. 2002.** The planar cell polarity gene strabismus regulates convergence and extension and neural fold closure in *Xenopus*. *Dev Biol*. 247:165.
- Greene, N. D., D. Gerrelli, H. W. Van Straaten, and A. J. Copp. 1998.** Abnormalities of floor plate, notochord and somite differentiation in the loop-tail (Lp) mouse: a model of severe neural tube defects. *Mech Dev*. 73:59.
- Gridley, T. 1997.** Notch signaling in vertebrate development and disease. *Mol Cell Neurosci* 9:103.

- Guan, K. L., and Y. Rao. 2003.** Signalling mechanisms mediating neuronal responses to guidance cues. *Nat Rev Neurosci.* 4:941.
- Guijarro, P., S. Simo, M. Pascual, I. Abasolo, J. A. Del Rio, and E. Soriano. 2006.** Netrin1 exerts a chemorepulsive effect on migrating cerebellar interneurons in a Dcc-independent way. *Mol Cell Neurosci.* 33:389.
- Gupta, A., K. Sanada, D. T. Miyamoto, S. Rovelstad, B. Nadarajah, A. L. Pearlman, J. Brunstrom, and L. H. Tsai. 2003.** Layering defect in p35 deficiency is linked to improper neuronal-glia interaction in radial migration. *Nat Neurosci.* 6:1284.
- Gurdon, J. B., P. Lemaire, and K. Kato. 1993.** Community effects and related phenomena in development. *Cell.* 75:831.
- Guthrie, S., and A. Lumsden. 1991.** Formation and regeneration of rhombomere boundaries in the developing chick hindbrain. *Development.* 112:221.
- Habas, R., I. B. Dawid, and X. He. 2003.** Coactivation of Rac and Rho by Wnt/Frizzled signaling is required for vertebrate gastrulation. *Genes Dev.* 17:295.
- Habas, R., Y. Kato, and X. He. 2001.** Wnt/Frizzled activation of Rho regulates vertebrate gastrulation and requires a novel Formin homology protein Daam1. *Cell.* 107:843.
- Hafezparast, M., R. Klocke, C. Ruhrberg, A. Marquardt, A. Ahmad-Annuar, S. Bowen, G. Lalli, A. S. Witherden, H. Hummerich, S. Nicholson, P. J. Morgan, R. Oozageer, J. V. Priestley, S. Averill, V. R. King, S. Ball, J. Peters, T. Toda, A. Yamamoto, Y. Hiraoka, M. Augustin, D. Korthaus, S. Wattler, P. Wabnitz, C. Dickneite, S. Lampel, F. Boehme, G. Peraus, A. Popp, M. Rudelius, J. Schlegel, H. Fuchs, M. Hrabe de Angelis, G. Schiavo, D. T. Shima, A. P. Russ, G. Stumm, J. E. Martin, and E. M. Fisher. 2003.** Mutations in dynein link motor neuron degeneration to defects in retrograde transport. *Science.* 300:808.
- Hagman, J., C. Belanger, A. Travis, C. W. Turck, and R. Grosschedl. 1993.** Cloning and functional characterization of early B-cell factor, a regulator of lymphocyte-specific gene expression. *Genes Dev.* 7:760.

- Hatten, M. E. 1999.** Central nervous system neuronal migration. *Annu Rev Neurosci* 22:511.
- Hattori, M., H. Adachi, M. Tsujimoto, H. Arai, and K. Inoue. 1994.** The catalytic subunit of bovine brain platelet-activating factor acetylhydrolase is a novel type of serine esterase. *J Biol Chem.* 269:23150.
- Heins, N., P. Malatesta, F. Cecconi, M. Nakafuku, K. L. Tucker, M. A. Hack, P. Chapouton, Y. A. Barde, and M. Gotz. 2002.** Glial cells generate neurons: the role of the transcription factor Pax6. *Nat Neurosci.* 5:308.
- Heisenberg, C. P., M. Tada, G. J. Rauch, L. Saude, M. L. Concha, R. Geisler, D. L. Stemple, J. C. Smith, and S. W. Wilson. 2000.** Silberblick/Wnt11 mediates convergent extension movements during zebrafish gastrulation. *Nature.* 405:76.
- Hiesberger, T., M. Trommsdorff, B. W. Howell, A. Goffinet, M. C. Mumby, J. A. Cooper, and J. Herz. 1999.** Direct binding of Reelin to VLDL receptor and ApoE receptor 2 induces tyrosine phosphorylation of disabled-1 and modulates tau phosphorylation. *Neuron.* 24:481.
- Higashijima, S., Y. Hotta, and H. Okamoto. 2000.** Visualization of cranial motor neurons in live transgenic zebrafish expressing green fluorescent protein under the control of the islet-1 promoter/enhancer. *J Neurosci.* 20:206.
- Hirai, S., A. Kawaguchi, R. Hirasawa, M. Baba, T. Ohnishi, and S. Ohno. 2002.** MAPK-upstream protein kinase (MUK) regulates the radial migration of immature neurons in telencephalon of mouse embryo. *Development.* 129:4483.
- Hirokawa, N., and R. Takemura. 2003.** Biochemical and molecular characterization of diseases linked to motor proteins. *Trends Biochem Sci.* 28:558.
- Hodge, T., and M. J. Cope. 2000.** A myosin family tree. *J Cell Sci.* 113 Pt 19:3353.
- Holzschuh, J., N. Wada, C. Wada, A. Schaffer, Y. Javidan, A. Tallafuss, L. Bally-Cuif, and T. F. Schilling. 2005.** Requirements for endoderm and BMP signaling in sensory neurogenesis in zebrafish. *Development.* 132:3731.

- Howell, B. W., T. M. Herrick, J. D. Hildebrand, Y. Zhang, and J. A. Cooper. 2000.** Dab1 tyrosine phosphorylation sites relay positional signals during mouse brain development. *Curr Biol.* 10:877.
- Hu, H. 2001.** Cell-surface heparan sulfate is involved in the repulsive guidance activities of Slit2 protein. *Nat Neurosci.* 4:695.
- Hutson, L. D., and C. B. Chien. 2002.** Wiring the zebrafish: axon guidance and synaptogenesis. *Curr Opin Neurobiol.* 12:87.
- Jacob, J., and S. Guthrie. 2000.** Facial visceral motor neurons display specific rhombomere origin and axon pathfinding behavior in the chick. *J Neurosci.* 20:7664.
- Jenny, A., R. S. Darken, P. A. Wilson, and M. Mlodzik. 2003.** Prickle and Strabismus form a functional complex to generate a correct axis during planar cell polarity signaling. *Embo J.* 22:4409.
- Jessell, T. M. 2000.** Neuronal specification in the spinal cord: inductive signals and transcriptional codes. *Nat Rev Genet.* 1:20.
- Jessen, J. R., J. Topczewski, S. Bingham, D. S. Sepich, F. Marlow, A. Chandrasekhar, and L. Solnica-Krezel. 2002.** Zebrafish trilobite identifies new roles for Strabismus in gastrulation and neuronal movements. *Nat Cell Biol.* 4:610.
- Jiang, S., and S. Ramachandran. 2004.** Identification and molecular characterization of myosin gene family in *Oryza sativa* genome. *Plant Cell Physiol.* 45:590.
- Kalil, K., and E. W. Dent. 2005.** Touch and go: guidance cues signal to the growth cone cytoskeleton. *Curr Opin Neurobiol.* 15:521.
- Kappler, J. A., C. J. Starr, D. K. Chan, R. Kollmar, and A. J. Hudspeth. 2004.** A nonsense mutation in the gene encoding a zebrafish myosin VI isoform causes defects in hair-cell mechanotransduction. *Proc Natl Acad Sci U S A.* 101:13056.
- Kato, G., and S. Maeda. 1999.** Neuron-specific Cdk5 kinase is responsible for mitosis-independent phosphorylation of c-Src at Ser75 in human Y79 retinoblastoma cells. *J Biochem.* 126:957.
- Kawauchi, T., K. Chihama, Y. Nabeshima, and M. Hoshino. 2006.** Cdk5 phosphorylates and stabilizes p27kip1 contributing to actin organization and cortical neuronal migration. *Nat Cell Biol.* 8:17.

- Kawauchi, T., K. Chihama, Y. V. Nishimura, Y. Nabeshima, and M. Hoshino. 2005.** MAP1B phosphorylation is differentially regulated by Cdk5/p35, Cdk5/p25, and JNK. *Biochem Biophys Res Commun.* 331:50.
- Keshvara, L., S. Magdaleno, D. Benhayon, and T. Curran. 2002.** Cyclin-dependent kinase 5 phosphorylates disabled 1 independently of Reelin signaling. *J Neurosci.* 22:4869.
- Kibar, Z., V. Capra, and P. Gros. 2007.** Toward understanding the genetic basis of neural tube defects. *Clin Genet.* 71:295.
- Kimmel, C. B., W. W. Ballard, S. R. Kimmel, B. Ullmann, and T. F. Schilling. 1995.** Stages of embryonic development of the zebrafish. *Dev Dyn.* 203:253.
- Kimmel, C. B., W. K. Metcalfe, and E. Schabtach. 1985.** T reticular interneurons: a class of serially repeating cells in the zebrafish hindbrain. *J Comp Neurol.* 233:365.
- Kitsukawa, T., A. Shimono, A. Kawakami, H. Kondoh, and H. Fujisawa. 1995.** Overexpression of a membrane protein, neuropilin, in chimeric mice causes anomalies in the cardiovascular system, nervous system and limbs. *Development.* 121:4309.
- Klein, T. J., and M. Mlodzik. 2005.** Planar cell polarization: an emerging model points in the right direction. *Annu Rev Cell Dev Biol* 21:155.
- Komuro, H., and P. Rakic. 1993.** Modulation of neuronal migration by NMDA receptors. *Science.* 260:95.
- Konno, D., S. Yoshimura, K. Hori, H. Maruoka, and K. Sobue. 2005.** Involvement of the phosphatidylinositol 3-kinase/rac1 and cdc42 pathways in radial migration of cortical neurons. *J Biol Chem.* 280:5082.
- Kostovic, I., and P. Rakic. 1980.** Cytology and time of origin of interstitial neurons in the white matter in infant and adult human and monkey telencephalon. *J Neurocytol.* 9:219.
- Krause, M., E. W. Dent, J. E. Bear, J. J. Loureiro, and F. B. Gertler. 2003.** Ena/VASP proteins: regulators of the actin cytoskeleton and cell migration. *Annu Rev Cell Dev Biol* 19:541.

- Kriegstein, A. R., and S. C. Noctor. 2004.** Patterns of neuronal migration in the embryonic cortex. *Trends Neurosci.* 27:392.
- Kruger, R. P., J. Aurandt, and K. L. Guan. 2005.** Semaphorins command cells to move. *Nat Rev Mol Cell Biol.* 6:789.
- Kuhn, T. B., E. T. Stoeckli, M. A. Condrau, F. G. Rathjen, and P. Sonderegger. 1991.** Neurite outgrowth on immobilized axonin-1 is mediated by a heterophilic interaction with L1(G4). *J Cell Biol.* 115:1113.
- Kuo, G., L. Arnaud, P. Kronstad-O'Brien, and J. A. Cooper. 2005.** Absence of Fyn and Src causes a reeler-like phenotype. *J Neurosci.* 25:8578.
- Kyriakopoulou, K., I. de Diego, M. Wassef, and D. Karagogeos. 2002.** A combination of chain and neurophilic migration involving the adhesion molecule TAG-1 in the caudal medulla. *Development.* 129:287.
- Lambert de Rouvroit, C., and A. M. Goffinet. 2001.** Neuronal migration. *Mech Dev.* 105:47.
- Landmesser, L. T. 2001.** The acquisition of motoneuron subtype identity and motor circuit formation. *Int J Dev Neurosci.* 19:175.
- Law, A. K., V. Pencea, C. R. Buck, and M. B. Luskin. 1999.** Neurogenesis and neuronal migration in the neonatal rat forebrain anterior subventricular zone do not require GFAP-positive astrocytes. *Dev Biol.* 216:622.
- Lemmon, V., S. M. Burden, H. R. Payne, G. J. Elmslie, and M. L. Hlavin. 1992.** Neurite growth on different substrates: permissive versus instructive influences and the role of adhesive strength. *J Neurosci.* 12:818.
- Lewis, K. E., and J. S. Eisen. 2003.** From cells to circuits: development of the zebrafish spinal cord. *Prog Neurobiol.* 69:419.
- Li, Z., N. M. Joseph, and S. S. Easter, Jr. 2000.** The morphogenesis of the zebrafish eye, including a fate map of the optic vesicle. *Dev Dyn.* 218:175.

- Libby, R. T., and K. P. Steel. 2000.** The roles of unconventional myosins in hearing and deafness. *Essays Biochem* 35:159.
- Liu, Y., and M. C. Halloran. 2005.** Central and peripheral axon branches from one neuron are guided differentially by Semaphorin3D and transient axonal glycoprotein-1. *J Neurosci.* 25:10556.
- Logan, C. Y., and R. Nusse. 2004.** The Wnt signaling pathway in development and disease. *Annu Rev Cell Dev Biol* 20:781.
- Louvi, A., S. S. Sisodia, and E. A. Grove. 2004.** Presenilin 1 in migration and morphogenesis in the central nervous system. *Development.* 131:3093.
- Lowery, L. A., and H. Sive. 2004.** Strategies of vertebrate neurulation and a re-evaluation of teleost neural tube formation. *Mech Dev.* 121:1189.
- Lumsden, A. 1990.** The cellular basis of segmentation in the developing hindbrain. *Trends Neurosci.* 13:329.
- Lumsden, A., and R. Keynes. 1989.** Segmental patterns of neuronal development in the chick hindbrain. *Nature.* 337:424.
- Lumsden, A., and R. Krumlauf. 1996.** Patterning the vertebrate neuraxis. *Science.* 274:1109.
- Luo, L. 2000.** Rho GTPases in neuronal morphogenesis. *Nat Rev Neurosci.* 1:173.
- Luskin, M. B. 1993.** Restricted proliferation and migration of postnatally generated neurons derived from the forebrain subventricular zone. *Neuron.* 11:173.
- Luskin, M. B., and C. J. Shatz. 1985.** Studies of the earliest generated cells of the cat's visual cortex: cogeneration of subplate and marginal zones. *J Neurosci.* 5:1062.
- Ma, X., S. Kawamoto, Y. Hara, and R. S. Adelstein. 2004.** A point mutation in the motor domain of nonmuscle myosin II-B impairs migration of distinct groups of neurons. *Mol Biol Cell.* 15:2568.
- Malatesta, P., E. Hartfuss, and M. Gotz. 2000.** Isolation of radial glial cells by fluorescent-activated cell sorting reveals a neuronal lineage. *Development.* 127:5253.

- Manzanares, M., P. A. Trainor, S. Nonchev, L. Ariza-McNaughton, J. Brodie, A. Gould, H. Marshall, A. Morrison, C. T. Kwan, M. H. Sham, D. G. Wilkinson, and R. Krumlauf. 1999.** The role of kreisler in segmentation during hindbrain development. *Dev Biol.* 211:220.
- Marin, O., J. Baker, L. Puelles, and J. L. Rubenstein. 2002.** Patterning of the basal telencephalon and hypothalamus is essential for guidance of cortical projections. *Development.* 129:761.
- Marin, O., A. S. Plump, N. Flames, C. Sanchez-Camacho, M. Tessier-Lavigne, and J. L. Rubenstein. 2003.** Directional guidance of interneuron migration to the cerebral cortex relies on subcortical Slit1/2-independent repulsion and cortical attraction. *Development.* 130:1889.
- Marin, O., and J. L. Rubenstein. 2001.** A long, remarkable journey: tangential migration in the telencephalon. *Nat Rev Neurosci.* 2:780.
- Marin, O., and J. L. Rubenstein. 2003.** Cell migration in the forebrain. *Annu Rev Neurosci* 26:441.
- Marlow, F., J. Topczewski, D. Sepich, and L. Solnica-Krezel. 2002.** Zebrafish Rho kinase 2 acts downstream of Wnt11 to mediate cell polarity and effective convergence and extension movements. *Curr Biol.* 12:876.
- Matise, M. P., D. J. Epstein, H. L. Park, K. A. Platt, and A. L. Joyner. 1998.** Gli2 is required for induction of floor plate and adjacent cells, but not most ventral neurons in the mouse central nervous system. *Development.* 125:2759.
- Metcalf, W. K., B. Mendelson, and C. B. Kimmel. 1986.** Segmental homologies among reticulospinal neurons in the hindbrain of the zebrafish larva. *J Comp Neurol.* 251:147.
- Metcalf, W. K., P. Z. Myers, B. Trevarrow, M. B. Bass, and C. B. Kimmel. 1990.** Primary neurons that express the L2/HNK-1 carbohydrate during early development in the zebrafish. *Development.* 110:491.
- Milev, P., P. Maurel, M. Haring, R. K. Margolis, and R. U. Margolis. 1996.** TAG-1/axonin-1 is a high-affinity ligand of neurocan,

phosphacan/protein-tyrosine phosphatase-zeta/beta, and N-CAM. *J Biol Chem.* 271:15716.

Miner, J. H., and P. D. Yurchenco. 2004. Laminin functions in tissue morphogenesis. *Annu Rev Cell Dev Biol* 20:255.

Miyata, T., A. Kawaguchi, H. Okano, and M. Ogawa. 2001. Asymmetric inheritance of radial glial fibers by cortical neurons. *Neuron.* 31:727.

Muller, M., N. Jabs, D. E. Lorke, B. Fritsch, and M. Sander. 2003. Nkx6.1 controls migration and axon pathfinding of cranial branchio-motoneurons. *Development.* 130:5815.

Murdoch, J. N., K. Doudney, C. Paternotte, A. J. Copp, and P. Stanier. 2001. Severe neural tube defects in the loop-tail mouse result from mutation of *Lpp1*, a novel gene involved in floor plate specification. *Hum Mol Genet.* 10:2593.

Nadarajah, B., P. Alifragis, R. O. Wong, and J. G. Parnavelas. 2002. Ventricle-directed migration in the developing cerebral cortex. *Nat Neurosci.* 5:218.

Nadarajah, B., P. Alifragis, R. O. Wong, and J. G. Parnavelas. 2003. Neuronal migration in the developing cerebral cortex: observations based on real-time imaging. *Cereb Cortex.* 13:607.

Nadarajah, B., J. E. Brunstrom, J. Grutzendler, R. O. Wong, and A. L. Pearlman. 2001. Two modes of radial migration in early development of the cerebral cortex. *Nat Neurosci.* 4:143.

Nadarajah, B., and J. G. Parnavelas. 1999. Gap junction-mediated communication in the developing and adult cerebral cortex. *Novartis Found Symp* 219:157.

Nadarajah, B., and J. G. Parnavelas. 2002. Modes of neuronal migration in the developing cerebral cortex. *Nat Rev Neurosci.* 3:423.

Nambiar, R. M., M. S. Ignatius, and P. D. Henion. 2007. Zebrafish *colgate/hdac1* functions in the non-canonical Wnt pathway during axial extension and in Wnt-independent branchiomotor neuron migration. *Mech Dev.* 124:682.

Nardelli, J., D. Thiesson, Y. Fujiwara, F. Y. Tsai, and S. H. Orkin. 1999. Expression and genetic interaction of transcription factors GATA-2 and GATA-3 during development of the mouse central nervous system. *Dev Biol.* 210:305.

- Noctor, S. C., A. C. Flint, T. A. Weissman, R. S. Dammerman, and A. R. Kriegstein. 2001.** Neurons derived from radial glial cells establish radial units in neocortex. *Nature*. 409:714.
- Noctor, S. C., A. C. Flint, T. A. Weissman, W. S. Wong, B. K. Clinton, and A. R. Kriegstein. 2002.** Dividing precursor cells of the embryonic cortical ventricular zone have morphological and molecular characteristics of radial glia. *J Neurosci*. 22:3161.
- Noden, D. M. 1983.** The role of the neural crest in patterning of avian cranial skeletal, connective, and muscle tissues. *Dev Biol*. 96:144.
- Ohsawa, R., T. Ohtsuka, and R. Kageyama. 2005.** Mash1 and Math3 are required for development of branchiomotor neurons and maintenance of neural progenitors. *J Neurosci*. 25:5857.
- Ohshima, T., and K. Mikoshiba. 2002.** Reelin signaling and Cdk5 in the control of neuronal positioning. *Mol Neurobiol*. 26:153.
- Ohshima, T., M. Ogawa, K. Takeuchi, S. Takahashi, A. B. Kulkarni, and K. Mikoshiba. 2002.** Cyclin-dependent kinase 5/p35 contributes synergistically with Reelin/Dab1 to the positioning of facial branchiomotor and inferior olive neurons in the developing mouse hindbrain. *J Neurosci*. 22:4036.
- Oster, S. F., and D. W. Sretavan. 2003.** Connecting the eye to the brain: the molecular basis of ganglion cell axon guidance. *Br J Ophthalmol*. 87:639.
- Ozmen, M., Y. Yilmaz, M. Caliskan, O. Minareci, and N. Aydinli. 2000.** Clinical features of 21 patients with lissencephaly type I (agyria-pachygyria). *Turk J Pediatr*. 42:210.
- Paglini, G., G. Pigino, P. Kunda, G. Morfini, R. Maccioni, S. Quiroga, A. Ferreira, and A. Caceres. 1998.** Evidence for the participation of the neuron-specific CDK5 activator P35 during laminin-enhanced axonal growth. *J Neurosci*. 18:9858.
- Park, M., and R. T. Moon. 2002.** The planar cell-polarity gene *stbm* regulates cell behaviour and cell fate in vertebrate embryos. *Nat Cell Biol*. 4:20.
- Parnavelas, J. G. 2000.** The origin and migration of cortical neurones: new vistas. *Trends Neurosci*. 23:126.

- Parnavelas, J. G., P. Alifragis, and B. Nadarajah. 2002.** The origin and migration of cortical neurons. *Prog Brain Res* 136:73.
- Parnavelas, J. G., S. A. Anderson, A. A. Lavdas, M. Grigoriou, V. Pachnis, and J. L. Rubenstein. 2000.** The contribution of the ganglionic eminence to the neuronal cell types of the cerebral cortex. *Novartis Found Symp* 228:129.
- Pata, I., M. Studer, J. H. van Doorninck, J. Briscoe, S. Kuuse, J. D. Engel, F. Grosveld, and A. Karis. 1999.** The transcription factor GATA3 is a downstream effector of Hoxb1 specification in rhombomere 4. *Development*. 126:5523.
- Pattyn, A., M. Hirsch, C. Goridis, and J. F. Brunet. 2000.** Control of hindbrain motor neuron differentiation by the homeobox gene Phox2b. *Development*. 127:1349.
- Pattyn, A., A. Vallstedt, J. M. Dias, M. Sander, and J. Ericson. 2003.** Complementary roles for Nkx6 and Nkx2 class proteins in the establishment of motoneuron identity in the hindbrain. *Development*. 130:4149.
- Paulus, J. D., and M. C. Halloran. 2006.** Zebrafish bashful/laminin-alpha 1 mutants exhibit multiple axon guidance defects. *Dev Dyn*. 235:213.
- Peng, M. Y., H. J. Wen, L. J. Shih, C. M. Kuo, and S. P. Hwang. 2002.** Myosin heavy chain expression in cranial, pectoral fin, and tail muscle regions of zebrafish embryos. *Mol Reprod Dev*. 63:422.
- Pollard, S. M., M. J. Parsons, M. Kamei, R. N. Kettleborough, K. A. Thomas, V. N. Pham, M. K. Bae, A. Scott, B. M. Weinstein, and D. L. Stemple. 2006.** Essential and overlapping roles for laminin alpha chains in notochord and blood vessel formation. *Dev Biol*. 289:64.
- Porcionatto, M. A. 2006.** The extracellular matrix provides directional cues for neuronal migration during cerebellar development. *Braz J Med Biol Res*. 39:313.
- Rader, C., E. T. Stoeckli, U. Ziegler, T. Osterwalder, B. Kunz, and P. Sonderegger. 1993.** Cell-cell adhesion by homophilic interaction of the neuronal recognition molecule axonin-1. *Eur J Biochem*. 215:133.

- Rakic, P. 1982.** Early developmental events: cell lineages, acquisition of neuronal positions, and areal and laminar development. *Neurosci Res Program Bull.* 20:439.
- Rakic, P. 1990.** Principles of neural cell migration. *Experientia.* 46:882.
- Rakic, P. 2000.** Molecular and cellular mechanisms of neuronal migration: relevance to cortical epilepsies. *Adv Neurol* 84:1.
- Rakic, P. 2000.** Illegal immigrations. *Neuron.* 27:409.
- Rauch, G. J., M. Hammerschmidt, P. Blader, H. E. Schauerte, U. Strahle, P. W. Ingham, A. P. McMahon, and P. Haffter. 1997.** Wnt5 is required for tail formation in the zebrafish embryo. *Cold Spring Harb Symp Quant Biol* 62:227.
- Reddy, A. S., and I. S. Day. 2001.** Analysis of the myosins encoded in the recently completed *Arabidopsis thaliana* genome sequence. *Genome Biol* 2:3.
- Reiner, O., R. Carrozzo, Y. Shen, M. Wehnert, F. Faustinella, W. B. Dobyns, C. T. Caskey, and D. H. Ledbetter. 1993.** Isolation of a Miller-Dieker lissencephaly gene containing G protein beta-subunit-like repeats. *Nature.* 364:717.
- Rivas, R. J., and M. E. Hatten. 1995.** Motility and cytoskeletal organization of migrating cerebellar granule neurons. *J Neurosci.* 15:981.
- Sakaguchi, T., A. Kuroiwa, and H. Takeda. 2001.** A novel sox gene, 226D7, acts downstream of Nodal signaling to specify endoderm precursors in zebrafish. *Mech Dev.* 107:25.
- Sambrook, J., Fritsch, E.F., and Maniatis, T. 1989.** Molecular cloning: A laboratory manual. Second edition. Cold Spring Harbor Press.
- Sapir, T., M. Elbaum, and O. Reiner. 1997.** Reduction of microtubule catastrophe events by LIS1, platelet-activating factor acetylhydrolase subunit. *Embo J.* 16:6977.
- Schilling, T. F., and C. B. Kimmel. 1997.** Musculoskeletal patterning in the pharyngeal segments of the zebrafish embryo. *Development.* 124:2945.

- Schmechel, D. E., and P. Rakic. 1979.** A Golgi study of radial glial cells in developing monkey telencephalon: morphogenesis and transformation into astrocytes. *Anat Embryol (Berl)*. 156:115.
- Schneider-Maunoury, S., P. Topilko, T. Seitandou, G. Levi, M. Cohen-Tannoudji, S. Pournin, C. Babinet, and P. Charnay. 1993.** Disruption of Krox-20 results in alteration of rhombomeres 3 and 5 in the developing hindbrain. *Cell*. 75:1199.
- Schwarz, Q., C. Gu, H. Fujisawa, K. Sabelko, M. Gertsenstein, A. Nagy, M. Taniguchi, A. L. Kolodkin, D. D. Ginty, D. T. Shima, and C. Ruhrberg. 2004.** Vascular endothelial growth factor controls neuronal migration and cooperates with Semaphorin 3A to pattern distinct compartments of the facial nerve. *Genes Dev*. 18:2822.
- Seiler, C., O. Ben-David, S. Sidi, O. Hendrich, A. Rusch, B. Burnside, K. B. Avraham, and T. Nicolson. 2004.** Myosin VI is required for structural integrity of the apical surface of sensory hair cells in zebrafish. *Dev Biol*. 272:328.
- Seitanidou, T., S. Schneider-Maunoury, C. Desmarquet, D. G. Wilkinson, and P. Charnay. 1997.** Krox-20 is a key regulator of rhombomere-specific gene expression in the developing hindbrain. *Mech Dev*. 65:31.
- Sellers, J. R. 2000.** Myosins: a diverse superfamily. *Biochim Biophys Acta*. 1496:3.
- Senzaki, K., M. Ogawa, and T. Yagi. 1999.** Proteins of the CNR family are multiple receptors for Reelin. *Cell*. 99:635.
- Shimada, Y., T. Usui, S. Yanagawa, M. Takeichi, and T. Uemura. 2001.** Asymmetric colocalization of Flamingo, a seven-pass transmembrane cadherin, and Dishevelled in planar cell polarization. *Curr Biol*. 11:859.
- Simon, H., and A. Lumsden. 1993.** Rhombomere-specific origin of the contralateral vestibulo-acoustic efferent neurons and their migration across the embryonic midline. *Neuron*. 11:209.
- Sittaramane, V., and A. Chandrasekhar. 2008.** Expression of unconventional myosin genes during neuronal development in zebrafish. *Gene Expr Patterns*. 8:161.

- Sobeih, M. M., and G. Corfas. 2002.** Extracellular factors that regulate neuronal migration in the central nervous system. *Int J Dev Neurosci.* 20:349.
- Soldati, T. 2003.** Unconventional myosins, actin dynamics and endocytosis: a menage a trois? *Traffic.* 4:358.
- Song, M. R. 2007.** Moving cell bodies: understanding the migratory mechanism of facial motor neurons. *Arch Pharm Res.* 30:1273.
- Song, M. R., R. Shirasaki, C. L. Cai, E. C. Ruiz, S. M. Evans, S. K. Lee, and S. L. Pfaff. 2006.** T-Box transcription factor Tbx20 regulates a genetic program for cranial motor neuron cell body migration. *Development.* 133:4945.
- Sousa, A. D., J. S. Berg, B. W. Robertson, R. B. Meeker, and R. E. Cheney. 2006.** Myo10 in brain: developmental regulation, identification of a headless isoform and dynamics in neurons. *J Cell Sci.* 119:184.
- Stafford, D., and V. E. Prince. 2002.** Retinoic acid signaling is required for a critical early step in zebrafish pancreatic development. *Curr Biol.* 12:1215.
- Stossel, T. P., J. Condeelis, L. Cooley, J. H. Hartwig, A. Noegel, M. Schleicher, and S. S. Shapiro. 2001.** Filamins as integrators of cell mechanics and signalling. *Nat Rev Mol Cell Biol.* 2:138.
- Strutt, D. 2001.** Planar polarity: getting ready to ROCK. *Curr Biol.* 11:R506.
- Studer, M. 2001.** Initiation of facial motoneurone migration is dependent on rhombomeres 5 and 6. *Development.* 128:3707.
- Studer, M., A. Lumsden, L. Ariza-McNaughton, A. Bradley, and R. Krumlauf. 1996.** Altered segmental identity and abnormal migration of motor neurons in mice lacking Hoxb-1. *Nature.* 384:630.
- Sumanas, S., P. Strege, J. Heasman, and S. C. Ekker. 2000.** The putative wnt receptor *Xenopus* frizzled-7 functions upstream of beta-catenin in vertebrate dorsoventral mesoderm patterning. *Development.* 127:1981.

- Suter, D. M., F. S. Espindola, C. H. Lin, P. Forscher, and M. S. Mooseker. 2000.** Localization of unconventional myosins V and VI in neuronal growth cones. *J Neurobiol.* 42:370.
- Suter, D. M., G. E. Pollerberg, A. Buchstaller, R. J. Giger, W. J. Dreyer, and P. Sonderegger. 1995.** Binding between the neural cell adhesion molecules axonin-1 and Nr-CAM/Bravo is involved in neuron-glia interaction. *J Cell Biol.* 131:1067.
- Tada, M., M. L. Concha, and C. P. Heisenberg. 2002.** Non-canonical Wnt signalling and regulation of gastrulation movements. *Semin Cell Dev Biol.* 13:251.
- Tada, M., and J. C. Smith. 2000.** Xwnt11 is a target of *Xenopus* Brachyury: regulation of gastrulation movements via Dishevelled, but not through the canonical Wnt pathway. *Development.* 127:2227.
- Tahinci, E., and K. Symes. 2003.** Distinct functions of Rho and Rac are required for convergent extension during *Xenopus* gastrulation. *Dev Biol.* 259:318.
- Takagi, S., Y. Kasuya, M. Shimizu, T. Matsuura, M. Tsuboi, A. Kawakami, and H. Fujisawa. 1995.** Expression of a cell adhesion molecule, neuropilin, in the developing chick nervous system. *Dev Biol.* 170:207.
- Takahashi, S., T. Saito, S. Hisanaga, H. C. Pant, and A. B. Kulkarni. 2003.** Tau phosphorylation by cyclin-dependent kinase 5/p39 during brain development reduces its affinity for microtubules. *J Biol Chem.* 278:10506.
- Takeuchi, M., J. Nakabayashi, T. Sakaguchi, T. S. Yamamoto, H. Takahashi, H. Takeda, and N. Ueno. 2003.** The prickle-related gene in vertebrates is essential for gastrulation cell movements. *Curr Biol.* 13:674.
- Tanaka, T., F. F. Serneo, H. C. Tseng, A. B. Kulkarni, L. H. Tsai, and J. G. Gleeson. 2004.** Cdk5 phosphorylation of doublecortin ser297 regulates its effect on neuronal migration. *Neuron.* 41:215.
- Tawk, M., C. Araya, D. A. Lyons, A. M. Reugels, G. C. Girdler, P. R. Bayley, D. R. Hyde, M. Tada, and J. D. Clarke. 2007.** A mirror-symmetric cell division that orchestrates neuroepithelial morphogenesis. *Nature.* 446:797.

- Taylor, J., N. Abramova, J. Charlton, and P. N. Adler. 1998.** Van Gogh: a new *Drosophila* tissue polarity gene. *Genetics*. 150:199.
- ten Donkelaar, H. J., M. Lammens, P. Wesseling, A. Hori, A. Keyser, and J. Rotteveel. 2004.** Development and malformations of the human pyramidal tract. *J Neurol*. 251:1429.
- Tessier-Lavigne, M., and C. S. Goodman. 1996.** The molecular biology of axon guidance. *Science*. 274:1123.
- Thisse, C., and B. Thisse. 1999.** Antivin, a novel and divergent member of the TGFbeta superfamily, negatively regulates mesoderm induction. *Development*. 126:229.
- Torban, E., C. Kor, and P. Gros. 2004.** Van Gogh-like2 (Strabismus) and its role in planar cell polarity and convergent extension in vertebrates. *Trends Genet*. 20:570.
- Torban, E., A. M. Patenaude, S. Leclerc, S. Rakowiecki, S. Gauthier, G. Andelfinger, D. J. Epstein, and P. Gros. 2008.** Genetic interaction between members of the Vangl family causes neural tube defects in mice. *Proc Natl Acad Sci U S A*. 105:3449.
- Torban, E., H. J. Wang, N. Groulx, and P. Gros. 2004.** Independent mutations in mouse Vangl2 that cause neural tube defects in looptail mice impair interaction with members of the Dishevelled family. *J Biol Chem*. 279:52703.
- Tree, D. R., J. M. Shulman, R. Rousset, M. P. Scott, D. Gubb, and J. D. Axelrod. 2002.** Prickle mediates feedback amplification to generate asymmetric planar cell polarity signaling. *Cell*. 109:371.
- Tsiotra, P. C., K. Theodorakis, J. Papamatheakis, and D. Karagozeos. 1996.** The fibronectin domains of the neural adhesion molecule TAX-1 are necessary and sufficient for homophilic binding. *J Biol Chem*. 271:29216.
- Tsukada, M., A. Prokscha, E. Ungewickell, and G. Eichele. 2005.** Doublecortin association with actin filaments is regulated by neurabin II. *J Biol Chem*. 280:11361.

- Tullio, A. N., P. C. Bridgman, N. J. Tresser, C. C. Chan, M. A. Conti, R. S. Adelstein, and Y. Hara. 2001.** Structural abnormalities develop in the brain after ablation of the gene encoding nonmuscle myosin II-B heavy chain. *J Comp Neurol.* 433:62.
- Tuxworth, R. I., and M. A. Titus. 2000.** Unconventional myosins: anchors in the membrane traffic relay. *Traffic.* 1:11.
- Uchida, Y., T. Ohshima, Y. Sasaki, H. Suzuki, S. Yanai, N. Yamashita, F. Nakamura, K. Takei, Y. Ihara, K. Mikoshiba, P. Kolattukudy, J. Honnorat, and Y. Goshima. 2005.** Semaphorin3A signalling is mediated via sequential Cdk5 and GSK3beta phosphorylation of CRMP2: implication of common phosphorylating mechanism underlying axon guidance and Alzheimer's disease. *Genes Cells.* 10:165.
- Usui, T., Y. Shima, Y. Shimada, S. Hirano, R. W. Burgess, T. L. Schwarz, M. Takeichi, and T. Uemura. 1999.** Flamingo, a seven-pass transmembrane cadherin, regulates planar cell polarity under the control of Frizzled. *Cell.* 98:585.
- Vanderlaan, G. 2006.** Differential roles for hedgehog signaling in motor neuron development. Dissertation submitted to the University of Missouri-Columbia.
- Vanderlaan, G., O. V. Tyurina, R. O. Karlstrom, and A. Chandrasekhar. 2005.** Gli function is essential for motor neuron induction in zebrafish. *Dev Biol.* 282:550.
- Veeman, M. T., D. C. Slusarski, A. Kaykas, S. H. Louie, and R. T. Moon. 2003.** Zebrafish prickles, a modulator of noncanonical Wnt/Fz signaling, regulates gastrulation movements. *Curr Biol.* 13:680.
- Volkman, D., T. Mori, U. K. Tirlapur, K. Konig, T. Fujiwara, J. Kendrick-Jones, and F. Baluska. 2003.** Unconventional myosins of the plant-specific class VIII: endocytosis, cytokinesis, plasmodesmata/pit-fields, and cell-to-cell coupling. *Cell Biol Int* 27:289.
- Wada, H., M. Iwasaki, T. Sato, I. Masai, Y. Nishiwaki, H. Tanaka, A. Sato, Y. Nojima, and H. Okamoto. 2005.** Dual roles of zygotic and maternal Scribble1 in neural migration and convergent extension movements in zebrafish embryos. *Development.* 132:2273.

- Wada, H., H. Tanaka, S. Nakayama, M. Iwasaki, and H. Okamoto. 2006.** Frizzled3a and Celsr2 function in the neuroepithelium to regulate migration of facial motor neurons in the developing zebrafish hindbrain. *Development*. 133:4749.
- Wallingford, J. B., and R. Habas. 2005.** The developmental biology of Dishevelled: an enigmatic protein governing cell fate and cell polarity. *Development*. 132:4421.
- Wallingford, J. B., and R. M. Harland. 2002.** Neural tube closure requires Dishevelled-dependent convergent extension of the midline. *Development*. 129:5815.
- Wallingford, J. B., B. A. Rowning, K. M. Vogeli, U. Rothbacher, S. E. Fraser, and R. M. Harland. 2000.** Dishevelled controls cell polarity during *Xenopus* gastrulation. *Nature*. 405:81.
- Walsh, C. A., and A. M. Goffinet. 2000.** Potential mechanisms of mutations that affect neuronal migration in man and mouse. *Curr Opin Genet Dev*. 10:270.
- Wang, F. S., J. S. Wolenski, R. E. Cheney, M. S. Mooseker, and D. G. Jay. 1996.** Function of myosin-V in filopodial extension of neuronal growth cones. *Science*. 273:660.
- Ward, M., C. McCann, M. DeWulf, J. Y. Wu, and Y. Rao. 2003.** Distinguishing between directional guidance and motility regulation in neuronal migration. *J Neurosci*. 23:5170.
- Warren, J. T., Jr., A. Chandrasekhar, J. P. Kanki, R. Rangarajan, A. J. Furley, and J. Y. Kuwada. 1999.** Molecular cloning and developmental expression of a zebrafish axonal glycoprotein similar to TAG-1. *Mech Dev*. 80:197.
- Wichterle, H., J. M. Garcia-Verdugo, and A. Alvarez-Buylla. 1997.** Direct evidence for homotypic, glia-independent neuronal migration. *Neuron*. 18:779.
- Wilkinson, D. G., and R. Krumlauf. 1990.** Molecular approaches to the segmentation of the hindbrain. *Trends Neurosci*. 13:335.
- Wilson, S. W., L. S. Ross, T. Parrett, and S. S. Easter, Jr. 1990.** The development of a simple scaffold of axon tracts in the brain of the embryonic zebrafish, *Brachydanio rerio*. *Development*. 108:121.

- Winter, C. G., B. Wang, A. Ballew, A. Royou, R. Karess, J. D. Axelrod, and L. Luo. 2001.** Drosophila Rho-associated kinase (Drok) links Frizzled-mediated planar cell polarity signaling to the actin cytoskeleton. *Cell*. 105:81.
- Wizenmann, A., and A. Lumsden. 1997.** Segregation of rhombomeres by differential chemoaffinity. *Mol Cell Neurosci* 9:448.
- Wolff, T., and G. M. Rubin. 1998.** Strabismus, a novel gene that regulates tissue polarity and cell fate decisions in Drosophila. *Development*. 125:1149.
- Wolman, M. A., V. K. Sittaramane, J. J. Essner, H. J. Yost, A. Chandrasekhar, and M. C. Halloran. 2008.** Transient axonal glycoprotein-1 (TAG-1) and laminin- α 1 regulate dynamic growth cone behaviors and initial axon direction in vivo. *Neural Develop.* 3:6.
- Wong, K., X. R. Ren, Y. Z. Huang, Y. Xie, G. Liu, H. Saito, H. Tang, L. Wen, S. M. Brady-Kalnay, L. Mei, J. Y. Wu, W. C. Xiong, and Y. Rao. 2001.** Signal transduction in neuronal migration: roles of GTPase activating proteins and the small GTPase Cdc42 in the Slit-Robo pathway. *Cell*. 107:209.
- Wu, X., G. Jung, and J. A. Hammer, 3rd. 2000.** Functions of unconventional myosins. *Curr Opin Cell Biol*. 12:42.
- Xie, Z., K. Sanada, B. A. Samuels, H. Shih, and L. H. Tsai. 2003.** Serine 732 phosphorylation of FAK by Cdk5 is important for microtubule organization, nuclear movement, and neuronal migration. *Cell*. 114:469.
- Xu, Q., G. Aildus, N. Holder, and D. G. Wilkinson. 1995.** Expression of truncated Sek-1 receptor tyrosine kinase disrupts the segmental restriction of gene expression in the *Xenopus* and zebrafish hindbrain. *Development*. 121:4005.
- Yamanaka, H., T. Moriguchi, N. Masuyama, M. Kusakabe, H. Hanafusa, R. Takada, S. Takada, and E. Nishida. 2002.** JNK functions in the non-canonical Wnt pathway to regulate convergent extension movements in vertebrates. *EMBO Rep*. 3:69.
- Yee, K. T., H. H. Simon, M. Tessier-Lavigne, and D. M. O'Leary. 1999.** Extension of long leading processes and neuronal

migration in the mammalian brain directed by the chemoattractant netrin-1. *Neuron*. 24:607.

Zisch, A. H., L. D'Alessandri, K. Amrein, B. Ranscht, K. H. Winterhalter, and L. Vaughan. 1995. The glypiated neuronal cell adhesion molecule contactin/F11 complexes with src-family protein tyrosine kinase Fyn. *Mol Cell Neurosci*. 6:263.

Vita

Vinoth Sittaramane was born in Trichy, Tamil Nadu, India. He finished high school in 1995 from Trichy. He received his Bachelor of Veterinary Sciences and Animal Husbandry (B.V.Sc & A.H) from Rajiv Gandhi College Of Veterinary and Animal Sciences, Pondicherry in 2000. Between 2000 and 2008, he received M.V.Sc in Animal Biotechnology from Indian Veterinary Research Institute and Ph.D in Biological Sciences from the University of Missouri-Columbia.